



**UNIVERSITY of the
WESTERN CAPE**

**Petrophysical evaluation and characterization of sandstone
reservoirs of the western Bredasdorp Basin, South Africa for well
D-D1 and E-AP1.**

Applied Geology (Petroleum Geology)

By

Maseko, Phindile Pearl

**Submitted in fulfillment of the requirements for the degree of M.Sc (Masters) in the
Department of Earth Science, University of the Western Cape**

Supervisor: Dr. Mimonitu Opuwari

March 2016

Abstract

The Bredasdorp Basin was formed consequent to extensional episodes during the initial stages of rifting in the Jurassic age. The basin acted as a local depocentre and was primarily infilled with late Jurassic and early Cretaceous shallow-marine and continental sediments. Two wells namely; D-D1 and E-AP1 were studied in order to evaluate the petrophysics and characterize sandstone reservoirs of the western Bredasdorp basin. This could be achieved by generating and comparing results from core analysis and wireline in order to determine if the two wells are comprised of good quality sandstone reservoirs and if the identified reservoirs produce hydrocarbons. A number of methods were employed in order to characterise and evaluate sandstone reservoir, these included; editing and normalization of raw wireline log data, classification of lithofacies on the basis of lithology, sedimentary structures, facies distribution, grain size variation, sorting of grains, fossils and bioturbation; calibration of log and core data to determine parameters for petrophysical interpretation; volume of clay; determination of porosity, permeability and fluid saturation, cut-off determination to distinguish between pay and non-pay sands. Borehole D-D1 is located in the western part of the Bredasdorp Basin. Only two reservoirs in well D-D1 indicated to have pay parameters with an average porosity ranging from 11.3% to 16%, average saturation from 0.6% to 21.5% and an volume of clay from 26.5% to 31.5%. This well was abandoned due to poor oil shows according to the geological well completion report. On the contrary well E-AP1 situated in the northwestern section of the basin showed good quality reservoir sandstones occurring in the 19082m to 26963m intervals though predominantly water saturated. Pay parameters for all five reservoirs in this well showed zero or no average porosity, saturation and volume of clay.

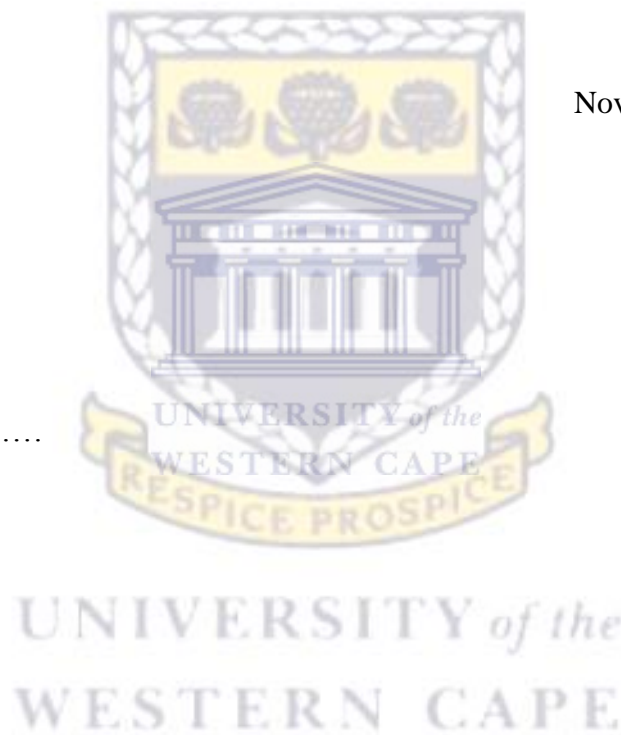
Declarations

I declare that this study on Petrophysical evaluation and characterization of sandstone reservoirs of the western Bredasdorp basin, South Africa for well D-D1 and E-AP1 is my own work, that it has not been submitted before for any degree or examination in any other university, and that all the sources I have used or quoted have been indicated and acknowledged by means of complete references.

Maseko Phindile Pearl

November 2014

.....
Signature



Acknowledgements

I would like to express my sincere gratitude to my supervisor Dr. M. Opuwari for his support, patience, motivation, guidance and immense knowledge. I could have not imagined having a better supervisor for my research.

My sincere thanks to Prof. Okujeni for always ensuring that all was well with me and gladly helped me when I needed his assistance.

A special thanks to my friend and colleague; Moses Magoba for his help and support throughout this study for giving his input and criticism where it was due.

Last but not least I would like to thank my parents and siblings for their support and believing in me through out my studies, not forgetting my new family who makes everyday a day filled with love, happiness and joy, my husband S'pha Buthelezi.

Above all I would like to thank the All Mighty God who gave me life in abundance, continues to protect, love, and bless me every new day.

I dedicate this to my mom and Amahle Zoé Buthelezi.



UNIVERSITY of the
WESTERN CAPE

Keywords

Bredasdorp Basin

Facies

Permeability

Porosity

Reservoir characterization

Sandstone



UNIVERSITY *of the*
WESTERN CAPE

Table of Contents

Abstract.....	i
Declaration.....	ii
Acknowledgement.....	iii
Keywords.....	iv
Table of content.....	v
List of figures.....	viii
List of tables.....	x
List of appendices.....	xi
CHAPTER 1: Introduction.....	1
1.1 Background.....	1
1.2 Thesis Outline.....	1
1.2.1.1 Chapter 1.....	1
1.2.1.2 Chapter 2.....	1
1.2.1.3 Chapter 3.....	2
1.2.1.4 Chapter 4.....	2
1.2.1.5 Chapter 5.....	2
1.2.1.6 Chapter 6.....	2
1.3 Aim.....	3
1.4 Objectives.....	3
1.5 History of Hydrocarbon exploration of South Africa Offshore.....	3
CHAPTER 2: Geological Background of the Bredasdorp Basin.....	6
2.1 Regional Geology of the Bredasdorp Basin.....	6
2.2 Tectonic Setting of the Bredasdorp Basin.....	10
2.3 Structural development of the Bredasdorp Basin.....	13
2.4 Thermal Gradient History of the Bredasdorp Basin.....	16
2.5 Source Rock Maturity.....	16
CHAPTER 3: Well Summary.....	18
3.1 Well D-D1.....	1

3.2 Well E-AP1.....	20
CHAPTER 4: Methodology.....	22
4.1 Flow Chart.....	22
4.2 Characteristics of selected wireline logs.....	23
4.2.1 Gamma Ray Log.....	24
4.2.2 Sonic log.....	24
4.2.3 Electrode Resistivity.....	26
4.2.4 Caliper.....	26
4.2.5 Neutron log.....	28
4.2.6 Density log.....	29
4.2.7 Combination of Neutron-Density Log.....	30
CHAPTER 5: Results.....	32
5.1 Conventional Core Analysis.....	32
5.1.1 Well D-D1 Core Analysis.....	32
5.1.2 Well E-AP1 Core Analysis.....	34
5.2 Lithofacies and Description.....	35
5.2.1 Well D-D1 Lithofacies.....	37
5.2.2 Well E-AP1 Lithofacies.....	38
5.3 Grain Density.....	39
5.3.1 Well D-D1 Grain Density.....	40
5.3.2 Well E-AP1 Grain Density.....	41
5.3.3 Comparison of grain density distribution for wells.....	42
5.4 Core Porosity.....	43
5.4.1 Well D-D1 Porosity.....	44

5.4.2 Well E-AP1 Porosity.....	48
5.5 Core Permeability.....	50
5.5.1 Well D-D1 Permeability.....	51
5.5.2 Well E-AP1 Permeability.....	53
5.6 Fluid Saturation.....	54
5.6.1 Well D-D1 Fluid saturation.....	55
5.6.2 Well E-AP1 Fluid saturation.....	57
5.6.3 Comparison of Porosity – Permeability and Facies Distribution.....	59
5.6.4 Permeability from Core Analysis (Permeability-Porosity Function).....	60
5.7 Cut-off determination.....	64
5.7.1 Porosity cut-off determination.....	65
5.7.2 Volume of shale cut-off determination.....	66
5.7.3 Water saturation cut-off determination.....	67
5.8 Determination of Net Pay.....	67
5.8.1 Well D-D1 Net pay.....	68
5.8.2 Well E-AP1 Net pay.....	72
CHAPTER 6: Conclusions.....	77
6.1 Recommendations.....	78
References.....	79
Appendix.....	83

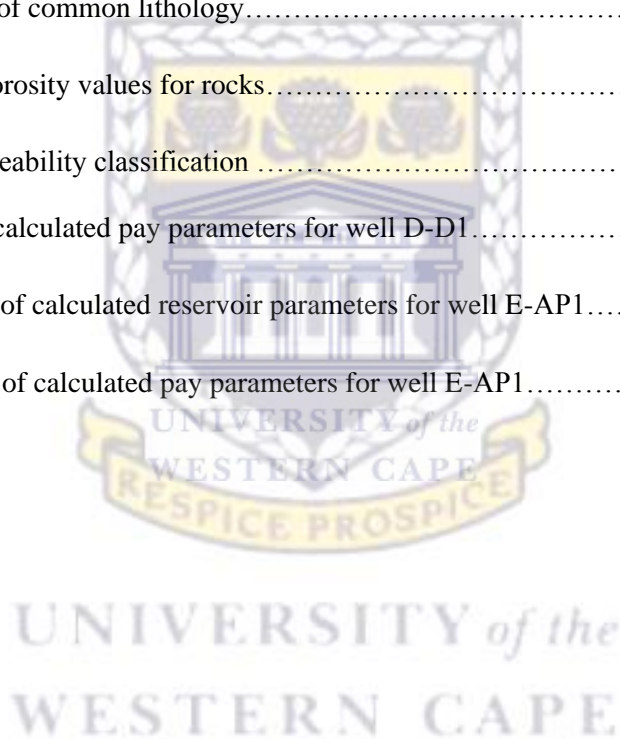
List of Figures

Figure 2.1.1: Paleogeography showing the break-up of Super Continent Pangaea and the development of the region around the Outeniqua Basin.....	6
Figure 2.1.2: Map showing the location of the study area within Block 9.....	7
Figure 2.1.3: Well location map.....	8
Figure 2.1.4: Structural Framework of the Bredasdorp Basin encircled in the map.....	9
Figure 2.2.1: Chronostratigraphy of the Bredasdorp Basin	12
Figure 2.3.1: Seismic profile with identified sequence boundaries (Top); and schematic cross section....	15
Figure 4.1: Flow chart of research methodology.....	22
Figure 4.2: Graphical representation of logs and reference to subsurface and hydrocarbons.....	23
Figure 4.2.1: Gamma ray tool.....	24
Figure 4.2.2: Sonic logging tool receiver (R) and transmitter (T).....	25
Figure 4.2.3: Normal device with electrodes A, M, N.....	26
Figure 4.2.4: Typical caliper response to various lithologies.....	27
Figure 4.2.5: (A) Compensation neutron tool drawing, and (B) schematic trajectories of a neutron in a limestone with no porosity and pure water.....	28
Figure 4.2.6: Compensation density sonde.....	29
Figure 4.2.7: The density-neutron cross-plot.....	31
Figure 5.2.1: Well D-D1 with core facies shown in track 3.....	37
Figure 5.2.2: Well E-AP1 with core facies shown in track 3.....	38
Figure 5.3.1: Histogram of well D-D1 core grain density.....	40
Figure 5.3.2: Histogram of well E-AP1 core grain density.....	41
Figure 5.3.3: Grain density histogram plot for well D-D1 and E-AP1.....	42

Figure 5.4.1a: Well D-D1 Porosity versus depth plot.....	45
Figure 5.4.1b: Well D-D1 Porosity versus depth plot.....	46
Figure 5.4.1.1: Well D-D1 Core Porosity histogram and plot against.....	47
Figure 5.4.2: Well E-AP1 Porosity versus depth plot.....	48
Figure 5.4.2.1: Well E-AP1 Core Porosity histogram and plot against.....	49
Figure 5.5.1a: Well D-D1 Permeability versus depth plot.....	52
Figure 5.5.1b: Well D-D1 Permeability versus depth plot.....	53
Figure 5.5.2: Well E-AP1 Permeability versus depth plot.....	54
Figure 5.6.1a: Well D-D1 Fluid saturation versus depth plot.....	56
Figure 5.6.1b: Well D-D1 Comparison of core and log saturation and porosity.....	57
Figure 5.6.2a: Well E-AP1 Fluid saturation versus depth plot.....	58
Figure 5.6.2b: Well E-AP1 Comparison of core and log saturation and porosity.....	58
Figure 5.6.3: Porosity Versus Klinkenberg Permeability.....	59
Figure 5.6.4a: Porosity-Permeability cross-plots for determination of functions.....	60
Figure 5.6.4b: Multi well for porosity-permeability cross-plots for determination of functions.....	61
Figure 5.6.4.1: Well D-D1 plot of predicted permeability overlaying original core permeability.....	62
Figure 5.6.4.2: Well E-AP1 plot of predicted permeability overlaying original core permeability.....	63
Figure 5.7.1: Multi well porosity-permeability and facies plot for cut-off determination.....	65
Figure 5.7.2: Volume of shale versus porosity plot for cut-off determination.....	66
Figure 5.7.3: Porosity versus water saturation plot for cut-off determination.....	67
Figure 5.8.1: Well D-D1 displaying calculated reservoir parameters and pay flag.....	72
Figure 5.8.2: Well E-AP1 displaying calculated reservoir parameters.....	81

List of Tables

Table 3.1.1: Rig and operational data for well D-D1.....	19
Table 3.1.2: Rig and operational data for well E-AP1.....	21
Table 5.1.1: Well D-D1 routine core analysis results.....	33
Table 5.1.2: Well E-AP1 routine core analysis results.....	34
Table 5.2: Lithofacies descriptions and classification of reservoir facies.....	36
Table 5.3: Matrix density of common lithology.....	39
Table 5.4: The range of porosity values for rocks.....	44
Table 5.5: Reservoir permeability classification	51
Table 5.8.1: Summary of calculated pay parameters for well D-D1.....	65
Table 5.8.2 (a): Summary of calculated reservoir parameters for well E-AP1.....	73
Table 5.8.2 (b): Summary of calculated pay parameters for well E-AP1.....	74



List of Appendices

Appendix A: Gamma Ray histogram for wells

Appendix B: RHOB vs NPHI for wells

Appendix C: RHOB vs DT for wells

Appendix D: ILD vs DT for wells

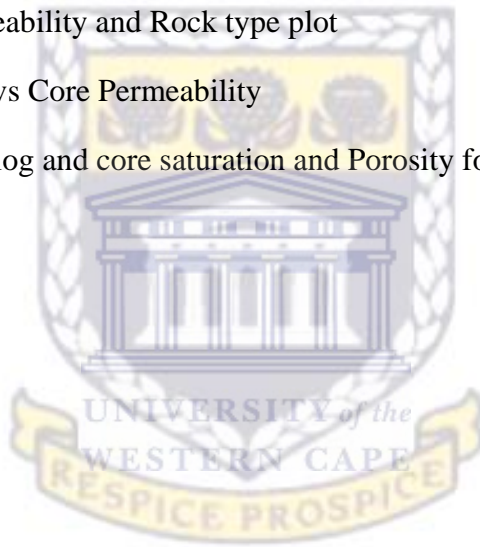
Appendix E: Core Porosity vs Core Permeability

Appendix F: Volume of Clay vs Core Porosity for wells

Appendix G: Porosity-Permeability and Rock type plot

Appendix H: Core Porosity vs Core Permeability

Appendix I: Comparison of log and core saturation and Porosity for reservoirs



UNIVERSITY of the
WESTERN CAPE

CHAPTER 1

1. Introduction

1.1 Background

The Bredasdorp Basin and its environs, is located on the South African continental shelf between Cape Agulhas and Mossel Bay. The basin is a sub-basin of the Outeniqua Basin. The basin is one of four delineated by the results from the seismic surveys and approximately 200 wells drilled in the course of exploration of hydrocarbons, extending for approximately 150 km E-W and 100 km N-S, with an acreage of approximately 15 000km².

Petroleum reservoir characterization can be described as a process that includes integrated analysing and understanding all available data from the well (Lombard and Akinlua, 2009). The integration of seismic interpretation with evaluation of petrophysical properties provides a comprehensive approach to reservoir characterization.

A predominance of the oil and gas that is currently produces worldwide is derived from reservoir rocks that contain hydrocarbon accumulations within its pore spaces. Porosity, permeability and shale volume are fundamental properties that govern the quality of reservoir rock as well as enable accurate estimation of potential hydrocarbon resources.

1.2 Thesis Outline

This thesis consists of a written report divided into six chapters of methods used to characterise and evaluate the petrophysics of sandstone reservoirs of well D-D1 and E-AP1 in the western part of the Bredasdorp Basin, South Africa. This could be achieved by generating and comparing results from core analysis and wireline in order to determine if the two wells are comprised of good quality sandstone reservoirs and if the identified reservoirs produce hydrocarbons. The data generated from core analysis and wireline is used to determine the volume of clay, porosity, permeability, fluid saturation, cut-off and net pay.

1.2.1 Chapter 1

Chapter 1 one gives a broad overview of the study area, the objectives to be achieved in the study and the history of the study area in terms of hydrocarbon exploration.

1.2.2 Chapter 2

Chapter 2 covers the regional geology of the Bredasdorp Basin, the tectonic setting giving detailed information on the structural development of the basin aligned with the chronostratigraphy of the study area. This chapter also covers the thermal gradient history and the source rock maturity of the basin.

1.2.3 Chapter 3

Chapter 3 summaries well D-D1 and E-AP1 based on their location, geology on cored intervals, exploration history, rig and operational data.

1.2.4 Chapter 4

Chapter 4 outlines all the methods that were used in order to achieve the objectives mentioned in Chapter 1. This chapter also gives detailed information on the wireline logging tools used to obtain logs that have been used in this study.

1.2.5 Chapter 5

Chapter 5 discusses a number of methods used in order to characterise and evaluate sandstone reservoir, these include editing and normalization of raw wireline log data ,classification of lithofacies on the basis of lithology, sedimentary structures, facies distribution, grain size variation, sorting of grains, fossils and bioturbation; calibration of log and core data to determine parameters for petrophysical interpretation; volume of clay; determination of porosity, permeability and fluid saturation, cut-off determination to distinguish between pay and non-pay sands.

1.2.6. Chapter 6

Chapter 6 concludes the thesis and also gives recommendations for future studies

1.3 Aim

This research aims to evaluate the petrophysics and characterize sandstone reservoirs of the western Bredasdorp basin, South Africa for well D-D1 and E-AP1. This could be achieved by generating and comparing results from core analysis and wireline in order to determine if the two wells are comprised of good quality sandstone reservoirs and if the identified reservoirs produce hydrocarbons.

1.4 Objectives

- ✓ Editing and normalization of raw wireline log data
- ✓ Classification of lithofacies
- ✓ Calibration of log and core data to determine parameters for petrophysical interpretation
- ✓ Volume of clay
- ✓ Determine porosity, permeability and fluid saturation
- ✓ Cut-off determination
- ✓ Net-pay determination

1.5 History of hydrocarbon exploration of South African Offshore

The Bredasdorp Basin is located on the South African continental shelf between Cape Agulhas and Mossel Bay (see Figure 2.1.2). The basin is essentially filled with Upper Jurassic and Lower Cretaceous synrift continental marine strata, Post Cretaceous and Cenozoic divergent rocks. The Bredasdorp Basin is delineated by the results from the seismic surveys and the ~200 wells drilled during the course of hydrocarbon exploration.

Prior to the start hydrocarbon exploration in the South African offshore in the late 1960's, there had been no geological studies of the continental shelf of South Africa. The presently understood geological history of the area in general and of the Bredasdorp Basin in particular therefore stems from this hydrocarbon exploration effort, which is still continuing. Indeed, it is only during the past 10 years, after many regional and local studies, that the geological history has become well enough understood for exploration success rates to improve dramatically. However, few of these studies have been published apart from some general reviews and presentation at Geocongress, Cape Town (1990). In step with this advancement has come an explosive growth in the understanding of the petroleum geochemistry of the basin. Many regional and well-specific studies of this nature have also been undertaken in offshore areas, almost entirely by SOEKOR. Very little of this information has been published.

Many hydrocarbon reservoirs within the Bredasdorp Basin have been found in Cretaceous sandstones. It is thought that the gas and oil they contain have been generated in one or more of the carbon-rich source rocks found within the limits of the basin or in the western part of the Southern Outeniqua Basin.

These hydrocarbons comprise of liquid oils and traces of high molecular weight hydrocarbons, considered to be residues after earlier oil charges, and wet gas with condensate. Concentrations of these hydrocarbons are commercially significant and are actively explored. Two reservoirs are currently producing gas-condensate and oil. The commercial viability of these occurrences is primarily related to the high monetary value of the liquid fraction compared of that of gas. Therefore it is of paramount importance to the exploration efforts to concentrate their search in those parts of the basin where such hydrocarbons are preferentially reservoired. This is achieved if the route that these hydrocarbons took when migration from their source rock to the present reservoir rock are known, where the timing of the migration episodes is understood and the volume available through each route can be reliably estimated. These can only be evaluated once the source rock for the hydrocarbon is identified, the fetch area is delineated, the maturation history is known and the relative quantities expelled from each source are calculated. Each of these is very difficult to determine and represents major challenges to the explorationist.

Prior to the present study, the distribution, thickness and richness of source rocks in the Bredasdorp Basin wells were established from inter-well comparisons using pyrolysis analyses (>24000) and optical studies (>3500) carried out on core and side wall core samples from 150 wells and 75 wells respectively. From the data it was determined that there were several different source rocks and that some were within the oil window, while some had passed through the oil window. No intersections of immature wet gas or oil-prone source rocks have been found.

The search for inherited characteristics of source rocks has been actively pursued by petroleum geochemists elsewhere for some time (Philippi, 1956; Bray and Evans, 1965). These earliest efforts concentrated on the composition of the oil amenable to gas chromatographic analysis. Those early methods were quickly adopted by other companies and refined so that correlations between source rocks and oils were frequently attempted using more detailed comparisons of the chemical and physical properties of hydrocarbons, with similar properties of bitumens in the supposed source rocks (Dow and Williams, 1974).

Those comparisons were based on the premise that hydrocarbons derived from each source rock should be distinguishable because they inherit characteristics of the original biological source material. Since it is known that some hydrocarbons are left behind in the source rock as bitumens after migration (Tissot and Welte, 1984), it is likely that chemical ‘fossils’ in the bitumens should match those found in reservoired hydrocarbons (Eglinton and Calvin, 1967).

These early correlation studies largely addressed characteristic aspects of low maturity whole oil and bulk source rock extracts using medium resolution gas chromatography. As the techniques became more widely used, the complexity of the hydrocarbons became evident. The high molecular weight fractions of the oils were evidently comprised of mixtures of hundreds of components which could only be separated by high resolution gas chromatography and later by mass spectrometry analysis. However, these methods proved to be less successful when dealing with higher maturity condensates and their sources, because the proportions of bulk and chromatographically resolvable groups of hydrocarbons decreased with increasing maturity. As a result, various fractionation and concentration steps were employed. The added advantage of using high resolution analyses of specific fractions was that they were able to establish identities of characteristic groups of compounds which could differentiate oils and source rocks without recourse to the short to medium-chain alkanes previously employed. This was a step forward as those alkanes were often subject to severe in reservoir alteration by biodegradation (Rogers *et al.*, 1974).

During the 1970’s and 1980’s, source rock-oil correlation methods available in South Africa were largely limited to those developed prior to the imposition of trade sanctions and technical embargo’s in the early 1970’s. These methods mostly comprised the high resolution gas chromatography techniques. Low resolution mass spectrometry analyses were possible but without calibration samples, the biological fossils or marker compounds could not be readily identified and compared with published literature. In addition, until the mid - 1980’s almost all the discovered hydrocarbons which were reservoired in quantity, and on which exploration focus was placed, were high maturity condensates. The known lack of success in determining oil; source correlations from such high maturity hydrocarbons, left little incentive for further study especially in view of the inaccessibility of the more modern analytical methods.

CHAPTER 2

Geological Background of the Bredasdorp Basin

2.1 Regional Geology of the Bredasdorp Basin

The date of the earliest break-up of Gondwana based on the volcanic evidence from eastern South Africa is $\sim 140 \pm 30$ Ma, while the western part of South Africa is $\sim 150 \pm 14$ Ma. Rifting is said to have started earlier in the east than the west. This conclusion agrees well with the proposed time of the first rifting events in the southern part of Africa based on the presence of mid-late Jurassic rocks in the South Atlantic (Gilbert, 1977). Separation between East and West Gondwana began along the progressively foundering rift zone between the Australasian plate and the African plate (Khanna and Pillay, 1986; Lawver et al., 1992). During this phase, continental sediments were deposited on the early syn-rift surface. During later stages of the sag, a seaway developed along the eastern margin of Africa gradually transgressing further south and bringing marine conditions to the southern coastal areas (Gilbert, 1990).

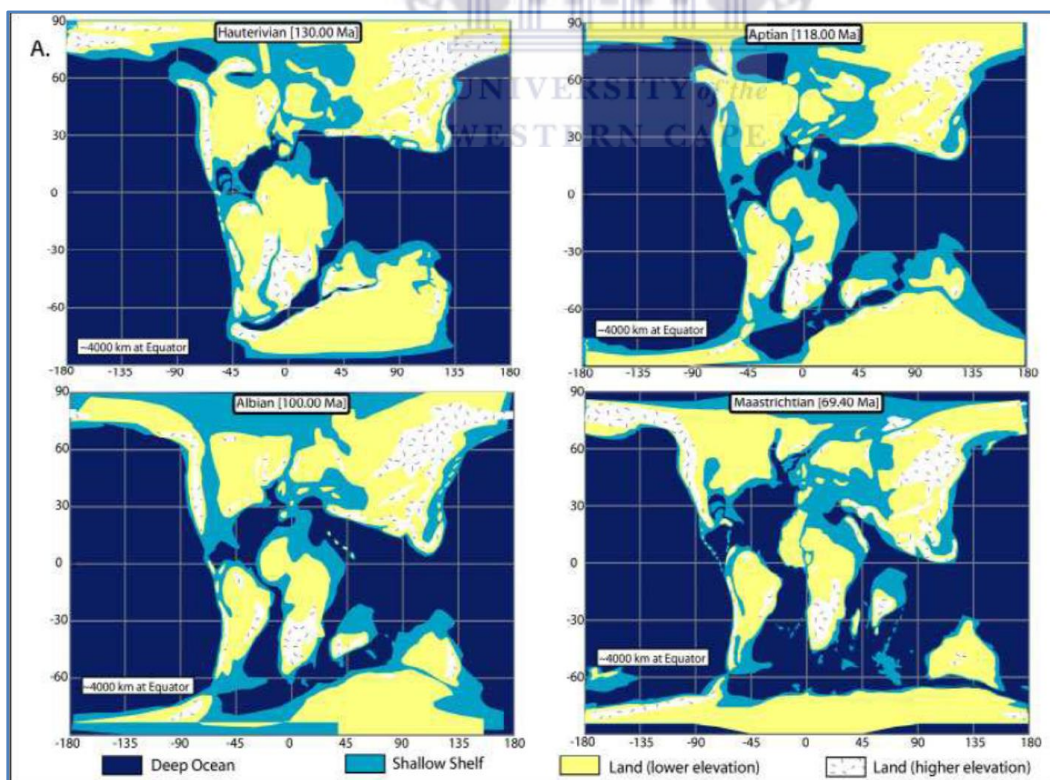


Figure 2.1.1: Paleogeography showing the break-up of Super Continent Pangea and the development of the region around the Outeniqua Basin (Gilbert, 1990).

The Outeniqua Basin, comprising of four sub-basins (Bredasdorp, Pletmos, Gamtoos and Algoa) was formed from dextral shearing processes of the South African margin which was initiated in the Early to Mid-Cretaceous. The rift phase of the south coast ended in the Lower Valanginian which is associated with drift-onset unconformity (1At1) (Petroleum Agency SA, 2004/2005). The drift-onset unconformity is simultaneous to the earliest oceanic crust in the South Atlantic. A complex series of micro plates such as the Falkland Plateau steadily moved southwestwards past the southern coast of Africa. These movements created some oblique rift half-graben sub-basins including the Bredasdorp Basin which may be regarded as failed rifts. Succeeding the rift phase was a transitional rift-drift phase featuring three phases of inversion related to continuous shearing. Transitional rift drift ended in the mid Albian as the Falkland Plateau separated from Africa and was followed by the development of a true passive margin.

The Bredasdorp Basin is a sub-basin of the Outeniqua Basin. This basin is situated off the south coast of the Republic of South Africa, southeast of Cape Town and west-southwest of Port Elizabeth. The Bredasdorp Basin was formed consequent to extensional episodes during the initial stages of rifting in the Jurassic age. The basin acted as a local depocentre and was primarily infilled with late Jurassic and early Cretaceous shallow-marine and continental sediments (Turner et al., 2000).



Figure 2.1.2: Map showing the location of the study area within Block 9 (Modified from Petroleum Agency SA, 2003).

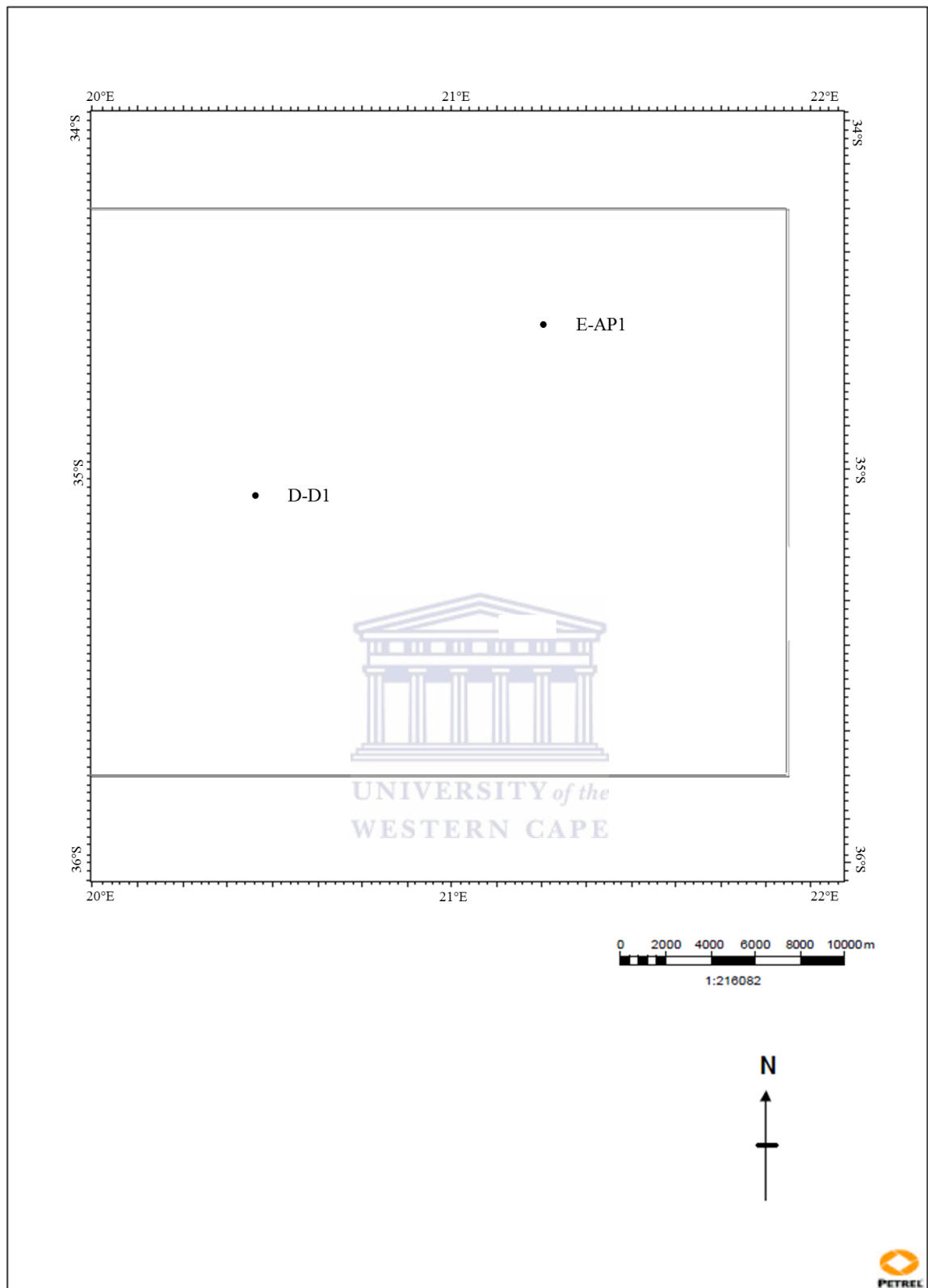


Figure 2.1.3: Well location map

The Bredasdorp Basin consists of the east-west Permo-Triassic Cape Fold Belt (CFB) to the north and by the lower-Cretaceous Agulhas Falkland Fracture Zone (AFFZ) to the southeast. The CFB is a northern verging fold and thrust belt whereas the AFFZ is a dextral transform fault formed during the separation of Africa and South America and it forms a boundary between continental and oceanic crusts. The basin formation is closely related to the break-up of Gondwanaland and subsequent development is related to thermal subsidence in response to a single rifting event. The synrift sedimentary sequence is composed of fluvial and shallow-marine sediments while the post-rift sequence is dominated by deep marine sediments (De Wit and Ransome, 1992).

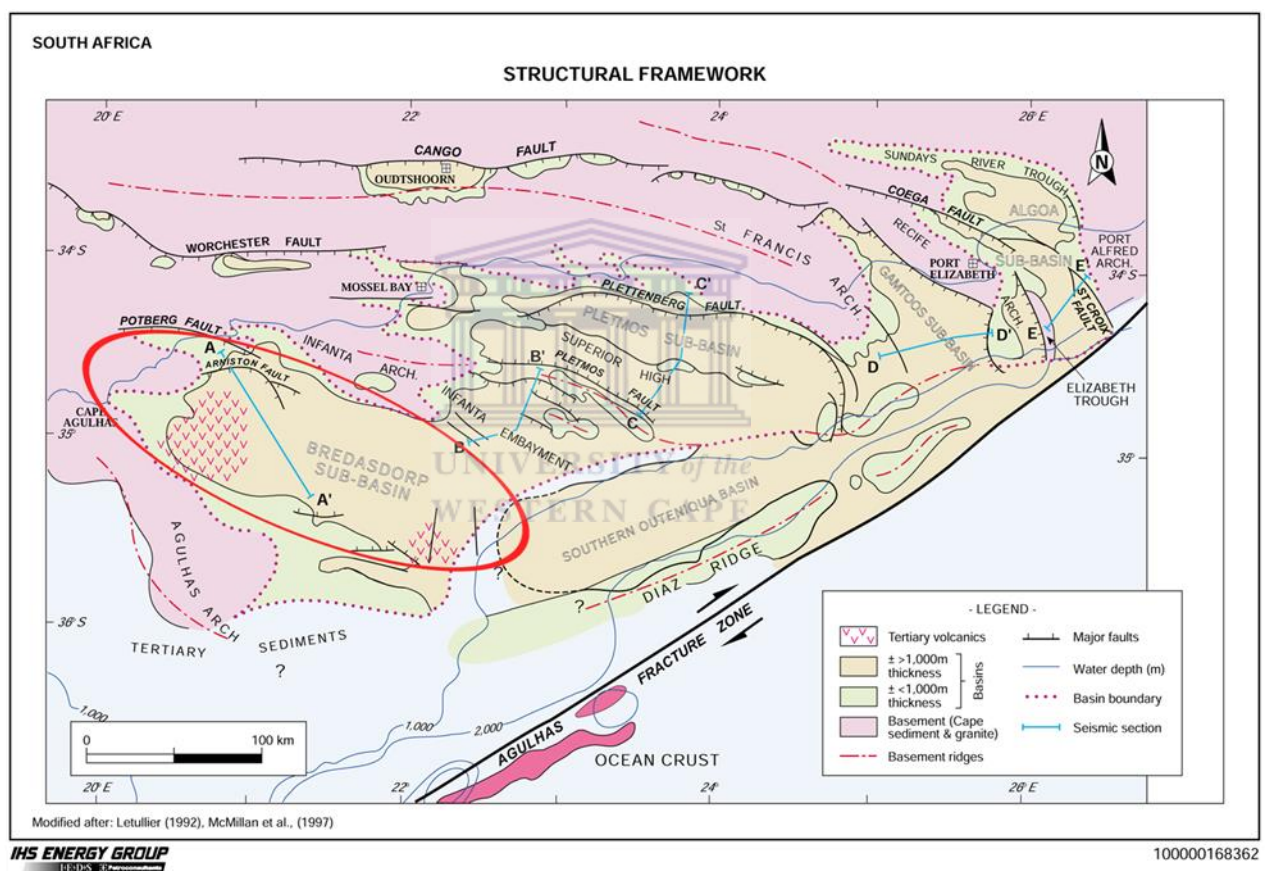


Figure 2.1.4: Structural Framework of the Bredasdorp Basin encircled in the map (After IHS basin monitor report, 2010).

2.2 Tectonic Setting of the Bredasdorp Basin

Break-up in the east dextral transtensional stresses gave rise to normal faulting in the northern Agulhas-Falkland Fracture Zone (McMillan et al., 1997). Faulting took place during the synrift stage between the Agulhas Arch and Infanta Arch, with normal faulting consequently resulting in graben and half-graben basins (Brown et al., 1995, McMillan et al., 1997). Continuous sedimentation from the basement to 1At1 until approximately 126 Ma from continental and marine sources. Rift faulting ceased during this period and post rift activity commenced (Brown et al., 1996). Horst structures contain condensed units and grabens contain expanded units at 1At1 thus evidence of differential subsidence is apparent in sedimentation (McMillan et al., 1997). Sediment supply into the Bredasdorp Basin was sourced from provenances in the north and northeast during rift phase comprising of orthoquartzites and slates from the Cape Supergroup and sandstones and shales from Karoo Supergroup (McMillan et al., 1997).

The unconformity that took place during 1At1 was triggered by upliftment of the arches and horst blocks (Brown et al., 1996) and subsequently terminated the active rift sedimentation (McMillan et al., 1997). This cycle essentially occurred in the central Bredasdorp Basin between ~126-117.5 Ma and this overlapped with late synrift activity of subsiding basins by rift faulting. This subsidence was rapid during 1At1 but started to diminish towards the end of the supercycle, between 1At1 to 5At1 (Brown et al., 1995, McMillan et al., 1997). Erosion subsequently occurred and carved submarine valleys as well as canyons into pre-1At1 units which provided channels for sediment supply into the deeper basin area from west, northwest and southwest (McMillan et al., 1997).

The Post-rift stage which took place between 117.5-112 Ma comprised of 6-12 cycles (Brown et al., 1995). Sequence 6At1 was produced by a high rate of regional subsidence. As subsidence and faulting slowed down the deposition of system tracts 8-12 occurred with sequence 7 which was removed by 8At1 erosion during 116-115Ma (Brown et al., 1995).

The sea level dropped during the Early Aptian (112 Ma) to mid-Albian (103 Ma) and this caused sediments to be eroded from high-stand shelf sandstones which were transported into the centre of the basin by turbidity currents from west to southwest (Turner et al., 2000). These sediments formed stacked, amalgamated channels and fan lobes of a coarsening upwards nature with reservoirs comprising of channel deposits defined by fining-upwards

(Turner et al., 2000) . The channels dominated the western to south-western area while the fan lobes are mostly in the eastern part of the basin (Turner et al., 2000). The channel of 13At1 sequence forms the site of oil accumulation while the 14At1 sequence contains basin floor-fan sandstones in the western part of the basin which contain oil bearing reservoirs (McMillan et al., 1997).

Erosion, minor warping and some uplift occurred during the Late Cenomanian, this phase is marked by 15At1 (McMillan et al., 1997). Shales with a rich content of plankton and other organic materials are found above 15At1 (McMillan et al., 1997). Propagation occurred between Turonian and Coniacian time. During the late Cretaceous a domal structure was formed in the south eastern region and these are said to be one of the few late structures forming in the basin (McMillan et al., 1997).

Sedimentation of high-stand shelf deposits containing glauconitic clays, biogenic clays with minor sands occurred during Tertiary era to present day. These sediments were acquired from the erosion of the Agulhas Arch flanks by uplift of the Late Cretaceous deposits (McMillan et al., 1997). The end of uplift of the arch and biogenic clay deposition in the southern part of the basin is marked by Early Miocene (McMillan et al., 1997).

Illustrated in Figure 2.2.1 below are the latter features constructed into a chronostratigraphic log. The figure displays the age interval of the basin from Pre-Mesozoic which forms the basement to Late Tertiary and major unconformity are marked accordingly. It also shows the main tectonic events sequentially which gave rise to the sediments deposited in their complementary environments from distal to proximal part of the basin.

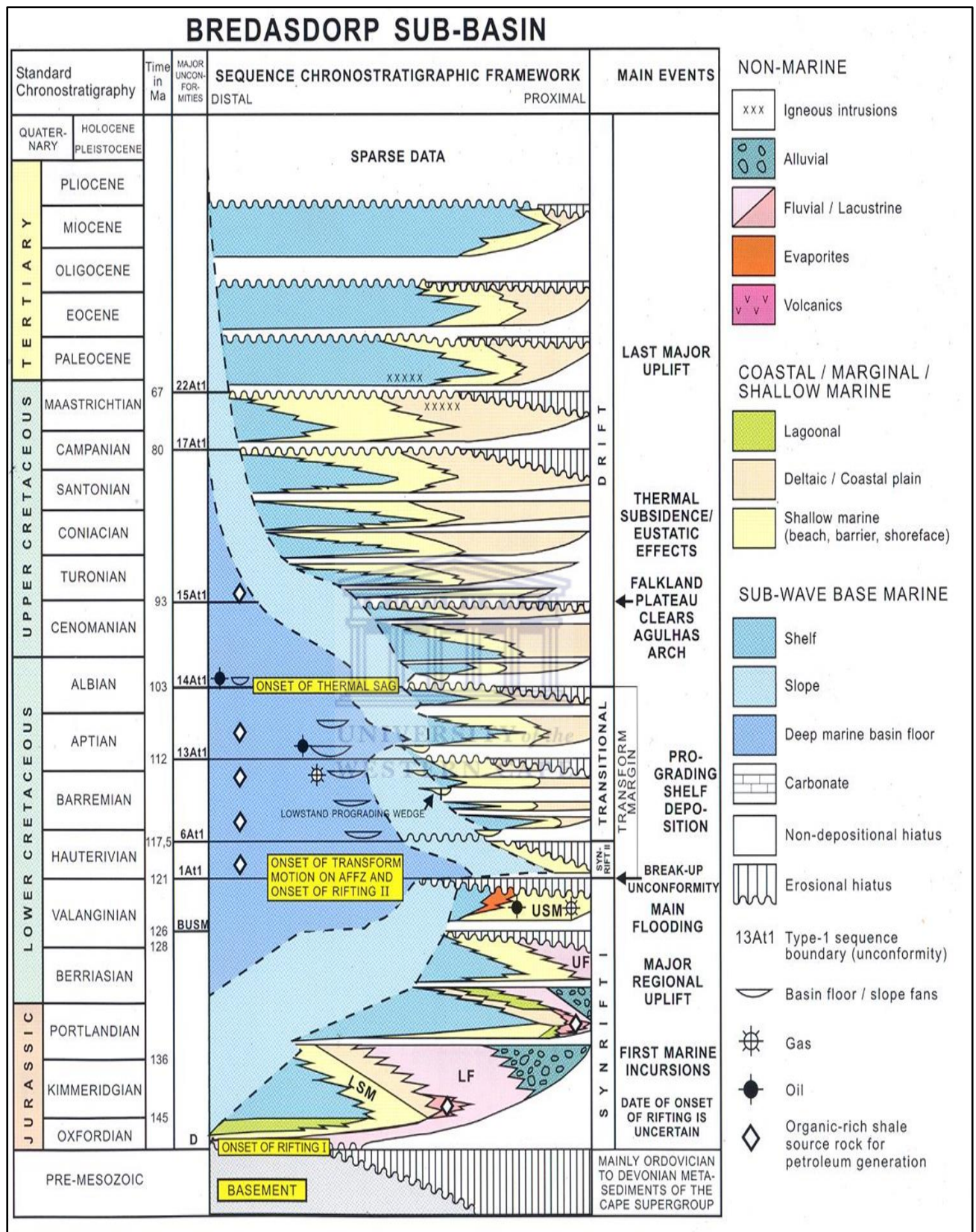


Figure 2.2.1: Chronostratigraphy of the Bredasdorp Basin (Petroleum Agency SA, 2003).

2.3 Structural development of the Bredasdorp Basin

The Bredasdorp Basin lies between two anticlinally dominated highs at Cape Infanta Agulhas. The Bredasdorp Basin is best described as a graben, a wide basement depression and with an asymmetric cross-section (Dingle et al., 1983).

The southern boundary of the Bredasdorp Basin formed subsequent to faulting and gently northward tilting flank of the Agulhas Arch which can be traced as a major subsurface feature to the southeast of Cape Agulhas. The upper division of the arch comprises of post-Paleozoic rocks such as Table Mountain Group quartzite and Bokkeveld shales over a granite core. The floor is relatively flat, however the western part which dips to the north-west direction such that the deepest parts of the basin lie close to its northern margin (Dingle et al., 1983).

The northern boundary of the basin, the basement descends rapidly through numerous small boundary faults from the Infanta Arch. The northern edge linearity is broken by minor deep grabens which form embayments onto the Infanta Arch. There are three horsts which project southeast and southwards into the basin, these horsts stand above the general level of the basin floor and are restricted by short curved faults.

The western part of the Bredasdorp Basin does not extend onshore, but breaks up into a small, narrow, northwest-southeast horsts graben, which extends to the coast, connecting Cape Agulhas and Cape Infanta (Dingle et al., 1983).

Rift Phase (Mid-Jurassic – Valagininian)

Extension driven subsidence and synrift basin fill characterized rift phase. Isostatic uplift on both flanks of the half graben resulted in erosional truncation of the late-rift sediments. Extreme marginal uplift and erosion of the northern flank removed the entire synrift sequence in places (Petroleum Agency SA, Brochure, 2004/5).

Early Drift Phase (Hauterivian – Early Barremian)

Prior onset of rapid thermal subsidence, continued uplift resulted in erosional truncation on the southern flank. Rapid subsidence and deposition of deep water sequence occurred within the graben (Petroleum Agency SA, Brochure, 2004/5).

Drift Phase (Barremian – Turonian)

Regional subsidence driven by thermal subsidence and sediment loading, with continuous minor displacement on the Arniston Fault. During early-Palaeozoic oil prone source in the half graben reached the main stage of generation. Minor subsidence continued until early Tertiary when alkaline affected southern flank, resulting in uplift and erosion (Petroleum Agency SA, Brochure, 2004/5).



UNIVERSITY *of the*
WESTERN CAPE

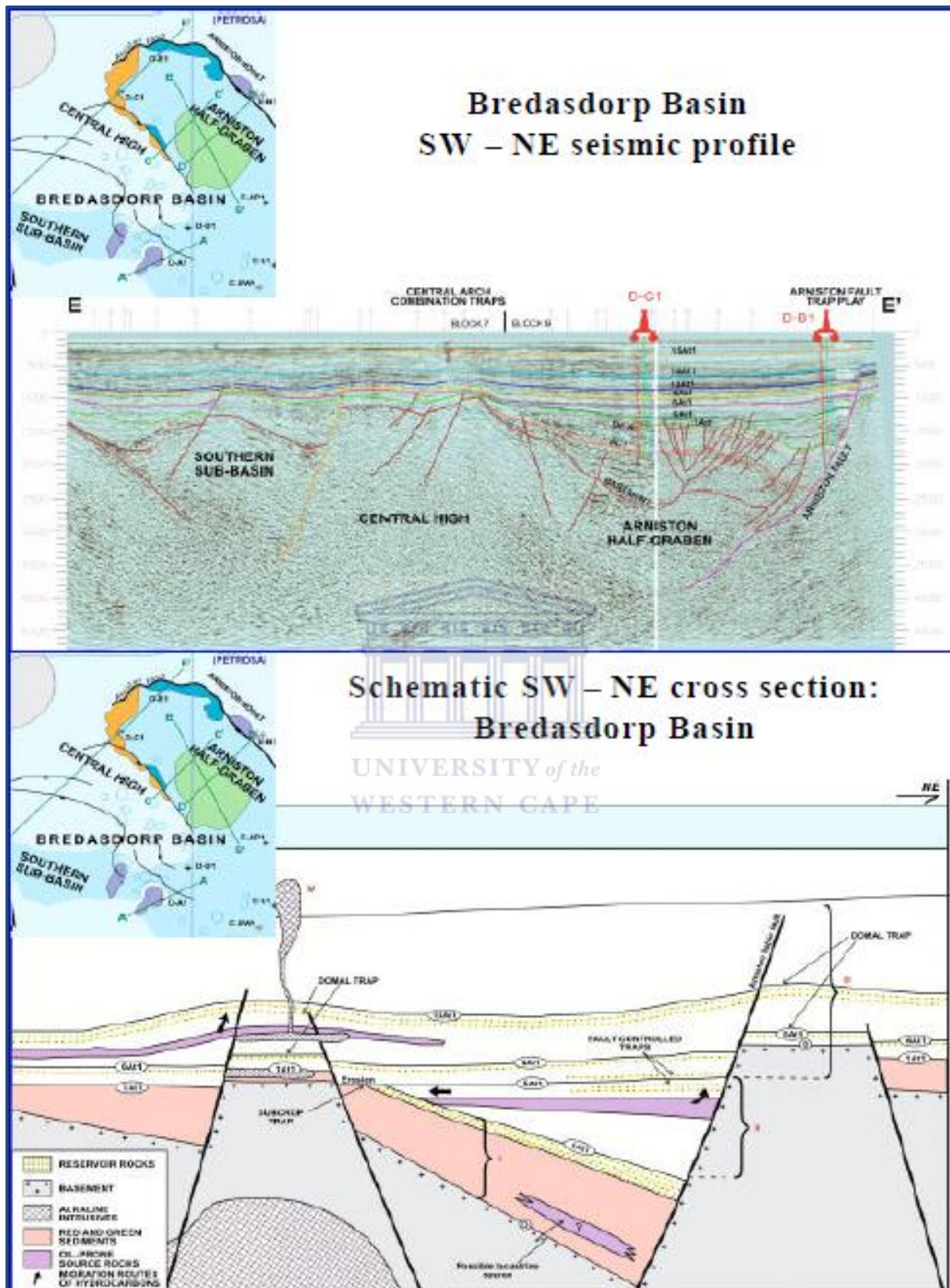


Figure 2.3.1: Seismic profile with identified sequence boundaries (Top); and schematic cross section (Bottom) (Modified from Broad, 2000).

2.4 Thermal Gradient history of the Bredasdorp Basin

The Bredasdorp Basin has a current thermal gradient of $35\text{--}49^{\circ}\text{C.km}^{-1}$, with a moderately high heat flow (Davies, 1997). Late Cretaceous had a reduced temperature gradient as a result of reduced heat flow and subsidence after rifting. The migration of Africa over a mantle plume during the Late Cretaceous to Early Tertiary experienced regional uplift which increased heat flow in the basin. Until approximately 80Ma, temperatures in the basin increased at a rate of $>3^{\circ}\text{C/Ma}$ (Davies, 1997). From ~80Ma to ~55Ma, sedimentation rates decreased consequently decreasing temperature to $<0.3^{\circ}\text{C/Ma}$. The temperature in Turonian source rocks for oil generation increased by $<10^{\circ}\text{C}$ during ~80Ma to ~55Ma (Davies, 1997). Temperatures increased by $\sim 20^{\circ}\text{C}$ during the migration of formation waters from the South-Outeniqua Basin into the Bredasdorp Basin post-Aptian sequences (Davies, 1997).

Maturation of the Aptian and older formations were affected by early burial, hotspot transit and hydrothermal event (Davies, 1997). The burial history of the Bredasdorp Basin is characterised by a thermal history due to variable heat flow rates all through the formation of the basin.

2.5 Source Rock Maturity

The geologic elements essential for oil and gas accumulation in adequate quantities to create a pool large enough to be worth producing are:

- ❖ Organic-rich source rocks
- ❖ Porous and permeable reservoir rocks to store the accumulated oil and gas
- ❖ A system of trap and seal to prevent the oil and gas from leaking away

A petroleum source rocks can be defined as a fine-grained sediment which in its natural setting has generated and released sufficient hydrocarbons to form commercial accumulation of oil and gas. For a source rock to be referred to as a petroleum source rock, it must have the quality and adequate amount of dispersed organic matter also referred to as kerogen and must also be matured. The quality of oil generated by any source rock depends on the ease of degradation of the constituent kerogen and the time-temperature relationship. Common petroleum source rocks are clays and carbonate muds (Broadet et al., 2006)

The Bredasdorp Basin is rich in gas and oil prone marine source rocks of the Kimmeridgian to Berriasian age. Known oil and gas source rocks of deep marine origin are situated in a

transitional rift-drift sequence and these are best developed in the Bredasdorp Basin. Sandstone reservoirs exist in both the synrift and drift segment; the reservoirs are shallow marine to fluvial where the drift sandstones are deep marine turbidite deposits. The trapping mechanisms within the synrifts are structural and as well as truncational. The drift shales provide the main seals (Broad et al., 2006).



UNIVERSITY *of the*
WESTERN CAPE

CHAPTER 3

Well Summary

3.1 Well D-D1

Borehole D-D1 is located in the western part of the Bredasdorp Basin, 10 km northeast of borehole D-A1 and 65km south-southeast of Cape Infanta.

The borehole was mainly designed to test for reservoired hydrocarbons within the near shore marine sequence beneath horizon 1At1 (refer to Figure 2.2.1) where approximately 570m of near shore sheet sandstones were identified.

Secondary targets included possible shelf and turbidite sandstone, hydrocarbon-bearing sandstones and conglomerates in the established meandering fluvial sequence.

The prognosed primary target compromises approximately 420m of interbedded conglomerates, pebbly sandstones and sandstones. Three cores cut towards the top of this interval indicate that the porosity-permeability (poroperm) qualities of these sandstones are very poor.

Sandstone development within the upper secondary target interval is not as good as expected and indications whilst drilling and from geophysical logs are that these sandstones are water-saturated.

A thick sequence (315m) of predominantly fair quality and wet gas-prone source rocks intersected.

The borehole was terminated at 3142m in continental argillaceous lithologies

No drill stem testing was recommended and the borehole was plugged and abandoned as a well with poor oil shows.

Table 3.1.1: Rig and operational data for well D-D1

Operator	SOEKOR (Pty) Ltd
Drilling contractor	Frontier
Rig	Actinia
Type	Semi submersible
Prospecting lease area	Southern offshore, Block D
Well classification	Wildcat
Trap classification	Structural
Location	10 km NE of borehole D-A1 and 65 km SSE of Infanta
Seismic reference	Line D-83-14, (Shortpoint 840)
Co-ordinates	Lat., 35° 01' 17, 46" S Long., 20° 59' 03, 68" E
Kelly bushing to sea-level	25 m
Water depth	77 m
Total depth (Driller)	3142 m
(Schlumberger)	3142 m
Spud date	1986-08-21
Drilling discontinued	1986-09-29
Rig moved off location	1986-05-10
Cores	1. 2850 m – 2862.2 m (100% recovery) 2. 2862.2 m – 2875.7 m (71.7% recovery) 3. 2875.7 m – 2880 m (65% recovery)
Drillstem test intervals	None performed
Final status	Well with poor oil shows

3.2 Well E-AP1

The E-AP1 borehole was drilled to test for hydrocarbon within stratigraphic closure at various levels in the E-AP1 prospect, located in the north-western section of the Bredasdorp Basin.

Delta-front sandstones within the upper part of the 7At1-to-8At1 (refer to Figure 2.2.1) sequence were to form the primary target. However, only rare, thin sandstone stringers occur within this interval.

Turbidite sandstones were identified in the 1At1-to-6At1, 6At1-to-7At1 and 13At1-to-13Amfs secondary target intervals. However, only rare, thin sandstone stringers occur within 1At1-to-6At1 sequence. Sandstones in the 13At1-to-13Amfs sequence are better developed than expected and appear to be fluvio-deltaic in origin.

Unexpected, good quality reservoir sandstone occurs in the 8At1-to-8Amfs intervals, but is predominantly water-saturated. Another unexpected thick sandstone sequence occurs immediately beneath the 13A type 1 unconformity, although it has poor reservoir properties.

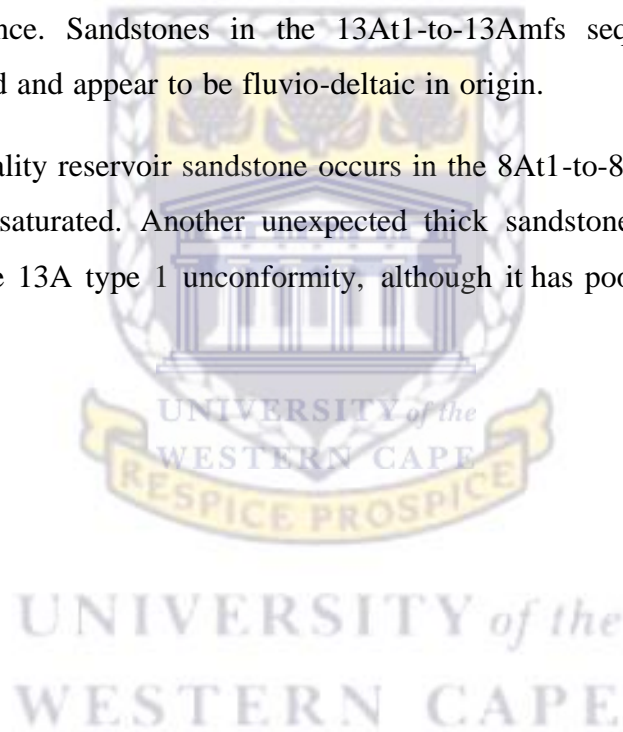


Table 3.1.2: Rig and operational data for well E-AP1

Operator	SOEKOR (Pty) Ltd, Gencor (15 percent participation)
Drilling contractor	Gisor
Rig	Actinia
Type	Semi-submersible, 6-caisson
Drilling depth rating	7620 m (25000 ft.)
Water depth rating	305 m (1000 ft.)
Prospecting lease area	Southern offshore, Block E
Well classification	Wildcat
Trap classification	Stratigraphic
Location	70 km SSW of Stilbaai
Seismic reference	Line E88-149, (Shotpoint 420)
Co-ordinates	Lat., 34° 58' 07, 65" S Long., 21° 10' 31, 12" E
Kelly bushing to sea-level	26 m
Water depth	84 m
Total depth (Driller) (Schlumberger)	3244 m 3244 m
Spud date	1989-02-15
Drilling discontinued	1989-03-19
Rig moved off location	1989-03-23
Cores	1. 2691m - 2704.5 m (96.3 % recovery)
Drillstem test intervals	None performed
Final status	Well with poor oil shows

CHAPTER 4

Methodology

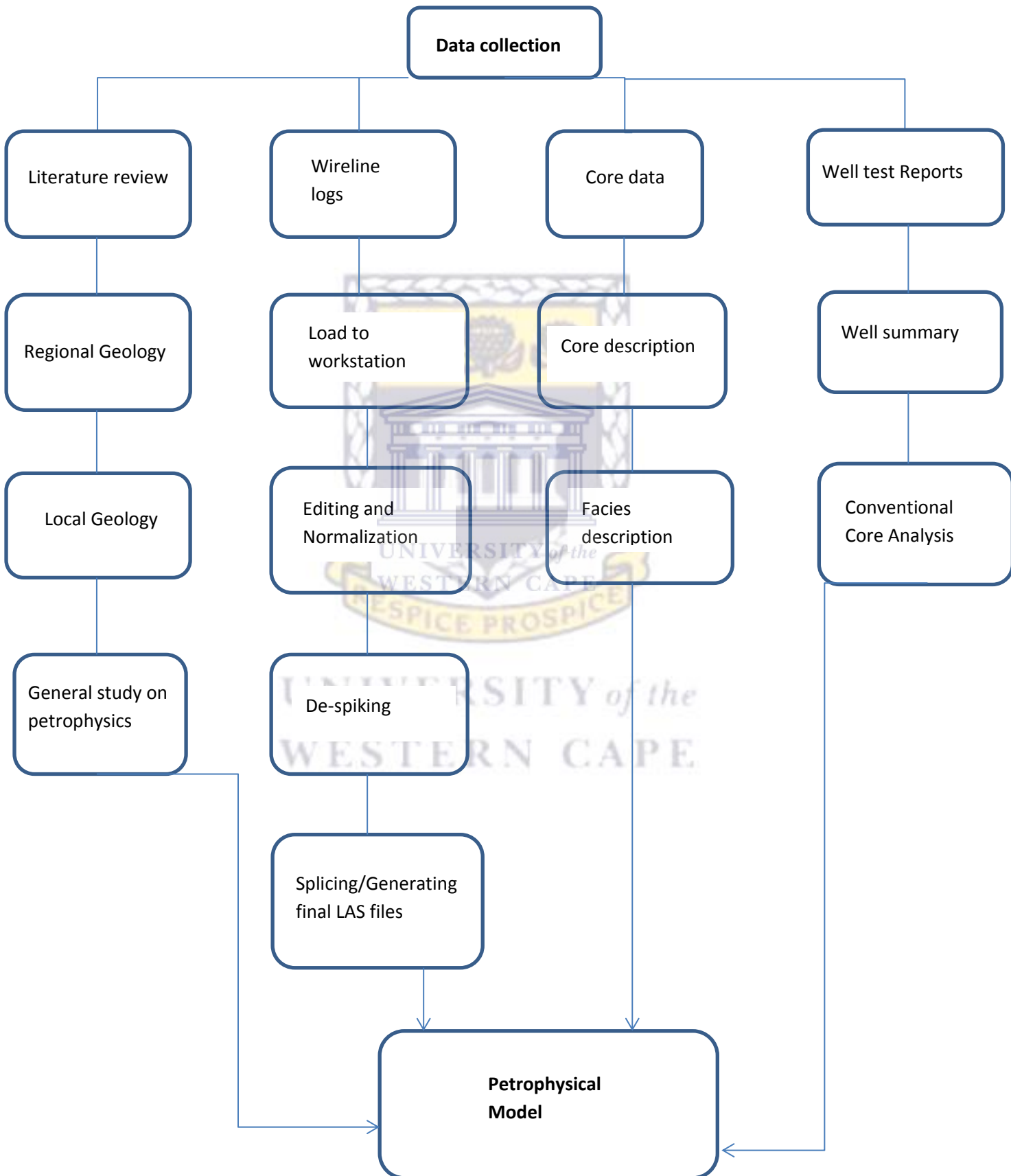


Figure 4.1: Flow chart of research methodology

4.2 Characteristics of selected wireline logs

Wireline logging tools are designed to handle specific logging limitations are being developed. These tools are the main source of accurate information on the depth as well as apparent and real thickness of beds. They yield information on the subsurface geology including formation boundaries, lithology, fluid content, and porosity. The wireline log suite obtained for this study includes gamma ray, resistivity and neutron density (Crain, 2000).

The geophysical wireline logs are the continuous records of geophysical parameters along a borehole. They are products of wireline logging which involves inserting a logging sensor or a combination of in the drill collar is lowered into the well bore by a survey cable and a continuous physical measurements (electrical, acoustical, nuclear, thermal and dimensional) are made (Crain, 2000).

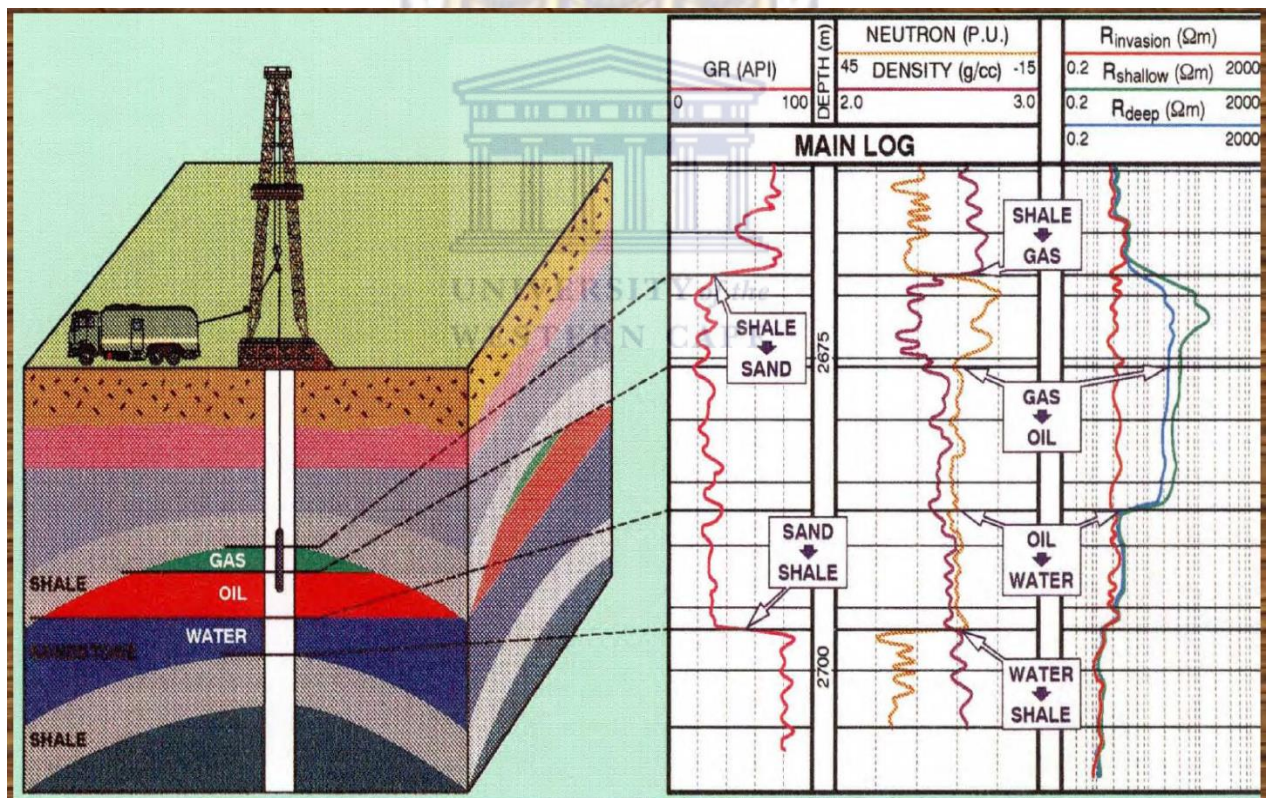


Figure 4.2: Graphical representation of logs and reference to subsurface and hydrocarbons (Van Ditzhuijzen et al, 2001).

4.2.1 Gamma ray log

Gamma ray log is a record of a formation's radioactivity. The radiation emanated from naturally-occurring uranium, thorium and potassium. The simple gamma ray log gives the radioactivity of the three elements combined, while the spectral gamma ray log shows the amount of each individual element contributing to this radioactivity. The geological significance of radiocativity lies in the distribution of these elements. Most rocks are radioactive to some degree, igneous and metamorphic rocks more so than sediments. However, amongst the sediments, shales have by far the strongest radiation. It is for this reason that the simple gamma ray log has been called the shale log while modern thinking shows that it is quite insufficient to equate gamma ray emission with shale occurrence (Rider, 2002).

Not all shales are radioactive, and all that is radioactive is not necessarily shale to derive shale volume. Qualitatively, in its simple form, it can be used to correlate, to suggest facies and sequences, and identify lithology (shaliness). The spectral gamma ray can be used additionally to derive a quantitative radioactive mineral volume and a more accurate shale volume. Qualitatively it can indicate dominant clay mineral types, give indications of depositional environment, indicate fractures and help to localize source rocks (Rider, 2002).

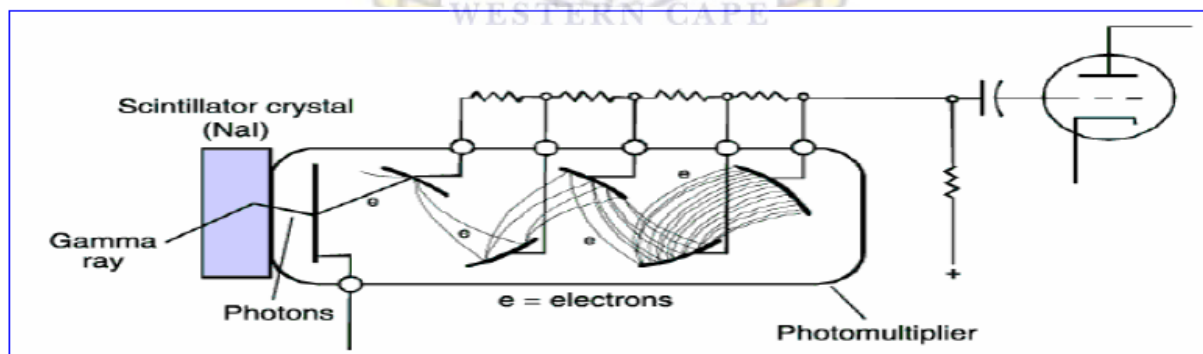


Figure 4.2.1: Gamma ray tool (Modified from Serra, 1984).

4.2.2 Sonic log

The sonic log provides a formation's interval transit time, designated delta-t. It is a measure of the formation's capacity to transmit sound waves. Geologically this varies with lithology and rock texture, notably porosity.

Quantitatively, the sonic log is used to evaluate porosity in liquid-filled holes. As an aid to seismic interpretation it can be used to give interval velocities and velocity profiles, and can be calibrated with the seismic section. Cross-multiplied with density, the sonic is used to produce the acoustic impedance log, the first step in making a synthetic seismic trace.

Qualitatively, for the geologist, the sonic log is sensitive to subtle textural variations in both sands and shales. It can help to identify lithology and may help to indicate source rocks, normal compaction and overpressure and to some extent fractures (Rider, 2002).

Modern sonic tools do not consist of just a single emitter and a single receiver, but of a number of both transmitters and receivers, the actual arrangement depending on the tool type. Modern designs allow unwanted borehole and tool effects to be largely eliminated and give a reliable measure of formation values even in quite poor borehole conditions (Rider, 2002).

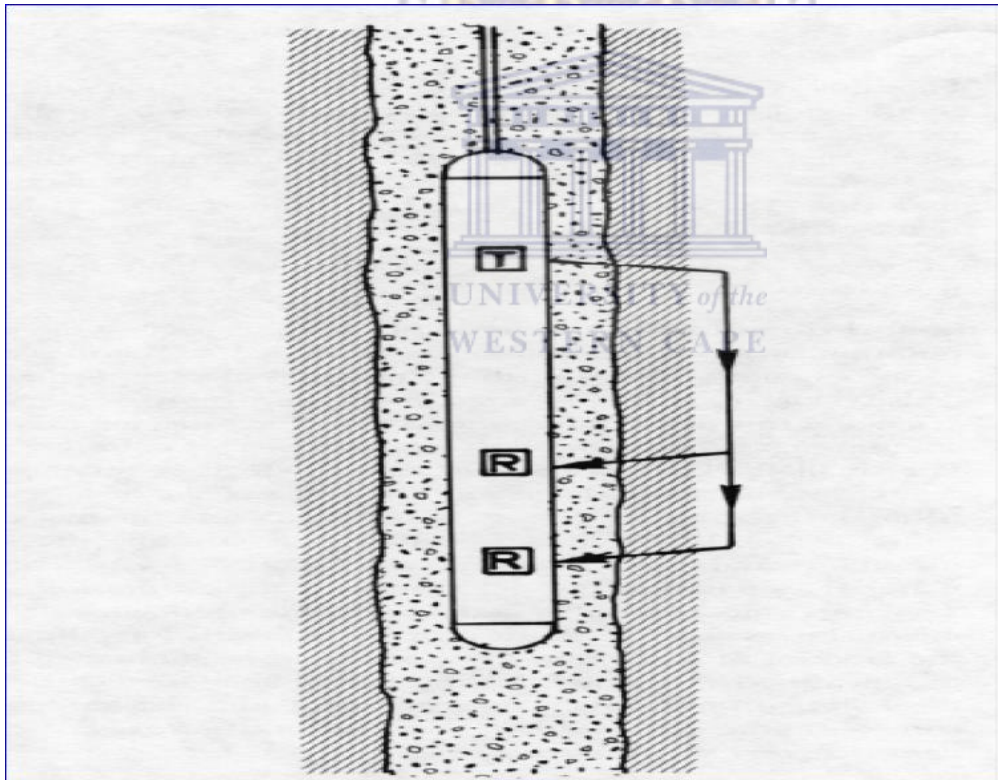


Figure 4.2.2: Sonic logging tool receiver (R) and transmitter (T) (Modified from http://www.spwla.org/library_info/glossary)

4.2.3 Electrode Resistivity

The second class resistivity measuring device is the electrode log. Electrodes in the borehole are connected to a power source and current flows from the electrodes through the borehole fluid into the formation and then to remote reference electrode. Typical examples of electrode resistivity tools include lateral logs, normal devices, microlaterolog, microlog, proximity log, and spherically focused logs (Rider, 2002).

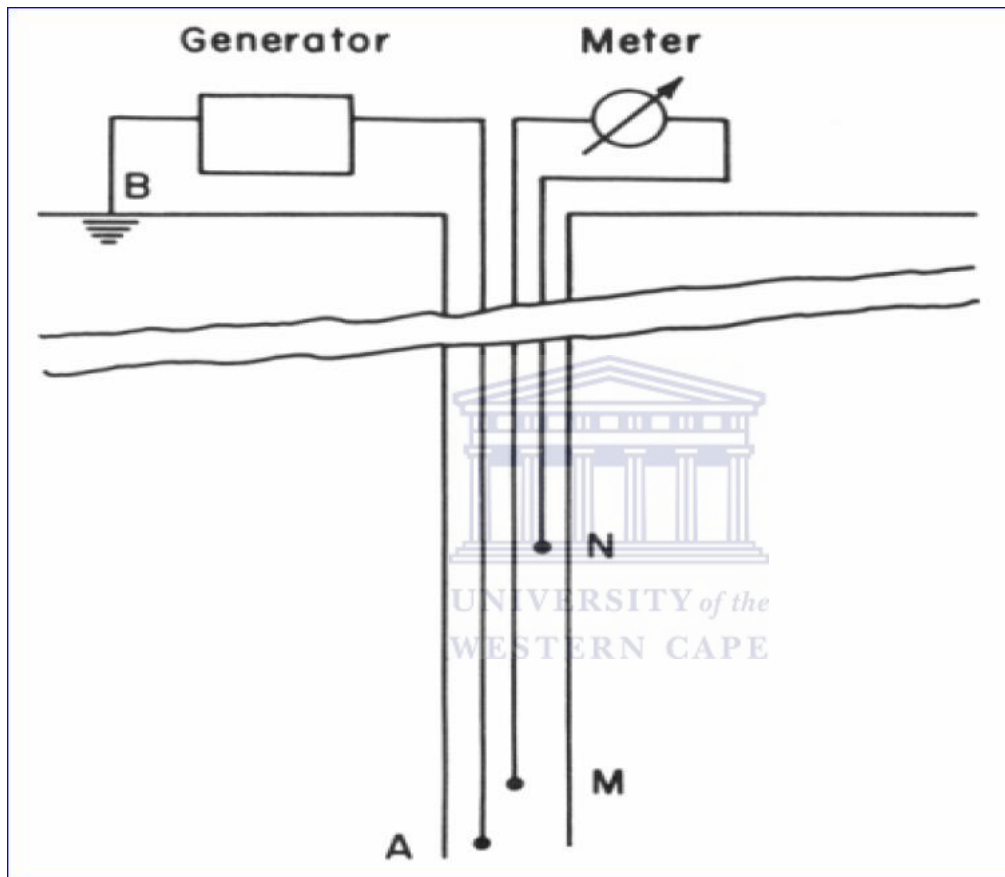


Figure 4.2.3: Normal device with electrodes A, M, N (Modified from Schlumberger, 2005).

4.2.4 Caliper

Caliper tools measure hole size and shape. The simple mechanical caliper measures the vertical profile of hole diameter. The more sophisticated borehole geometry tools record two simultaneous caliper and give an accurate borehole shape and orientation (Rider, 2002).

The mechanical caliper measures variations in borehole diameter with depth. The measurements are made by two articulated arms pushed against the borehole wall. The arms are linked to the cursor of the variable resistance. Lateral movement of the arms is translated

into movements of the cursor along the resistance, and hence variations in electrical output. The variations in output are translated into dipmeter variations after a simple calibration (Rider, 2002).

Frequently logging tools are automatically equipped with caliper, such as the micrologs and density-neutron tools where the caliper arm is used to apply the measuring head of the tool to the borehole wall. Sophisticated, dual caliper tools, such as the Borehole Geometry Tool of Schlumberger, also exist specifically for measuring hole size and volume. However, today, such information is generally taken from dipmeter tools, which acquire geometry data in order to derive dip. These tools have four pads fixed at right angles, opposite pairs being linked but independent of the perpendicular set. This, in terms of geometry, gives two independent calipers at 90°. The tool also contains gyroscopic orientation equipment so that the azimuth of the two calipers are permanently defined (Rider, 2002).

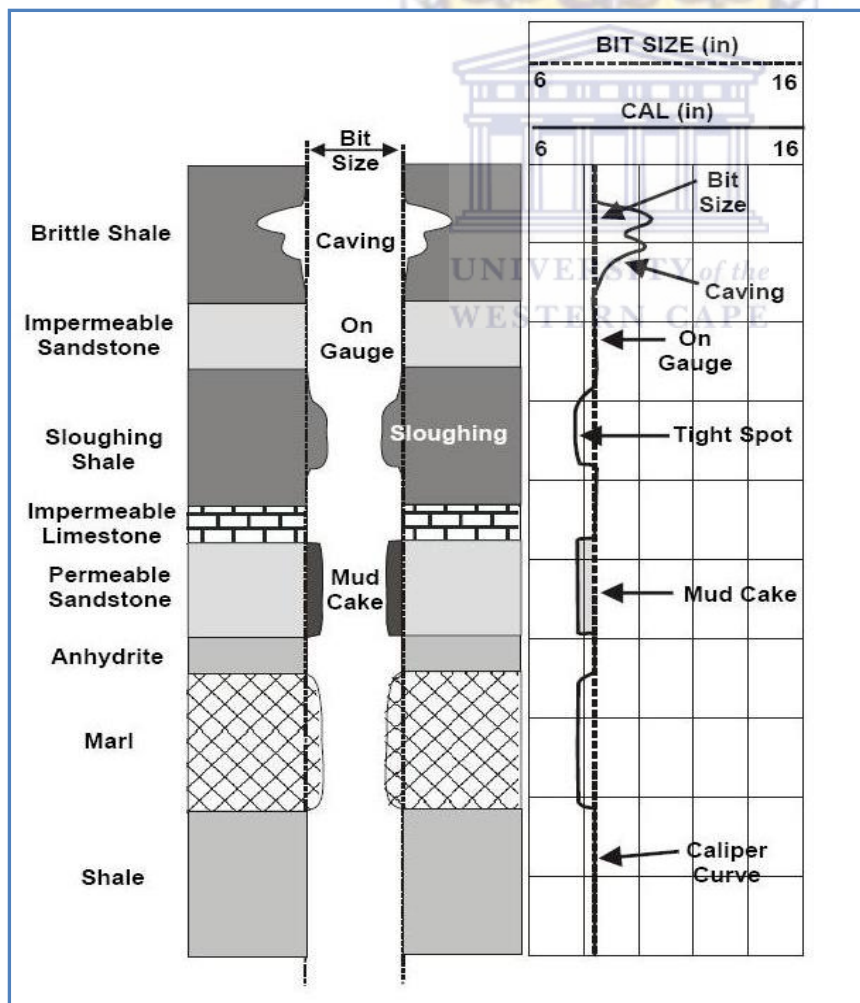


Figure 4.2.4: Typical caliper response to various lithologies (Western Atlas, 1992).

4.2.5 Neutron log

The neutron log provides a continuous record of a formation's reaction to fast neutron bombardment. It is quoted in terms of neutron porosity units, which are related to a formation's hydrogen index, an indication of its richness in hydrogen. Formations modify neutrons rapidly when they contain abundant nuclei, which in the geological context are supplied by H_2O . The log is therefore principally a measure of a formation's water content, be it bound water, water crystallization or free pore-water. This hydrogen richness is called the hydrogen index (HI) which is defined as the weight (%) hydrogen in the formation/wt (%) hydrogen in water, where $HI_{\text{water}} = 1$. However, the oilfield interest in water is as a pore fluid filler and porosity indicator so that the neutron log response is given directly in neutron porosity units. Neutron porosity is real porosity in clean limestones, but other lithologies require conversion factors (Rider, 2002).

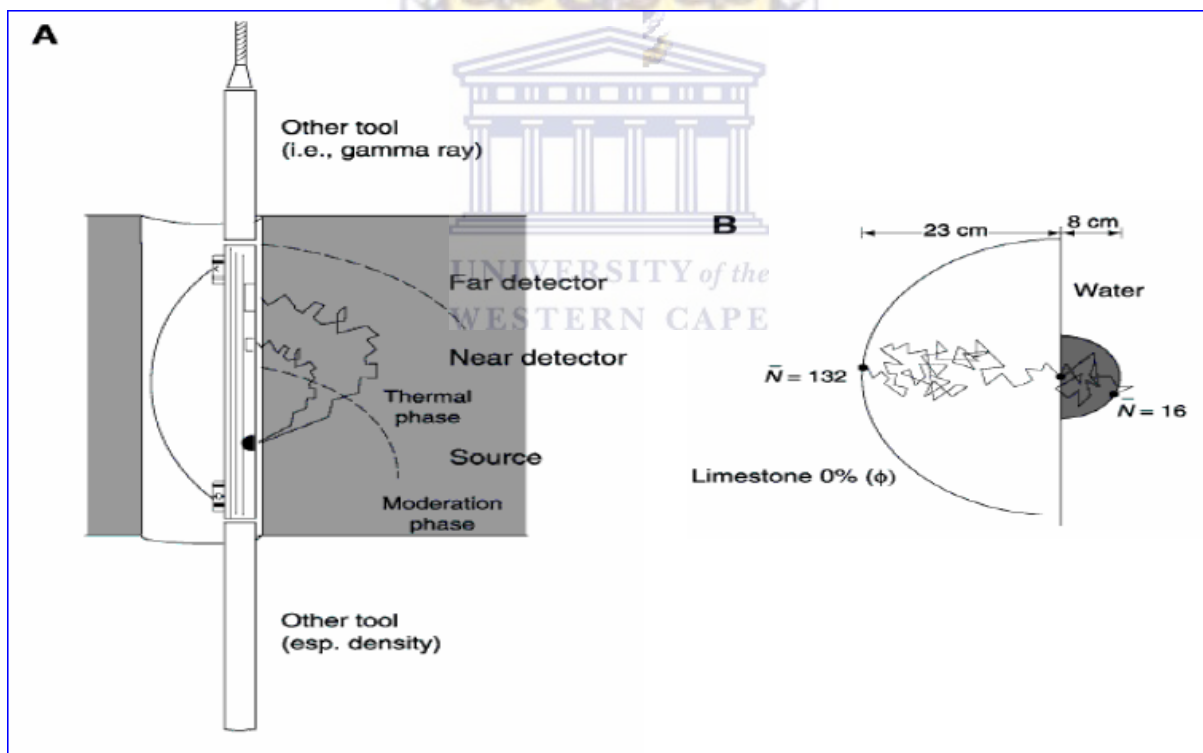


Figure 4.2.5: (A) Compensation neutron tool drawing, and (B) schematic trajectories of a neutron in a limestone with no porosity and pure water (Modified from Rider, 1996)

Neutron tools today generally consists of a fast neutron source and two detectors. The source bombards the formation with neutron and the detectors measure their loss of energy as they pass through it. Tool sources are mostly chemical, such as plutonium-beryllium (PuBe) or americium-beryllium (AmB), which produce fast neutrons with a peak energy level around

4Mev. These are most common. Infrequently, high energy neutrons at up to 14MeV are produced using accelerometers, in which the neutrons are created by bombarding a target with charged particles (Rider, 2006).

4.2.6 Density log

The density log is a continuous record of a formation's bulk density. This is the overall density of a rock including solid matrix and the fluid enclosed in the pores. Geologically, bulk density is a function of the density of the minerals forming a rock and volume of free fluids which it encloses. It is also used to calculate acoustic impedance. Qualitatively, it is a useful lithology indicator, can be used to identify certain minerals, can help to assess source rock organic matter content and may help to identify overpressure and fracture porosity (Rider, 2006). Formation bulk density (ρ_b) is a function of matrix density (ρ_{ma}), porosity and formation fluid density (ρ_f)

Density porosity is defined as:

$$\Phi_{den} = \frac{\rho_{ma} - \rho_b}{\rho_{ma} - \rho_f}$$

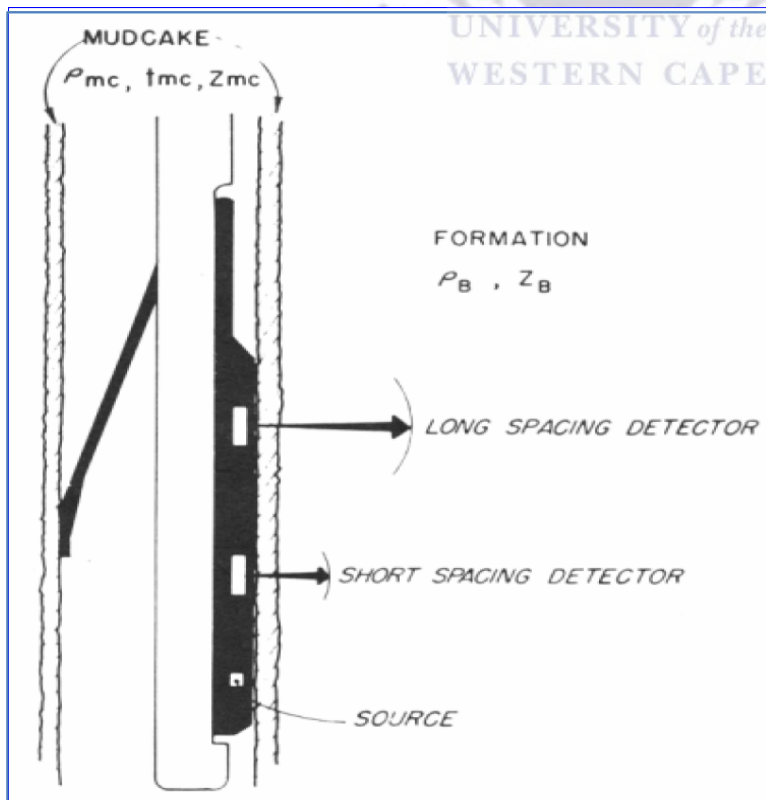


Figure 4.2.6: Compensation density sonde (modified after Wahl et al, 1964)

The standard density tools have a collimated gamma ray source and two detectors which allow compensation for borehole effects when their readings are combined and compared in calculated ratios. The near detector response is essentially due to borehole influences which, when removed from the far detector response enhance the formation effects. The most recent tools use efficient scintillations detectors which separate high and low gamma ray energy levels. This allows a better evaluation of borehole effects, so providing a more accurate density measurement (Rider, 2006).

4.2.7 Combination of Neutron-Density Log

Clean formations

Both the neutron and the density log are difficult to use for gross lithology identification. However, once combined, they become probably the best available indicator. Both the neutron log and the density log should be showing the same parameter – porosity. A neutron-log value of zero corresponds to a bulk density of 2.70g/cm^3 . A cross-plot of density-log values against neutron-log values will show a straight-line relationship a point on the line corresponding to a particular porosity (Rider, 2002).

Shale and shaly formations

Clean formations and the ideal reactions described above form the minority of cases. Shale is usually present. Pure shale is recognized on the neutron-density combination when the neutron value is high relative to the density value. It gives a large positive separation to the logs, the neutron well to the left of the density. If shale become diluted by matrix grains such as quartz or calcite with low hydrogen indexes, the neutron-log value decreases rapidly. Such a change is not seen so markedly on the density log since the matrix density of shales ($2.65\text{-}2.7\text{ g/cm}^3$) is similar to that of quartz and calcite ($2.65\text{-}2.71\text{ g/cm}^3$). On the log combination, the result is a decrease in the neutron-log value and a decrease in the log separation. The decreases continue until clean formation values are reached. Ideally, the changes from pure shale to clean formation are progressive on both logs as the volume of the shale decreases (Rider, 2002).

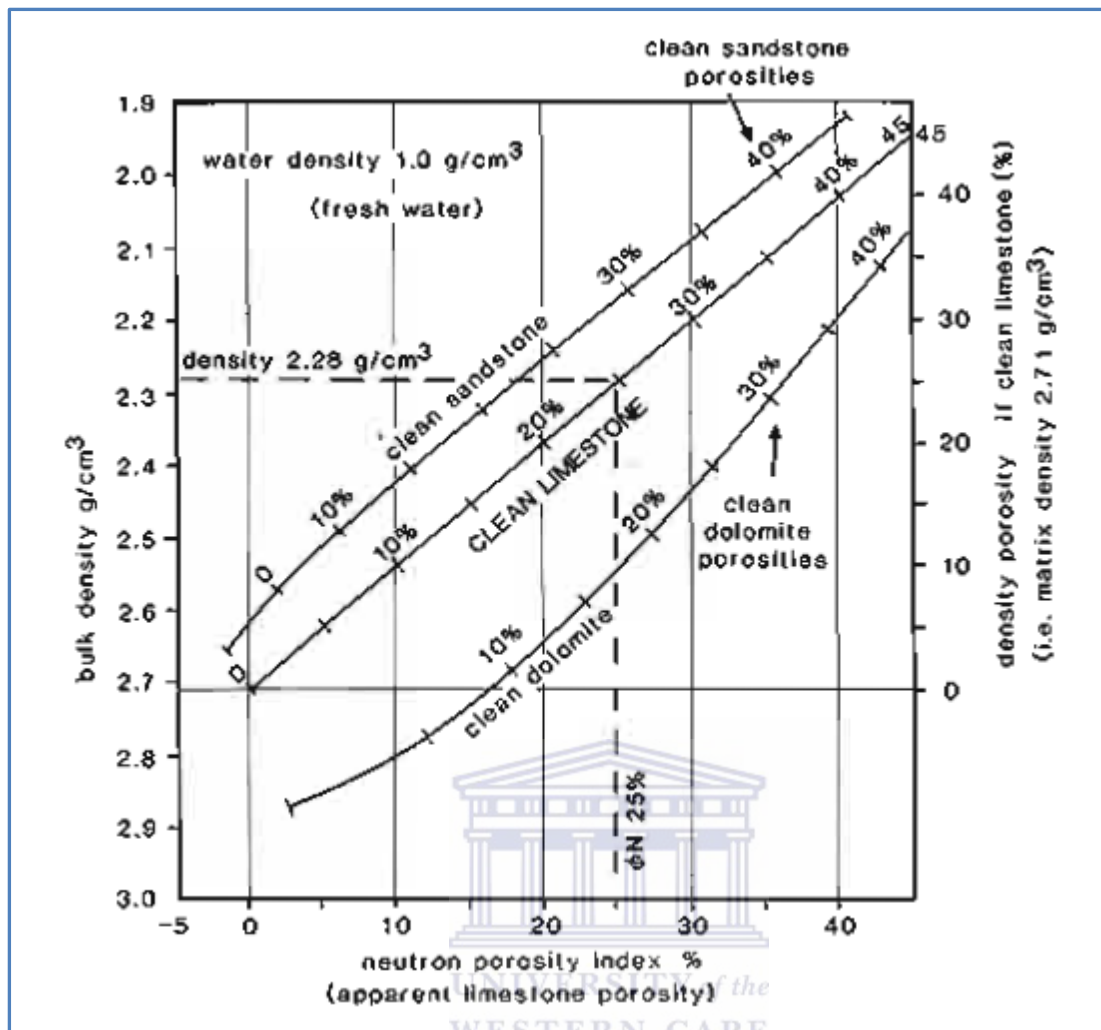


Figure 4.2.7: The density-neutron cross-plot (Modified from Schlumberger, 2005).

CHAPTER 5

Results

5.1 Conventional Core Analysis

Conventional cores are used as a reference to compare with the lithology interpreted from the wireline logs. Core data essentially complement log data. The conventional core analysis is the logging, sampling, and analysis of cores whereby a portion of each interval to be analysed is selected to represent the interval of interest. Cores also give proper understanding of wireline logs and provide an interpreter that recorded real subsurface lithologies. Detailed studies employed in core analysis can assist in the reduction of uncertainty associated with reservoir and seal distribution quality. The analysis was done for well D-D1 and E-AP1 of the cored intervals in order to determine the petrophysical properties of reservoir formations.

5.1.1 Well D-D1 Core analysis

Core #1 was cut from 2853.3m to 2868.2 m (100% recovery) and comprised of interbedded siltstones, pebbly sandstone and fine grained sandstones. Core #2 was cut from 2868.2 m to 2875.7 (71.1% recovery) and comprises of continuation of the above sandstone interval with minor interbedded pebbly sandstones. A third core (#3) was cut back-to-back with core # 2 from 2875.7 m to 2877m (65% recovery) and also comprise of tight fine grained sandstones with interbedded pebbly sandstones. Hydrocarbon fluorescence was noted in trace amounts throughout the entire core interval, particularly with core # 2. The routine core analysis measurements were provided in excel spreadsheet format and the measurements were available for horizontal plugs which includes; grain density, gas expansion, porosity, air and liquid permeabilities and fluid saturations. Porosity values obtained from core analysis results range from 0.9% to 6.6% while the maximum permeability measured was 0.65 millidarcies. Table 5.5.1 below displays the results obtained from the conventional core measurements of well D-D1.

Table 5.1.1: Well D-D1 routine core analysis results

Depth (m)	Permeability (KL)	Permeability (Ka)	Porosity (%)	Sw (%)	So (%)	Sg (%)	Grain Density (g/cc)
Core 1							
2853.3	0.02	0.041	0.015				2.7
2853.8	0.02	0.041	0.022				2.71
2854	0.01	0.028	0.013				2.71
2855.4	0.05	0.087	0.065				2.7
2855.9	0.05	0.088	0.07				2.7
2856.1	0.1	0.169	0.046	0.56	0.11	0.33	2.7
2856.3	0.07	0.118	0.033	0.71	0	0.29	2.69
2856.7	0.02	0.03	0.009				2.71
2857.2	0.02	0.038	0.015				2.7
2858.2	0.02	0.035	0.007				2.7
2859.7	0.02	0.031	0.012	0.84	0	0.16	2.72
2860.5	0.02	0.04	0.013				2.7
2862.5	0.02	0.042	0.028				2.71
2864.6	0.03	0.044	0.027				2.7
2866.1	0.01	0.025	0.009	0.86	0	0.14	2.73
2868.2	0.03	0.047	0.027				2.7
Core 2							
2868.2	0.02	0.04	0.034	0.98	0	0.02	2.69
2869.9	0.03	0.051	0.01	0.92	0	0.08	2.72
2869.5	0.03	0.051	0.021	0.86	0	0.14	2.68
2869.9	0.03	0.051	0.014	0.84	0	0.16	2.7
2870.2	0.65	0.952	0.066	0.54	0.1	0.36	2.69
2672.3	0.02	0.046	0.027	0.87	0	0.13	2.69
2873.5	0.02	0.046	0.026	0.89	0	0.11	2.67
2873.9	0.03	0.05	0.013	0.89	0	0.11	2.69
2874	0.02	0.041	0.008	0.93	0	0.07	
2875.7	0.07	0.127	0.059	0.95	0	0.05	2.69
Core 3							
2876.9	0.03	0.06	0.055	0.89	0	0.11	2.7
2877	0.03	0.21	0.024	0.89	0	0.11	2.7

5.1.2 Well E-AP1 Core analysis

Core #1 was cut from 2691 m to 2704.5m and comprises predominantly of siltstone with approximately 4m and sandstone in the top section. Although uniform bright fluorescence was recorded at the base of the sandstone, hydrocarbon shows were generally only poor to moderate. Core analysis results indicate mainly water-saturation, oil and gas-saturation values of up to 15% and 47% respectively were recorded. A maximum permeability of 16 mD was measured and porosities range between 4% and 14%. Table 5.1.2 below displays the results obtained from the conventional core measurements of well E-AP1.

Table 5.1.2: Well E-AP1 routine core analysis results

Depth (m)	Permeability (KL)	Permeability (Ka)	Porosity (%)	Sw (%)	So (%)	Sg (%)	Grain Density (g/cc)
2691.07	0.01	0.01	0.019				2.66
2691.31	0.07	0.11	0.01				2.66
2691.61	3.5	4.7	0.097				2.64
2691.8	1	1.5	0.094	0.68	0.14	0.18	2.66
2692.1	2.7	3.7	0.091				2.64
2692.37	2.9	4	0.109				2.67
2692.66	0.54	0.8	0.109	0.53	0	0.47	2.65
2692.9	0.02	0.3	0.01				2.66
2693.15	0.05	0.08	0.027				2.67
2693.37	2.9	4	0.11	0.61	0	0.39	2.66
2693.77	0.36	0.55	0.085				2.76
2694.02	16	20	0.136				2.64
2694.4	0.01	0.04	0.044	0.78	0	0.22	2.71
2694.4	0	0.01	0.039	0.78	0	0.22	2.71
2694.66	2.3	3.2	0.12				2.68
2694.91	6.5	8.4	0.13				2.64
2695.25	15.3	18.08	0.149	0.44	0.15	0.41	2.64
2695.25	13.8	16.3	0.142	0.44	0.15	0.41	2.64
2695.69	0.06	0.11	0.01				2.67
2695.92	0.01	0.01	0.01				2.66

5.2 Lithofacies Description

Core description is an essential starting point for reservoir characterization. This chapter presents the detailed description of the two wells D-D1 and E-AP1 as no core was cut for D- A1. An interpretation of facies is derived based on the lithology and other specific characteristics of the rock type. Graphic descriptions of core at various depth and scales are done in order to integrate with logs.

Lithofacies were described on the basis of lithology, sedimentary structures, facies distribution, grain size variation, sorting of grains, fossils and bioturbation. This description helps to find a relation between log and core data.






The list below shows the various lithofacies defined by core examination for both well D-D1 and E-AP1.

- Facies A1: Poorly sorted carbonaceous sandstone facies
- Facies A2: Massive clean sandstone facies
- Facies A3: Dark grey claystone facies
- Facies A4: Conglomerate with subrounded grains
- Facies A5: Well sorted siltstone



UNIVERSITY of the
WESTERN CAPE

Table 5.2: Lithofacies descriptions and classification of reservoir facies

Facies	Description	Reservoir quality	Facies photo
A1	Carbonaceous sandstone is poorly sorted, tight, very fine to coarse grained. Occasional water escape structures, such as sand dykes.	Fair	
A2	Massive clean sandstone is well sorted nature and generally medium grain size. Water escape and loading structures also occur.	Very Good	
A3	A dark grey glauconitic claystone forms this facies. It shows poor bedding and is intensely slumped.	Non Reservoir	
A4	Tight, coarse grained conglomerate with subrounded grains.	Good	
A5	Siltstone is well sorted and tight. Moderately to fine grains with loading structures.	Poor	

5.2.1 Well D-D1 Lithofacies

In well D-D1 five lithofacies were identified. These were facies type A1, A2, A3, A4 and A5 as shown in figure 5.2.1 below in track 3. In terms of reservoir quality, lithotype A2 represents a very good petrophysical reservoir with good permeability and porosity values, followed by lithotype A4. Facies A5 has poor reservoir quality while facies A3 is a non reservoir.

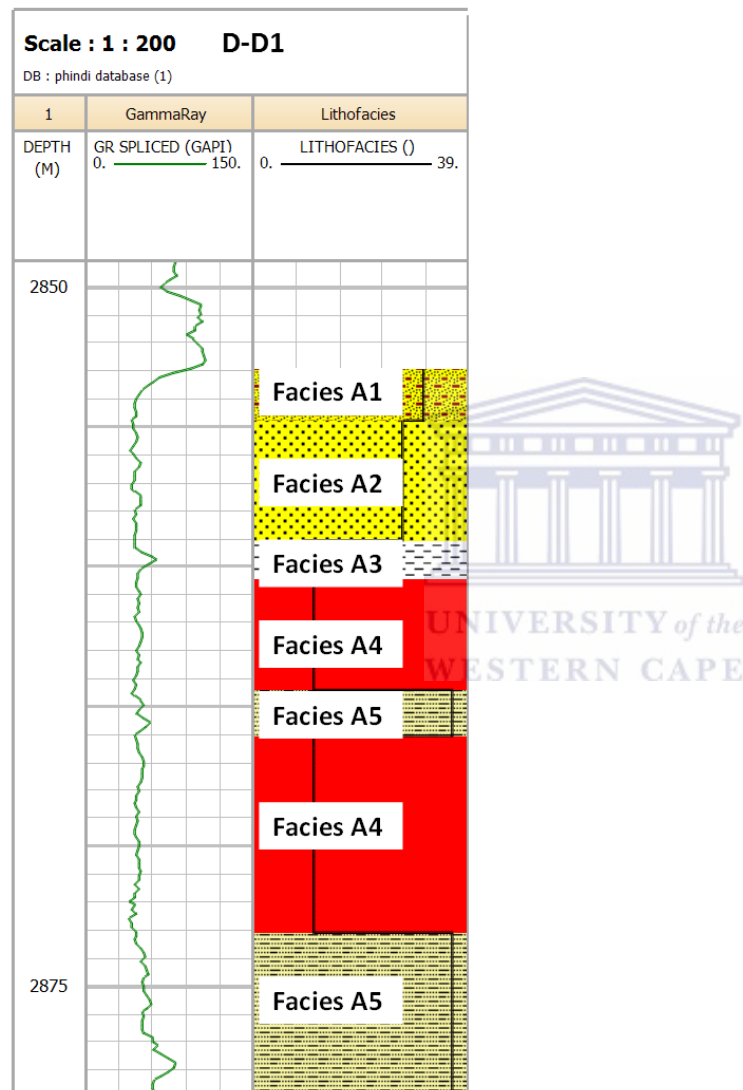


Figure 5.2.1: Well D-D1 with core facies shown in track 3.

5.2.2 Well E-AP1 Lithofacies

In well E-AP1 three lithofacies were identified. These were facies type A1, A2 and A3 as shown in figure 5.2.2 below in track 3. In terms of reservoir quality lithotype A2 represents a very good petrophysical reservoir with good permeability and porosity values, facies A1 shows moderate quality, whilst facies A3 is considered a non reservoir.

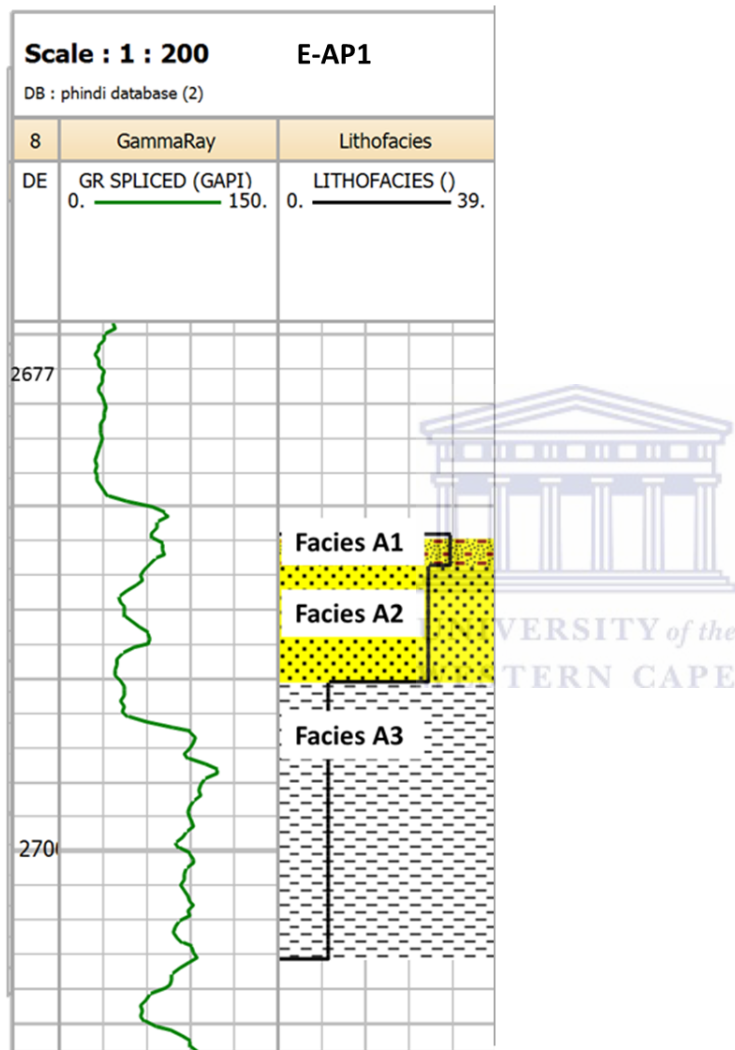


Figure 5.2.2: Well E-AP1 with core facies shown in track 3.

5.3 Grain Density

As used in log and core analysis grain density refers to all the solid material in the rock excluding the pore spaces containing fluids. Since, when interpreting the measurements, no effort is made to distinguish grains from other solid material. The grain density of core samples is calculated from the measured dry weight divided by the grain volume. In logs, grain density is calculated from density log, using an estimate of porosity and knowledge of the fluid content. The value of the grain density depends on the density and proportion of the individual mineral components. Table 5.3 below shows the matrix densities of some common lithologies.

Table 5.3: Matrix density of common lithology

Lithology	Matrix value (g/cm ³)
Clay minerals	2.02 – 2.81
Chlorite	2.81
Illite	2.61
Kaolinite	2.55
Smectite	2.02
Coal	1.19
Halite	2.04
Sandstone (quartz)	2.65
Limestones	2.71
Dolomites	2.85
Orthoclase	2.57
Plagioclase	2.59
Anhydrite	2.98
Siderite	3.88
Pyrite	4.99

(Schlumberger, 2003)

5.3.1 Well D-D1 Grain Density

The grain density of well D-D1 ranges from 2.67 to 2.73 g/cc with an average value of 2.7 g/cc and a standard deviation of 0.0124 g/cc as shown in the figure 5.3.1 below.

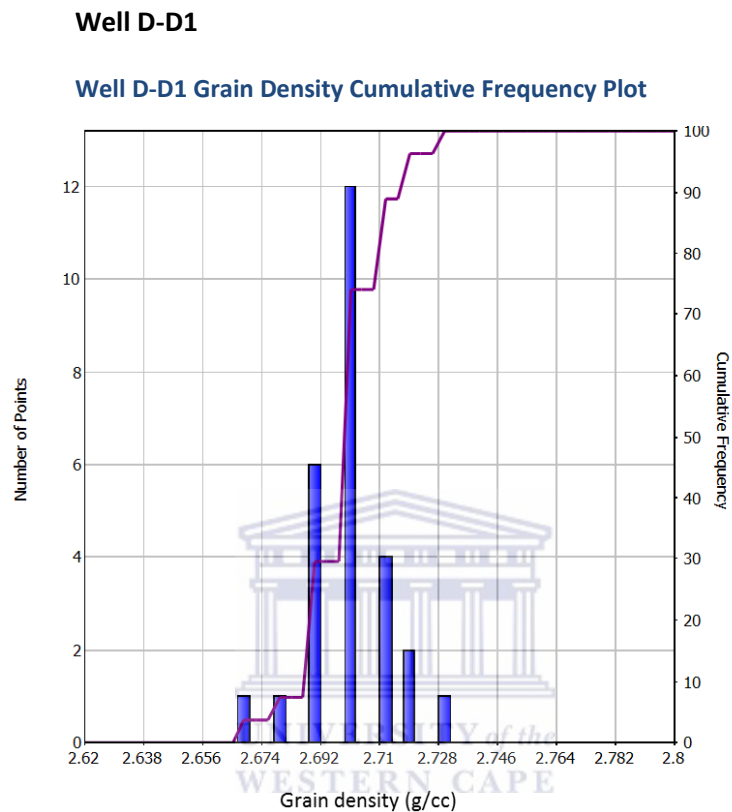


Figure 5.3.1: Histogram of well D-D1 core grain density

There is not much variation in well D-D1 as the grain density varies between 2.67 to 2.73 g/cc, which suggests the presence of clay minerals as seen from Table 5.3 and this is consistent for the entire core. This suggests that sandstone in this well had very high content of clay minerals. The high grain density value of 2.71 g/cc at 2853.7 m depth, suggests the presence of very thin interval of calcite.

5.3.2 Well E-AP1 Grain Density

The grain density of well E-AP1 ranges from 2.64 to 2.76 g/cc with an average value of 2.6 g/cc and a standard deviation of 0.02956 as shown in the figure 5.3.2 below.

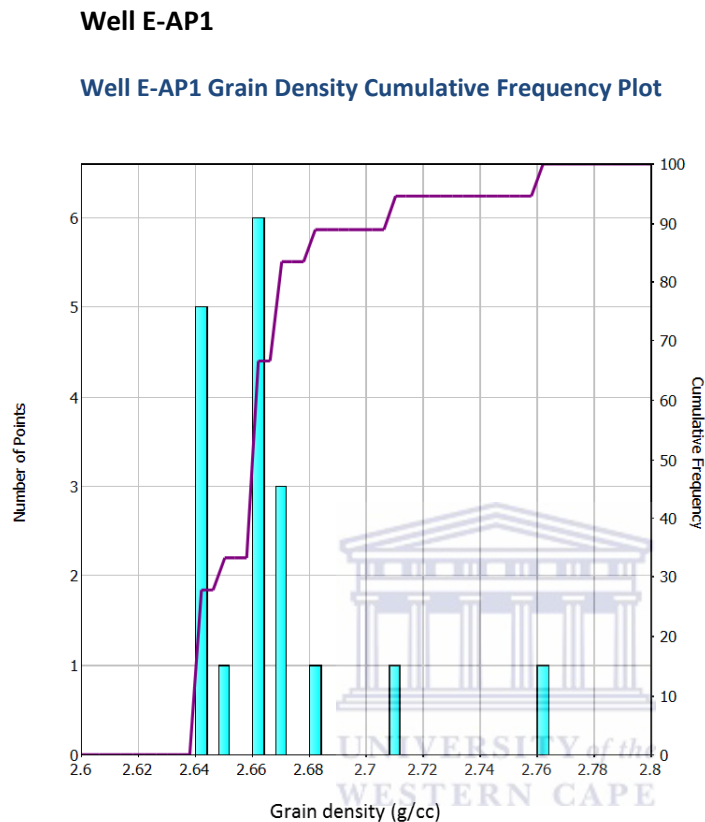


Figure 5.3.2: Histogram of well E-AP1 core grain density

A grain density value of 2.65 g/cc at 2692.66m depth suggests a clean sandstone (quartz) as seen from the core results. The grain density value of 2.71 g/cc at 2853.7m depth, suggests the presence of very thin interval of calcite. The grain density value from 2691.07m to 2692.10m depth range between 2.64 - 2.66 g/cc, suggesting the presence of clay minerals, and this is also observed between the measured depth of 2694.9m to 2695.25m. The high grain density observed in E-AP1 could be due iron rich clay (Chloride).

5.3.3 Comparison of grain density distribution for wells

The grain density value for all wells with core analysis results showed a range of 2.64 to 2.76 g/cc with a mean value of 2.68 g/cc and a standard deviation of 0.027 g/cc. Well D-D1 showed the highest mean density value of 2.7 g/cc whilst E-AP1 had a density value of 2.6 g/cc. The presence of calcite for both wells was observe to be significantly small.

All well

Grain Density Cumulative Frequency Plot

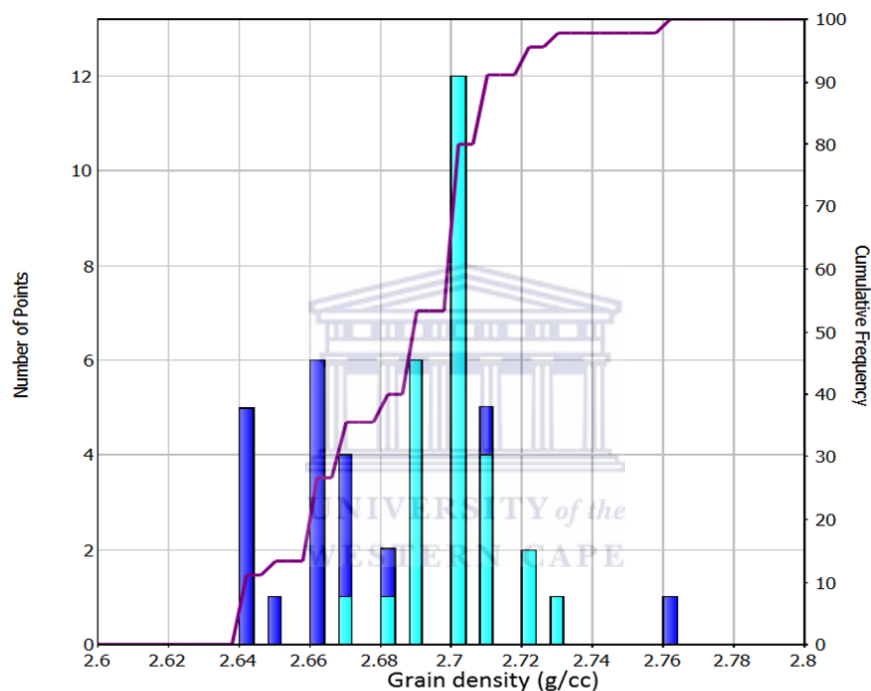


Figure 5.3.3: Grain density histogram plot for well D-D1 and E-AP1

5.4 Core Porosity

The determination of porosity can be generally considered to be the least complex stage in petrophysical interpretation. However, this stage is extremely important, since it defines the quantity of hydrocarbons present in the reservoir. Porosity is said to be the percentage of the volume of the rock that is not occupied by the solid framework of the reservoir, and this is used to determine the amount of water or other fluids that a rock may contain. Subsequent to the cleaning of core plug and removing fluids porosity is determined from the grain volume and the bulk volume of the sample. Various types of porosity are estimated using different techniques. Porosities for petroleum reservoirs ranges from approximately 5% to 45%.

Then initial (pre-diagenesis) porosity is affected by three major micro-structural parameters. These are grain size, grain packing, particle shape, and the distribution of grain sizes. However, the initial porosity is rarely found in real rocks, as these have subsequently been affected by secondary controls on porosity such as compaction and geochemical diagenetic processes. There are a number of factors that used to determine the magnitude of porosity in sediments, and these include grain sorting, degree of cementation, amount of compaction and methods of grain packing (Djebbar and Donaldson, 1999). When grains vary in size and are mixed together, sorting is said to be poor as a result porosity will be reduced. If all grains are of the same size, sorting is regarded as good and thus porosity will be increased. Porosity is also controlled by a huge range of secondary processes that result in compaction and dilatation. These can be categorized into mechanical processes, such as stress compaction, plastic deformation, brittle deformation, fracture evolution and geochemical processes such as dissolution and precipitation upon mineralogical changes (Djebbar and Donaldson, 1999).

In recently deposited, unconsolidated sediments, such as those that are found on the floor of a lake, porosity may be high (values up to 80%). However, more common materials, such as loose sands can have porosities as high as 45% that are either extremely unstable or stabilized by cements. Sandstones generally lie in the range 5% to 20%. Table 5.4 below gives approximate ranges of porosities for some lithologies (Djebbar and Donaldson, 1999).

Table 5.4: The range of porosity values for rocks.

Lithology	Porosity ranges (%)
Unconsolidated sands	35-45
‘Reservoir’ sandstones	15-35
Compact sandstones	5-15
Shales	0-45
Clays	0-45
Massive limestones	5-10
Vuggy limestones	10-40
Dolomite	10-30
Chalk	5-40
Granite	<1
Basalt	<0.5
Gneiss	<2
Conglomerate	1-15

5.4.1 Well D-D1 Porosity

The core porosity values for well D-D1 range from 1.2 % to 10.1 % at cored intervals. The low porosity intervals observed are as a result of siltstone and claystone interbedded lamina. Low porosity values that are associated with claystone are observed from 2859.2-2860.5m depth (Figure 5.4.1a), whilst low porosity values that are as a result of siltstone are observed at various depths which include 2864.4 – 28659m and 2873 - 2879.4m depth (Figure 5.4.1 b). The high porosity intervals were associated massive sandstone and conglomerate. Moderate porosity intervals for carbonaceous and massive sandstone were observed from 2852.9 - 2859.2 m depth. High porosity values associated with conglomerate were observed between 2860.5 -2859m (Figure 5.4.1a) and 2866.2 - 2873m depth (Figure 5.4.1 b).

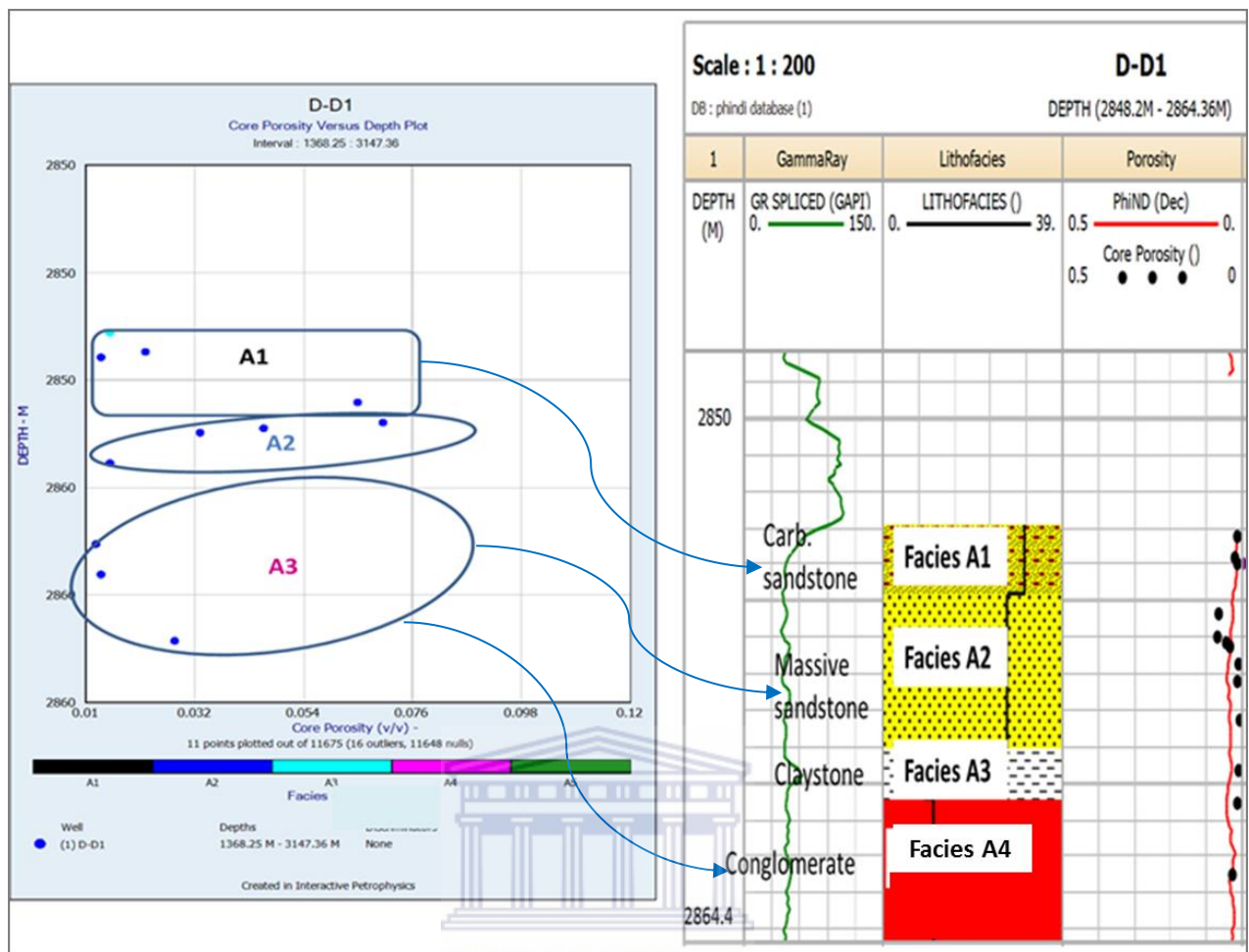


Figure 5.4.1a: Well D-D1 Porosity versus depth plot.

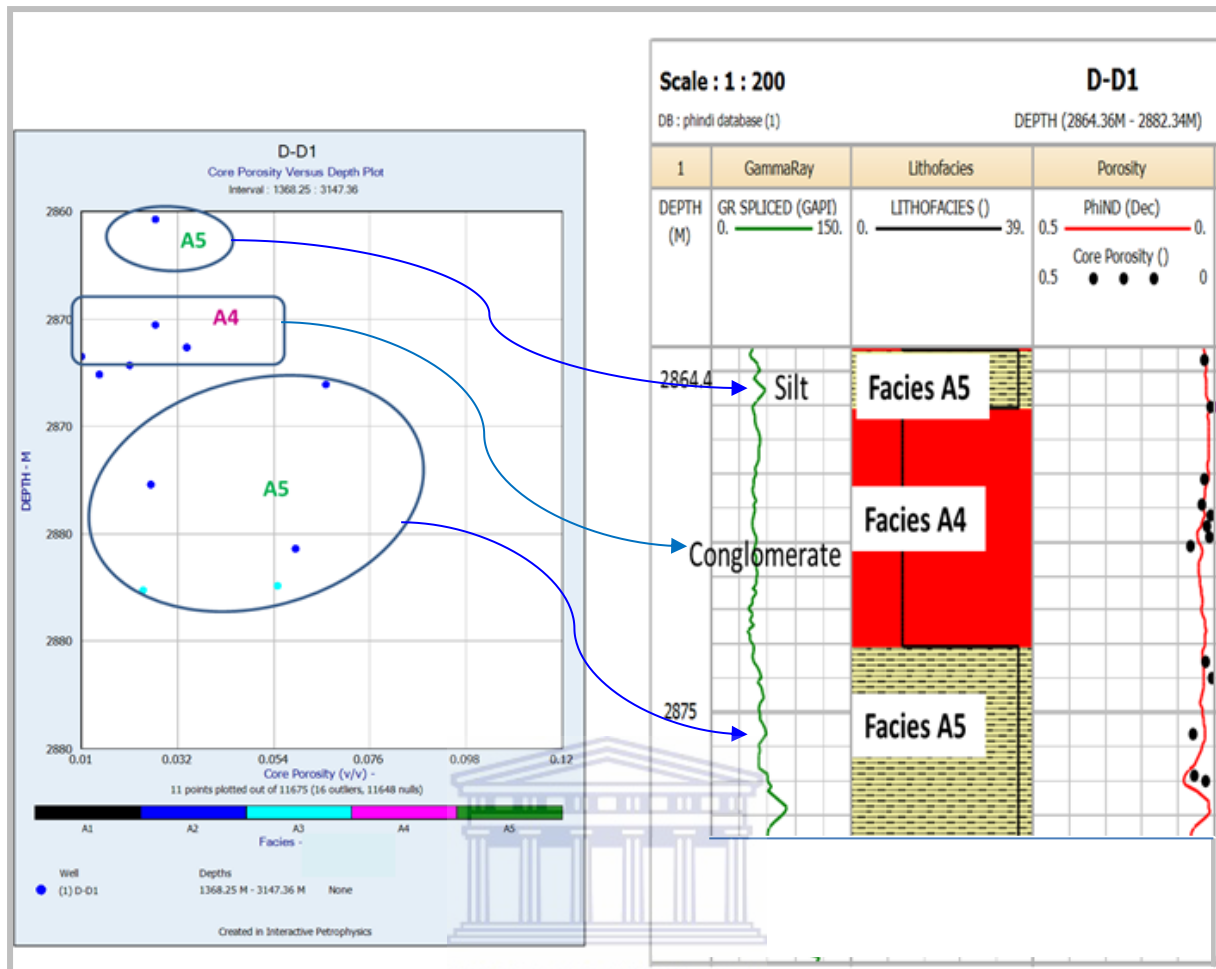


Figure 5.4.1b: Well D-D1 Porosity versus depth plot

Well D-D1

Core Porosity Histogram

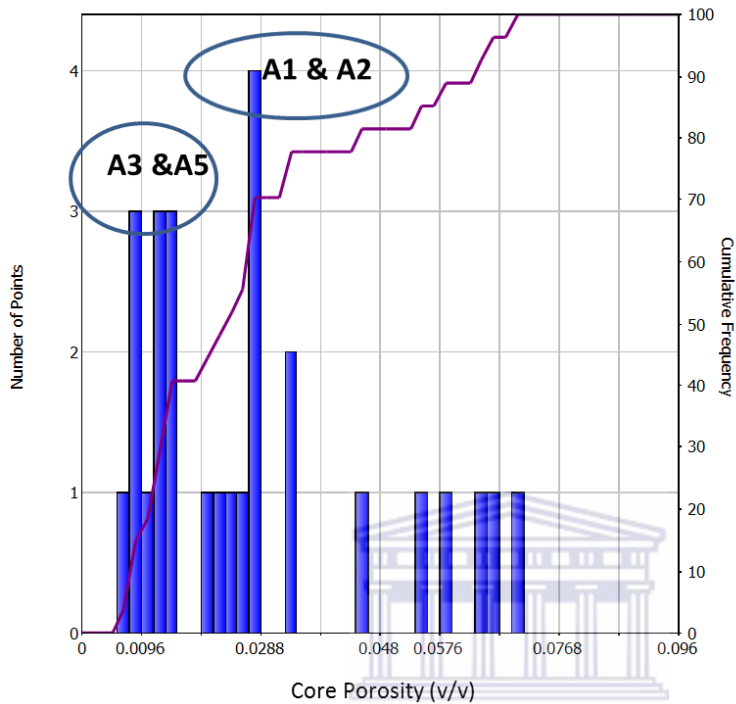


Figure 5.4.1.1: Well D-D1 Core Porosity histogram and plot against

The differences in variations of porosity in the zones could be associated to the type of facies present. The interval porosity values that are less than 6% is associated with facies type A3 and A5 (claystone and siltstone respectively). The interval values that are more than 18% may be attributed to sandstone (facies type A1).

5.4.2 Well E-AP1 Porosity

The core porosity values for well E-AP1 range from 1.8 % to 16.2 % at cored intervals. The low porosity intervals observed are associated with claystone interbedded lamina. Low porosity values that are associated with claystone are observed from 2695.0 – 2703.1m depth (Figure 5.4.2). Porosity values associated with carbonaceous sandstone appeared high while those of massive sandstone appeared to be slightly higher than the latter (Figure 5.4.2). These high porosity intervals are observed from 2690.8m – 2695m depth.

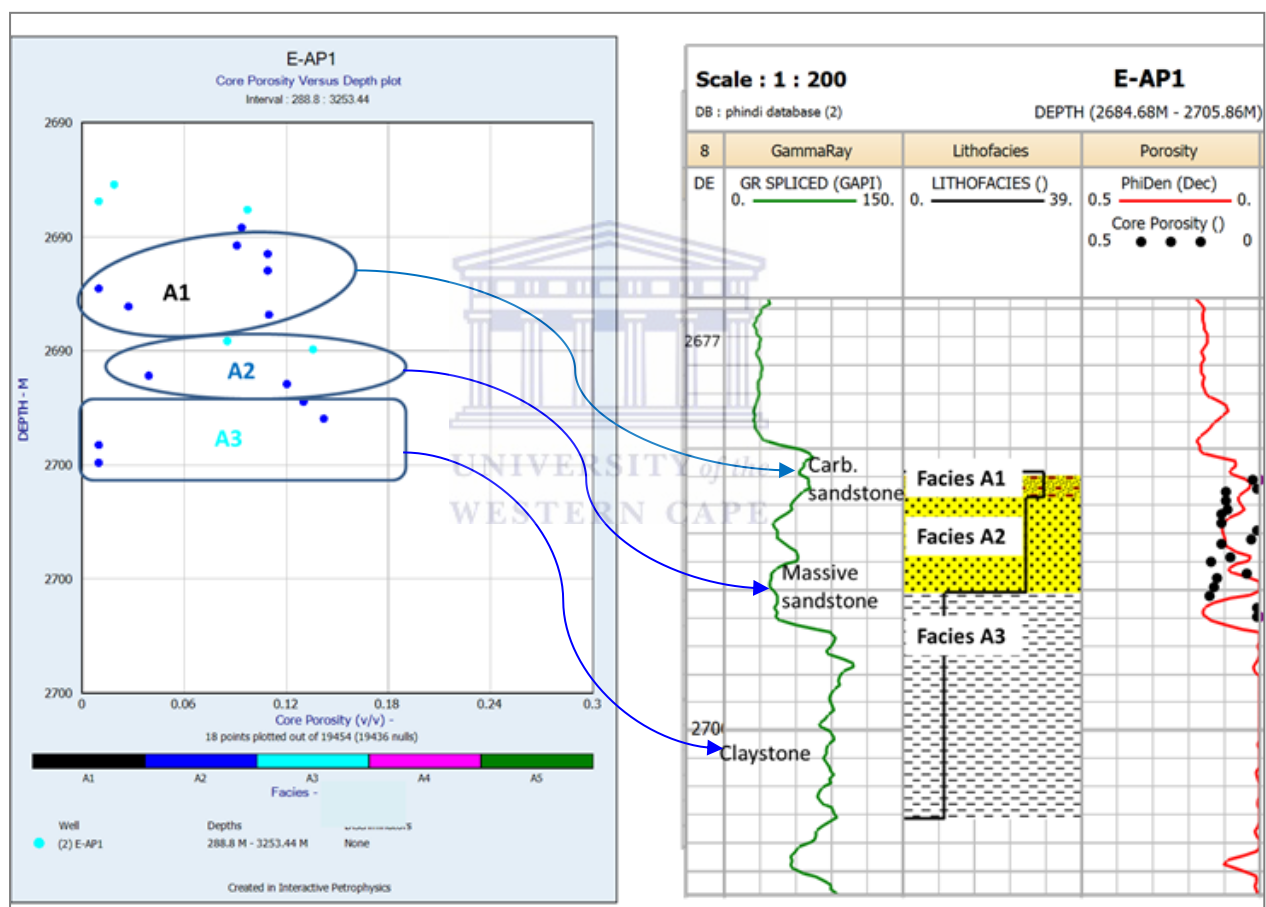


Figure 5.4.2: Well E-AP1 Porosity versus depth plot.

Well E-AP1

Core Porosity Histogram

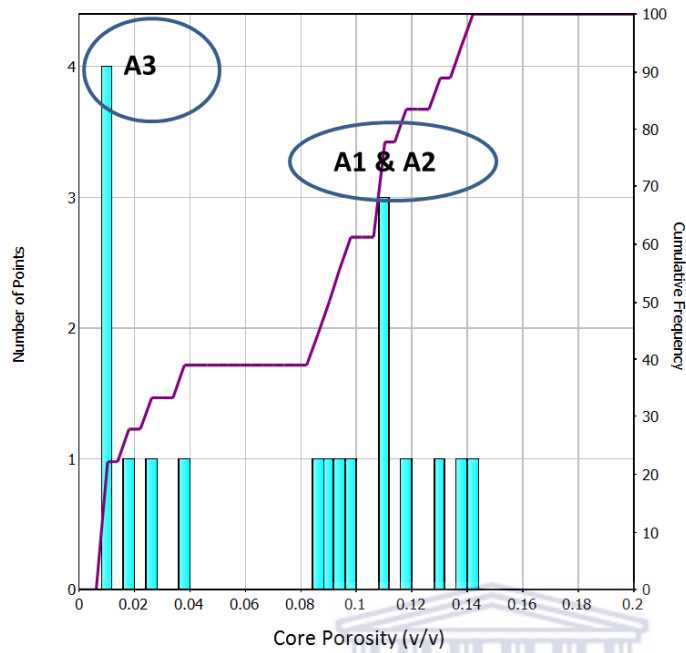


Figure 5.4.2.1: Well E-AP1 Core Porosity histogram and plot against

The differences in variations of porosity in the zones could be associated to the type of facies present. The interval porosity values that are less than 6% is associated with facies type A3 (Claystone). The interval values that are more than 6% may be attributed to carbonaceous sandstone (facies type A1).

5.5 Core Permeability

The permeability of a rock is a measure of ease which the rock will permit the passage of fluids. Permeability is a secondary property of detrital rocks and it is directly dependent on primary properties of composition, texture, and structure. If composition is assumed to be essentially constant and the small-scale effects of bedding are ignored, then texture is of first importance. Permeability depends on the textural elements that determine both size, shape of pores, and this dependency may be expressed by the functional relation:

$$K = f(D, s, SH, P)$$

Where K is the permeability and the independent variables are mean grain size, D; sorting, s; mean grain shape, SH; and packing, P. The first two variables, grain size and sorting are measured in dimensions of length, shape is expressed as a ratio, and packing is most commonly given as porosity or percent of voids.

Permeability of reservoirs may vary from less than 1 mD to over 1000 mD. In order to determine the permeability for core plugs, the plugs were placed in a compliant sleeve within a cylinder. Pressure is put on sleeve to ensure that injected gas or liquid flows parallel to the core plug axis. Gas is usually injected with an inflow pressure and flows almost linearly through the plugs to atmospheric pressure. The permeability is then determined from Darcy's law. For the purpose of flow in rocks it is usually assumed that the flow is laminar. Permeability to a single fluid is different to the permeability where more than one fluid phase is flowing. When there are two or more immiscible fluid phases flowing, relative permeability is used. A correction is done on the gas or air permeability which is known as Klinkenberg Correction. This correction is done due to differences in flow physics between gas and liquid especially in low permeable media. The permeability values are regarded as permeabilities to air and liquid. Gas permeability corrected from the Klinkenberg effect is said to be equivalent to the permeability if a liquid medium is present in the pores. The permeability of rocks varies enormously from 1 nanodarcy, nD (1×10^{-9} D) to 1 microdarcy, μ D (1×10^{-6} D) for granites, shales and clays that form cap-rocks or compartmentalize a reservoir, to several darcies from extremely good reservoir rocks. In general a cut-off of 1 mD is applied to reservoir rock below which the rock is not considered as a reservoir rock unless unusual circumstances apply. For reservoir rocks permeabilities can be classified as in Table 5.5 below.

Table 5.5: Reservoir permeability classification

Permeability values (mD)	Classification
Less than 1	Poor
Between 1 and 10	Fair
Between 10 and 50	Moderate
Between 50 and 250	High
Between 250 and 1000	Very High
Above 1000	Exceptional

(Modified after Djebbar, 1999)

5.5.1 Well D-D1 Permeability

The permeability for well D-D1 was measured both vertically and horizontally. The horizontally measured permeability is recognized as the rock permeability since it is measured parallel to the bedding which is the major contributor to fluid flow into a reservoir. The core permeability values for well D-D1 were recorded as permeability to air and liquid. Gas permeability corrected for the Klinkenberg effect is said to be equivalent to the permeability if a liquid medium is present in the pores. The air permeability values range from 0.021 mD to 0.169 mD while the liquid permeability values range from 0.01 mD to 0.10 mD. Liquid permeability values were used in this study. Plot of permeability in log scale against depth in linear scale is illustrated in Figure 5.5.1a and 5.5.1b below.

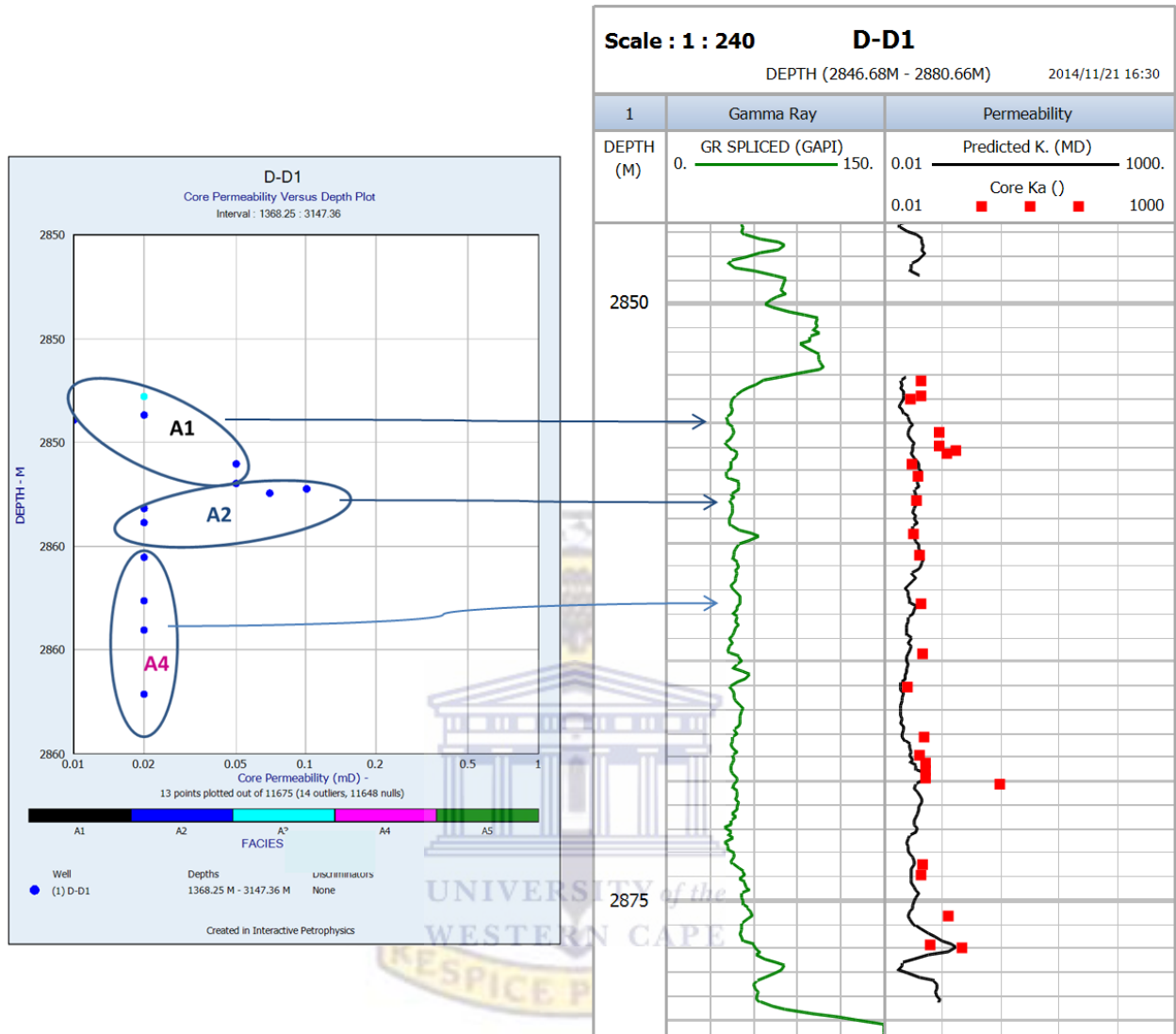


Figure 5.5.1a: Well D-D1 Permeability versus depth plot.

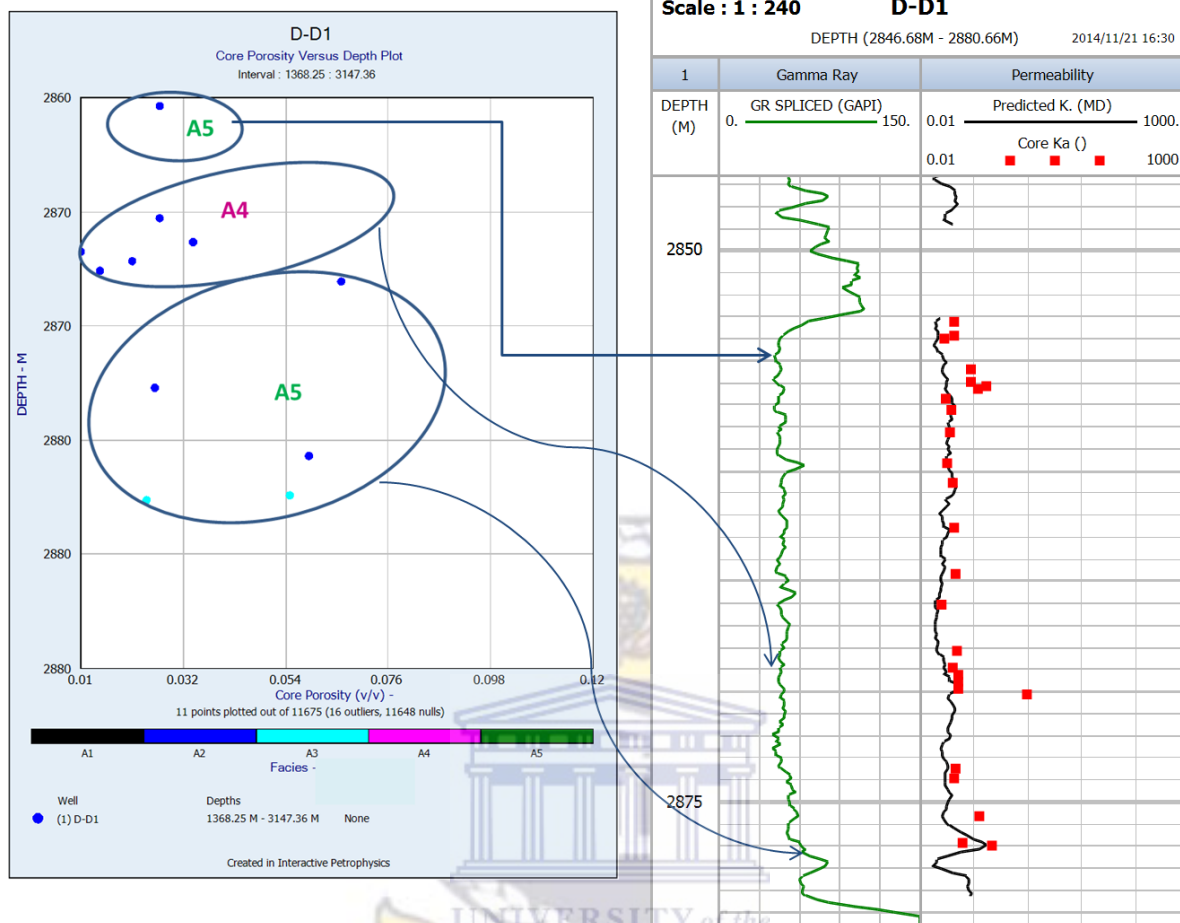


Figure 5.5.1b: Well D-D1 Permeability versus depth plot.

Well D-D1 displays poor permeability (<1 mD) from 2852.9 m to 2879.4 m depth of the cored intervals. This is especially observed in intervals where claystone and siltstone are present, these are indicated as facies type A3 and A5 respectively.

5.5.2 Well E-AP1 Permeability

The permeability for well E-AP1 was also measured both vertically and horizontally. The horizontally measured permeability is recognized as the rock permeability since it is measured parallel to the bedding which is the major contributor to fluid flow into a reservoir. The core permeability values for well E-AP1 were recorded as permeability to air and liquid. The air permeability values range from 0.01 mD to 20.00 mD while the liquid permeability values range from 0.01 mD to 16.00 mD. Liquid permeability values were used in this study. The permeability plot in log scale against depth in linear scale is illustrated in Figure 5.5.2 below.

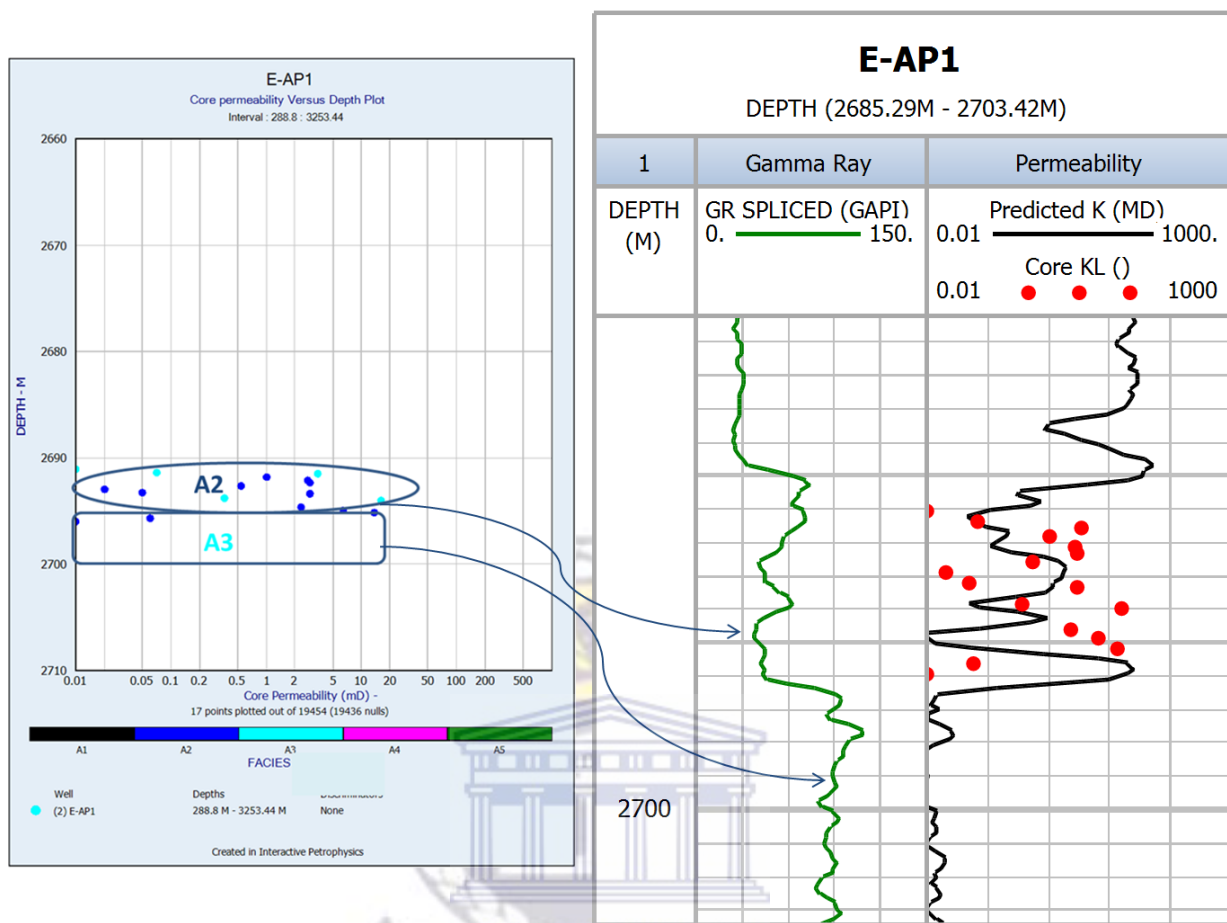


Figure 5.5.2: Well E-AP1 Permeability versus depth plot.

Well E-AP1 displays poor permeability values (<1 mD) shown in the depth interval of 2695.3m to 2703.0m in the plot and this due to the claystone interval indicated as facies type A3. Moderate to good permeability values were observed in the depth interval of 2695m to 2691.5m in the plot and this was as a result of the well sorted carbonaceous sandstone and the massive sandstone, which are indicated as facies type A1 and A2 respectively.

5.6 Fluid saturation

The saturation of a formation is considered as the fraction of its portion volume occupied by the fluid. In this study, three saturations used were; water saturation (S_w), oil saturation (S_o) and gas saturation (S_g). The summation of all saturation in a given rock must equal 100 percent and water saturation of a formation can vary from 100 percent to a much smaller percentage but will never be zero since there is always a small amount of capillary water or irreducible water that cannot be displaced. For an oil or gas bearing reservoir, not all the

hydrocarbon saturation can be removed, some of the oil or gases remain trapped in the pore volume and this phenomenon is called residual oil saturation. Water saturation calculation:

$$S_w = [(a / F^m) * (R_w / R_t)]^{(1/n)}$$

S_w : water saturation, F : porosity, R_w : formation water resistivity R_t : observed bulk resistivity, a : a constant (often taken to be 1), m : cementation factor (varies around 2), n : saturation exponent (generally 2)

5.6.1 Well D-D1 Fluid saturation

The fluid saturations in well D-D1 recorded were water saturation (S_w) with an average value of 84.5 %, oil saturation (S_o) of an average value of 1.31 % and gas saturation (S_g) value of 15.1%. Fluid saturations were only recorded at intervals sandstone (facies type A1 and A2) depth of 2850m to 2859m (Figure 5.6.1) . Oil saturation is noticeably low, only increasing from 10% to 12% while gas saturation increases from 5 % to 38 % at this depth. Water saturation is noticeably high, increasing from 56 % to 98 %. The water and hydrocarbon saturation were constant at a depth of 2853 m and this could be an indication of a transition zone.

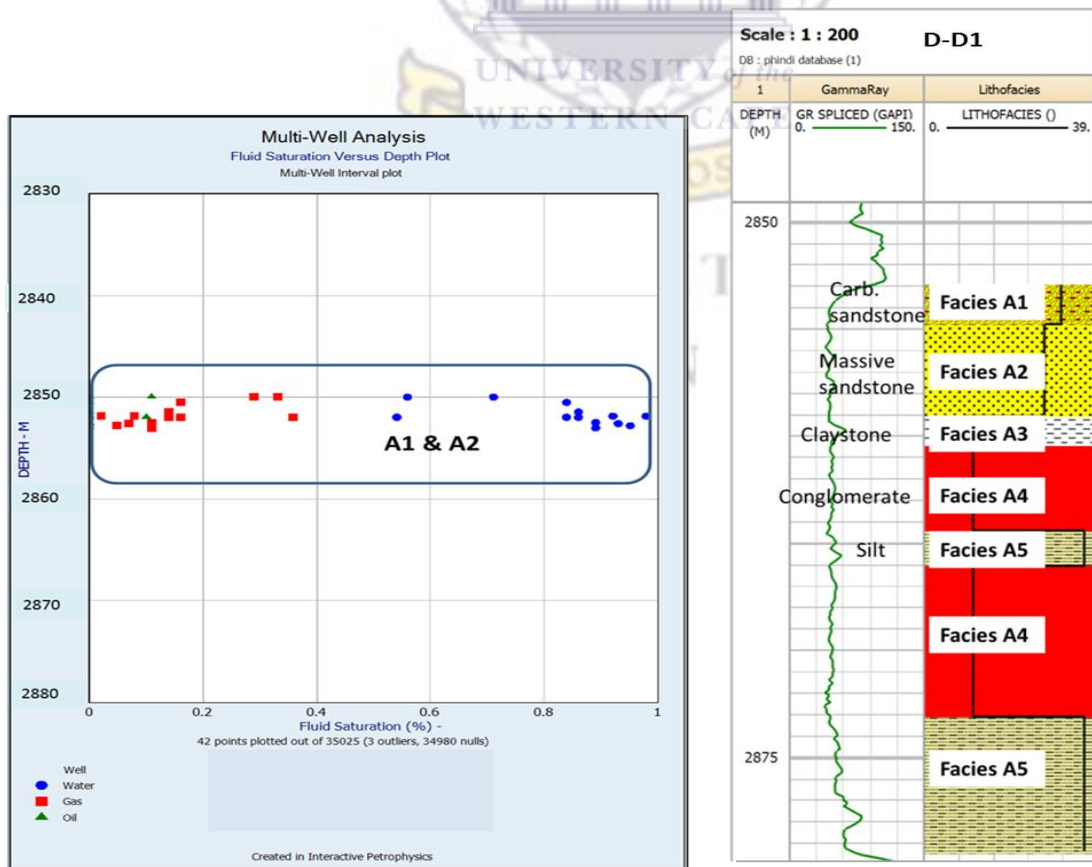


Figure 5.6.1a: Well D-D1 Fluid saturation versus depth plot

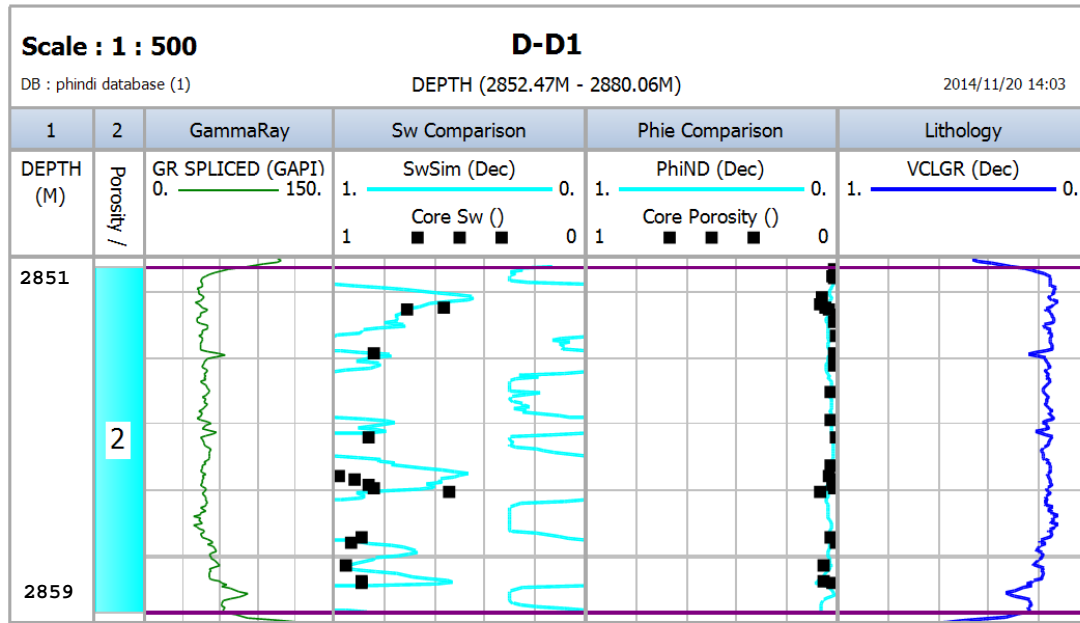


Figure 5.6.1b: Well D-D1 Comparison of core and log saturation and porosity

5.6.2 Well E-AP1 Fluid saturation

The fluid saturations in well E-AP1 recorded were water saturation (S_w) with an average value of 61 %, oil saturation (S_o) of an average value of 6.3 % and gas saturation (S_g) value of 33 %. Fluid saturations were only recorded at intervals associated with sandstone (facies type A1 and A2) depth of 2690.9m to 2695.0m (Figure 5.6.2).

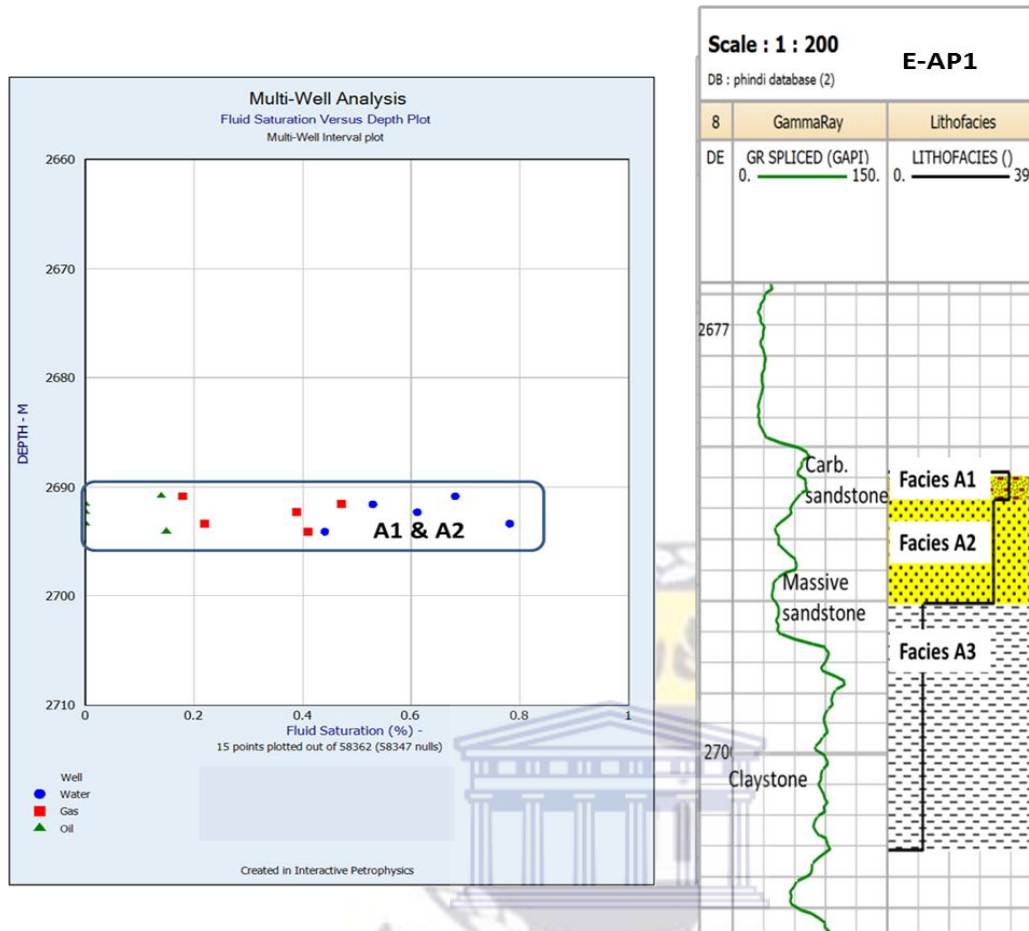


Figure 5.6.2a: Well E-AP1 Fluid saturation versus depth plot.

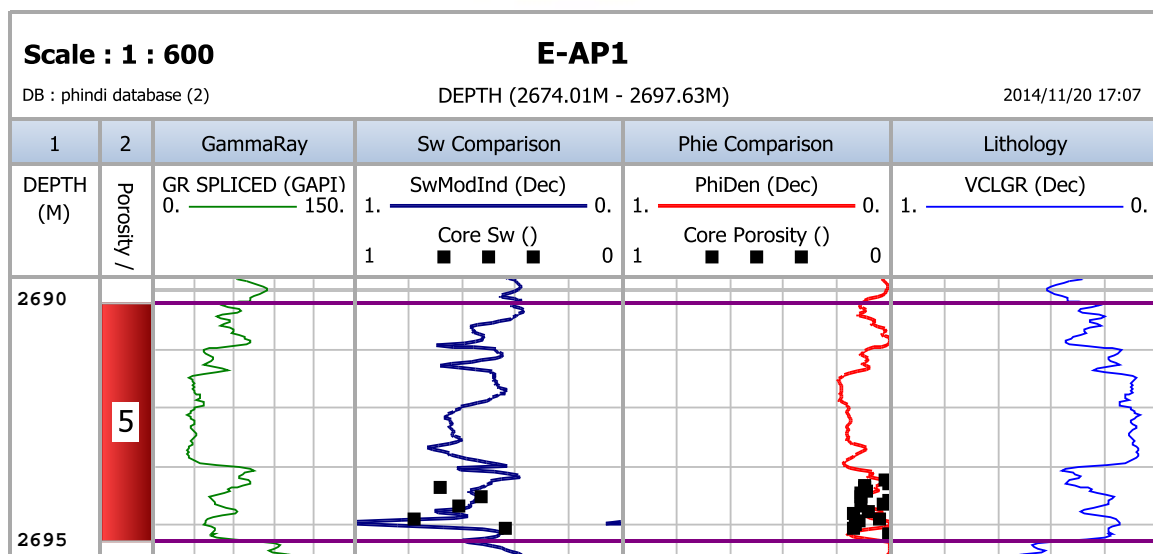


Figure 5.6.2b: Well E-AP1 Comparison of core and log saturation and porosity

5.6.3 Comparison of Porosity – Permeability and Facies Distribution

The porosity-permeability cross plots are used to distinguish between rock types and also display the trend between porosity and permeability. The most obvious control on permeability is porosity. This is because larger porosities mean that there are many more broader pathways for fluid flow. Almost invariably, a plot of permeability against porosity for a formation results in a clear trend with a degree of scatter associated with the other influences controlling the permeability. For the best results, poroperm cross plots ought to be constructed for a whole well with widely varying lithologies. The result is often a disappointing cloud of data in which the individual trends are not obvious. Sandstones are extremely well controlled by the porosity, while carbonates have a more diffuse cloud indicating that porosity has an influence, but there are other factors controlling the permeability. In the case of carbonates, there can exist high porosities that do not give rise to high permeabilities since the connectivity of the vugs that make up the pore spaces are poorly connected. Poroperm trends for various lithologies can be plotted, and form a map of poroperm relationships, as shown in figure 5.6.3 below.

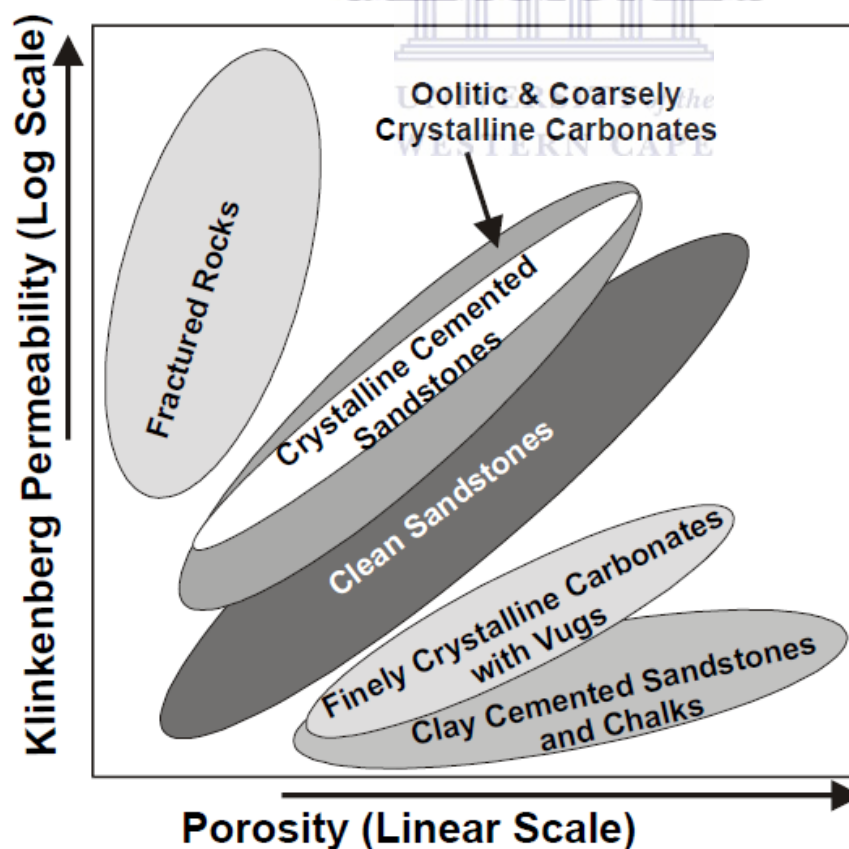


Figure 5.6.3: Porosity Versus Klinkenberg Permeability

5.6.4 Permeability from Core Analysis (Permeability-Porosity Function)

The permeability- Porosity function was done in order to establish a correlation between core permeability and porosity and other wireline log porosity responses. The aim was to predict permeability in uncored intervals and also to estimate permeability in wells without core data. This was done for well D-D1 and E-AP1. The core porosity was plotted on the x-axis in a linear scale against the core permeability on the y-axis in log scale, and facies and gamma ray on the z-axis as shown on the figure 5.6.4a and 5.6.4b below.

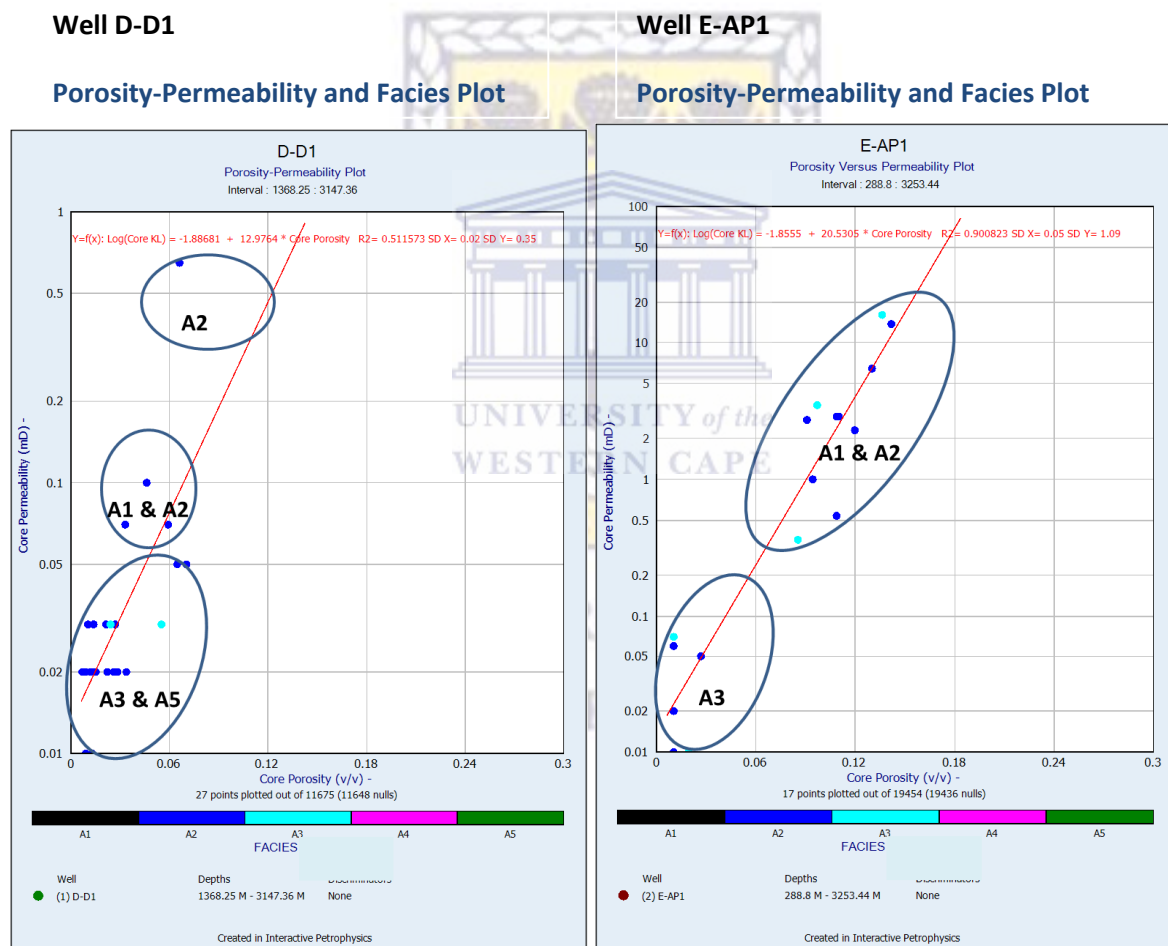


Figure 5.6.4a: Porosity-Permeability cross-plots for determination of functions

All well

Porosity-Permeability and Facies Plot

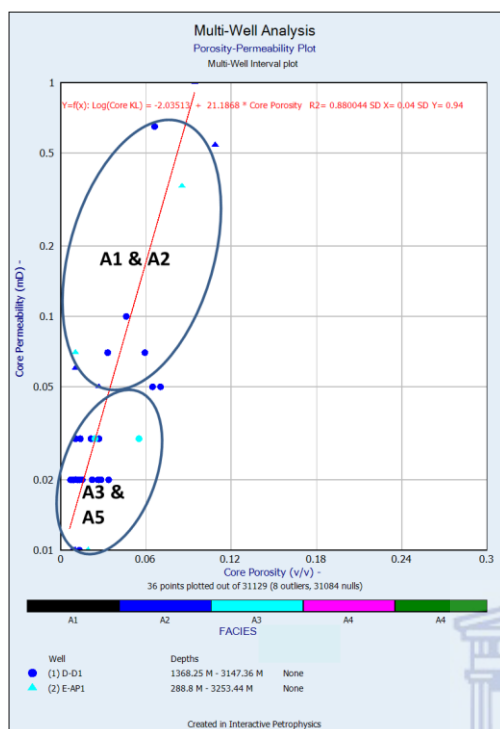


Figure 5.6.4b: Multi well for porosity-permeability cross-plots for determination of functions

Table 5.6.3 with permeability-porosity functions was established from the cross plots as seen in figure 5.3.2 and 5.3.3 above.

Table 5.6.4: Established porosity permeability functions for wells.

Well	Porosity-permeability functions	Correlation Coefficient (R^2)
D-D1	$\text{Log (Core KL)} = -1.88681 + 12.9764 * \text{Core Porosity}$	0.511573
E-AP1	$\text{Log (Core KL)} = 2.42162 + 2.09814 * \text{Core Porosity}$	0.825722
All Wells	$\text{Log (Core KL)} = -2.03513 + 21.1868 * \text{Core Porosity}$	0.880044

The functions established in table 5.6.3 above have been validated by comparing predicted permeabilities from functions against the original core measured permeabilities. The comparison of the functions are illustrated in the figure below (5.6.4.1 and 5.6.4.2) and with the predicted permeabilities in wells D-D1 and E-AP1.

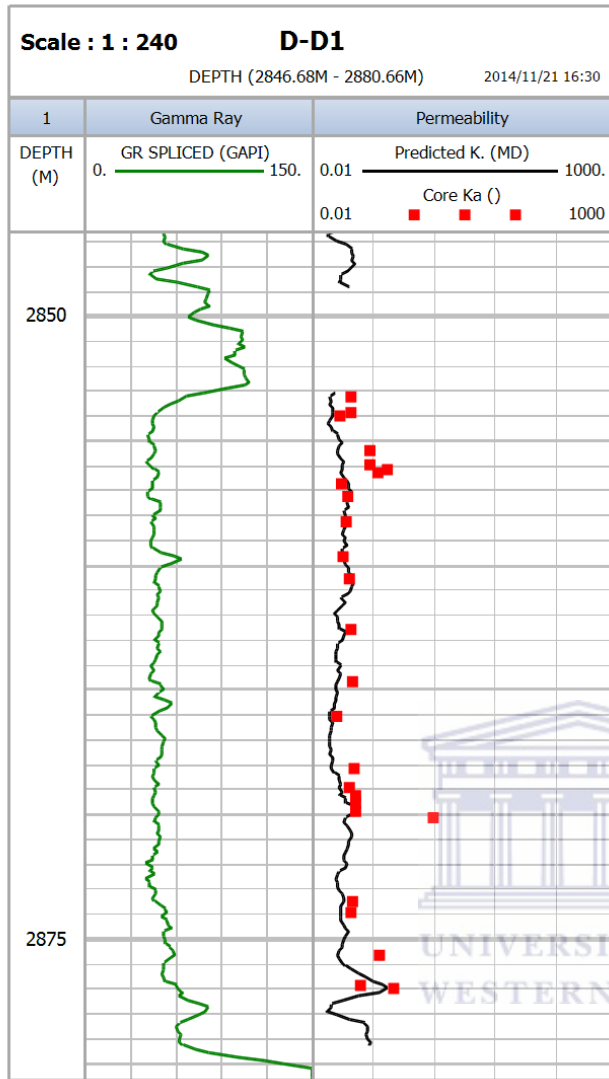


Figure 5.6.4.1: Well D-D1 plot of predicted permeability overlaying original core permeability

In well D-D1, the predicted permeability values from log derived porosity match very well with the core measured permeability. There is a good relationship between the two curves as they both portray similar trend pattern.

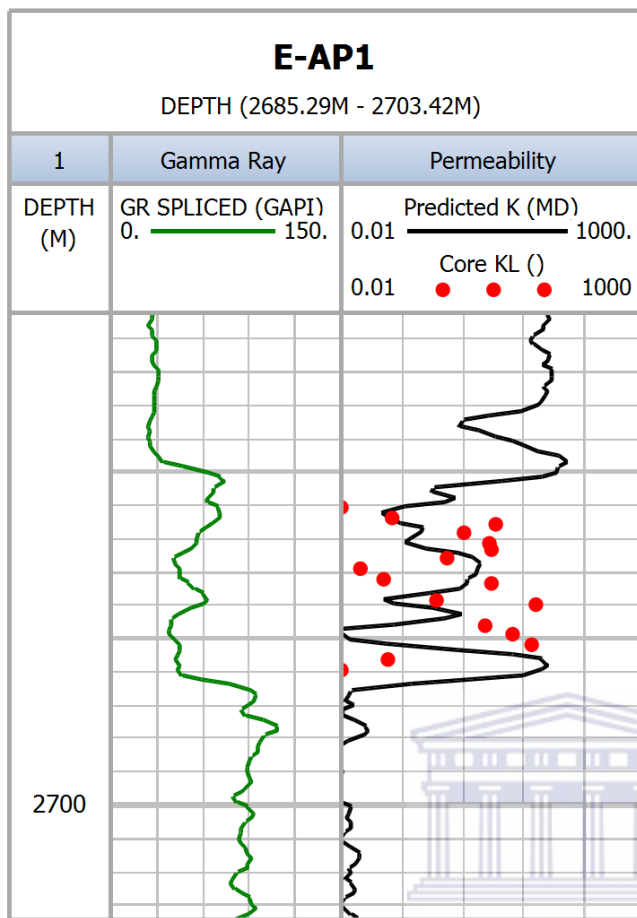


Figure 5.6.4.2: Well E-AP1 plot of predicted permeability overlaying original core permeability in track 4

In well E-AP1, the predicted permeability values from log derived porosity do not match very well with the core measured permeability. There is not a good relationship between the two curves as they both portray different trend pattern.

5.7 Cut-off determination

Identifying proper petrophysical cut-off parameters is necessary to eliminate the non-reservoir rocks, calculate the net reservoir rocks in the area of interest and establish an economical reserve estimate. One of the most important steps is to establish the linkage between conventional core measurement and a reference parameter that differentiates between reservoir and non-reservoir rock. Cut-off of petrophysical parameters is the most famous tool for determining net pays. In 2005, Worthington and Cosentino provided a comprehensive study on the role of cut-offs in determining net pays. They collected and summarized various combinations of cut-offs of shale volume, porosity, permeability, water saturation, resistivity and moveable hydrocarbon. In 2006, Jensen and Menke introduced a statistical method to determine cut-offs in a way to minimize error of calculating net or gross ratio. The evaluation of hydrocarbon volumes require cut-offs so that net reservoir intervals (net pay) that contain adequate hydrocarbon potentials and allow sufficient hydrocarbon flow can be identified.

Net pay is defined on fluids produced and flow rate criteria, Rocks with adequate permeability to flow fluids at commercially significant rates are classified as net reservoirs. If they produce hydrocarbons at a commercially viable hydrocarbon/water ratio, they are classified as net pay (Suzanne & Robert, 2004). The permeability cut-off is often considered as the controlling parameter in net pay since it is dependent on a limited number of parameters which include the fluid mobility, pressure differential and reservoir drive mechanism. A common arbitrary approach of determining permeability cut-off is set permeability cut-off for gas reservoir net pay at 0.1 mD and oil reservoir net pay at 1.0 mD.

A non-reservoir rock may have porosity and permeability that is too low and zero hydrocarbon saturation. The major control is usually the lithology. Shales are classified as non-reservoir rocks, they often contain hydrocarbon with high saturations but have very low porosity and permeability for the hydrocarbon to be extracted. However sandstones could be considered as reservoir rocks provided that they contain adequate hydrocarbon that could be extracted (George and Stiles, 1978).

5.7.1 Porosity cut-off determination

To discriminate between reservoir and non-reservoir, each data point had to meet a porosity cut-off. The effective porosity had to be equal to or greater than 8 percent of the total reservoir volume. This cut-off was established using core porosity and permeability data. Illustrated below is a multi-well porosity-permeability and facies cross plot used for cut-off determination.

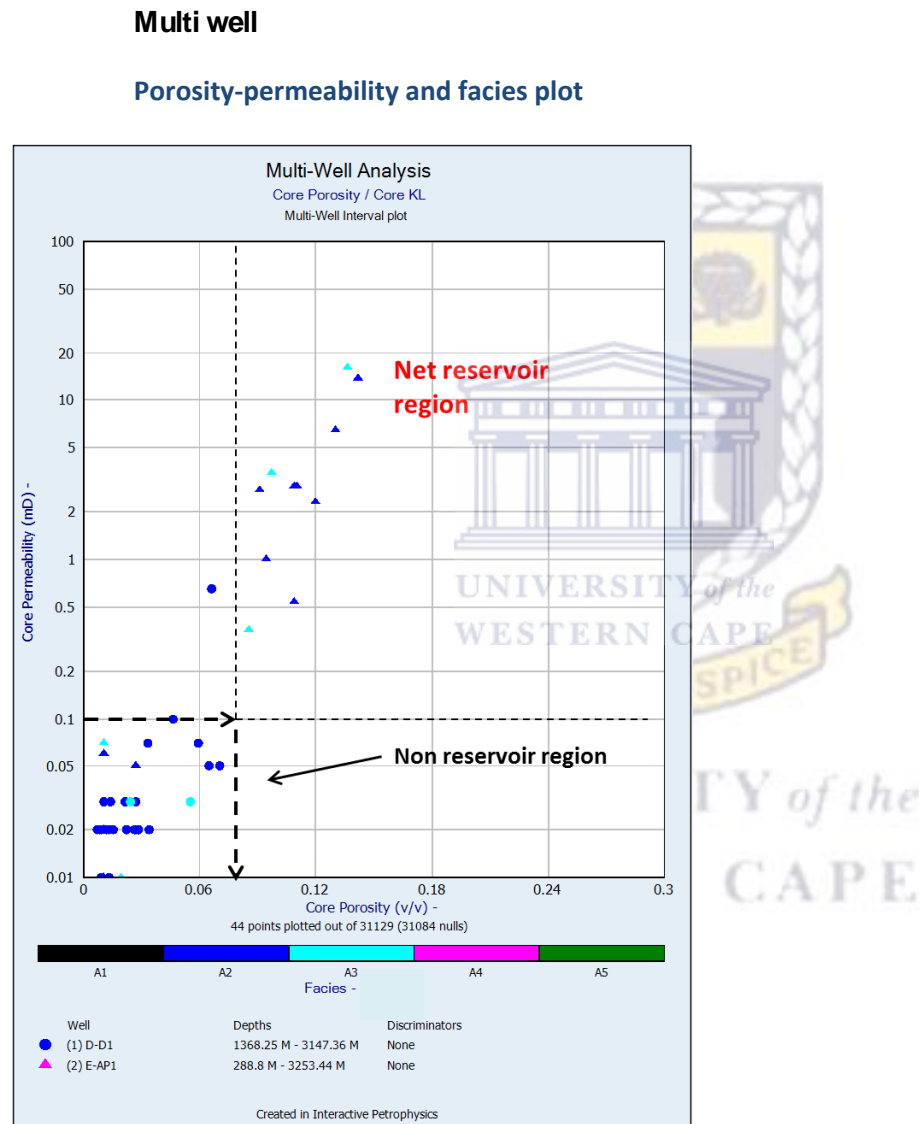


Figure 5.7.1: Multi well porosity-permeability and facies plot for cut-off determination.

5.7.2 Volume of shale cut-off determination

To discriminate between reservoir and non-reservoir rock, each sample point had to meet a shale cut-off. All rocks volume of shale had to be equal to or less that 30 percent of the total reservoir. Illustrated below is a multi-well volume of shale versus porosity and gamma-ray used to establish the volume of shale cut-off.

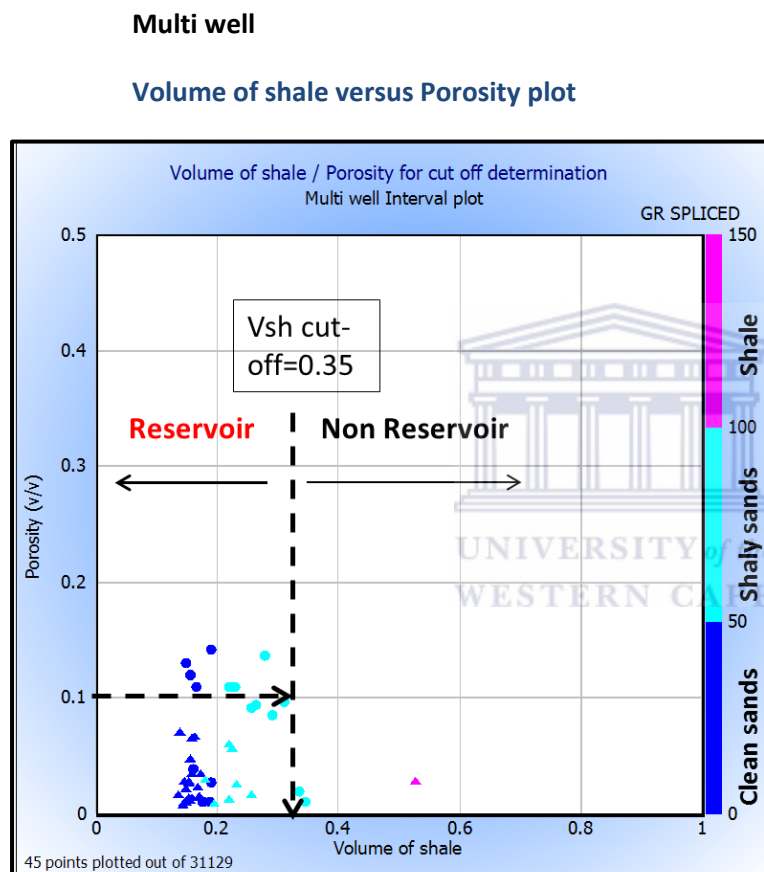


Figure 5.7.2: Volume of shale versus porosity plot for cut-off determination.

The plot illustrated above shows the volume of shale cut-off value for reservoir and non reservoir rock which is defined at 0.35. This consequently means that rocks with volume of shale value of more than 0.35 percent were regarded as shale and not classified as reservoir rock. Whilst, rocks with volume of shale value equal to or less than 35 percent were regarded as reservoir rock

5.7.3 Water saturation cut-off determination

Water saturation cut-off distinguishes between hydrocarbon bearing sandstones; productive and wet intervals. Intervals with water saturation of more than 65 percent were defined as wet or non-productive intervals. Water saturation cut-off > 65 percent is reasonable for deep gas reservoirs. Illustrated below is a multi-well water saturation versus porosity cross plot.

Multi well

Porosity versus Water saturation plot

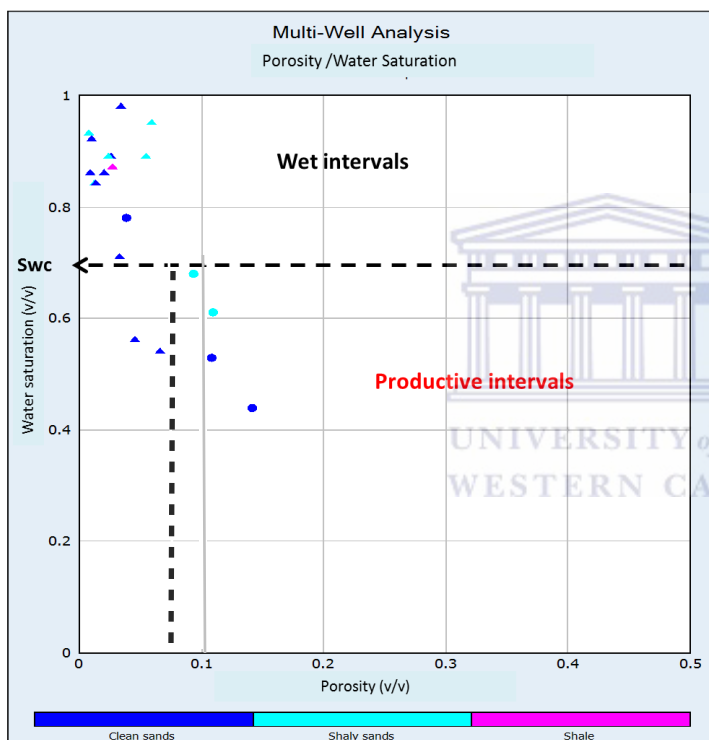


Figure 5.7.3: Porosity versus water saturation plot for cut-off determination.

5.8 Determination of Net Pay

Net Pay is defined as the thickness of rock that contributes to economically viable production with today's technology, today's prices, and today's costs. Net pay is obviously a moving target since technology, prices, and costs vary almost daily. Tight reservoirs or shaly zones that were bypassed in the past are now prospective pay zones due to new technology and continued demand for hydrocarbons. Net pay is determined by applying appropriate cut-offs to reservoir properties so that unproductive or uneconomic layers are not counted. This can be done with both log and core data (Worthington, 2008).

The main use of logs is for the identification of the depth of stratigraphic formation boundaries and their correlation between wells. In addition, logs also provide valuable information on the study area because they can be used for rock type recognition: Sandstone can usually be distinguished easily from shales in most logs. This information can be used to give both depth and thickness of sandstones at the well location, as well as for tracing them between wells (Worthington, 2008)

The difference between gross and net pay is made by applying cut-off values in the petrophysical analysis. In this study, cut-off values of porosity (≥ 0.1), volume of shale (≤ 0.3) and water saturation (≤ 0.65) were used to classify pay intervals, viz. intervals with porosity equal to and greater than 10 percent and volume of shale less or equal to 30 percent and water saturation less than or equal to 65 percent were considered as net pay intervals.

The net to gross ratio is the thickness of net sand divided by the thickness of gross sand. Thus ratio is frequently used to represent the quality of a reservoir zone and for volumetric hydrocarbon calculations.

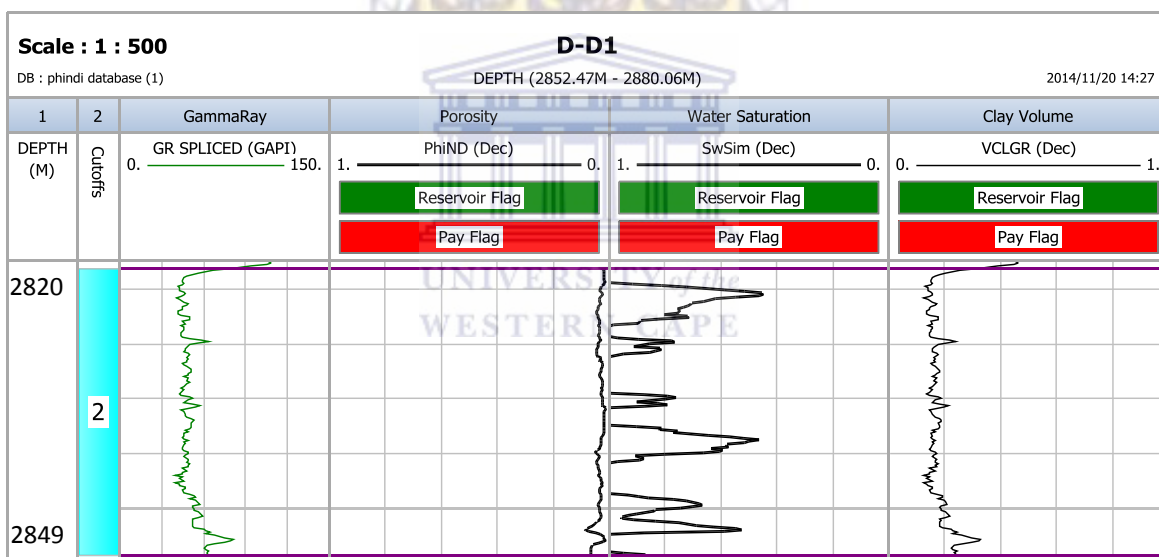
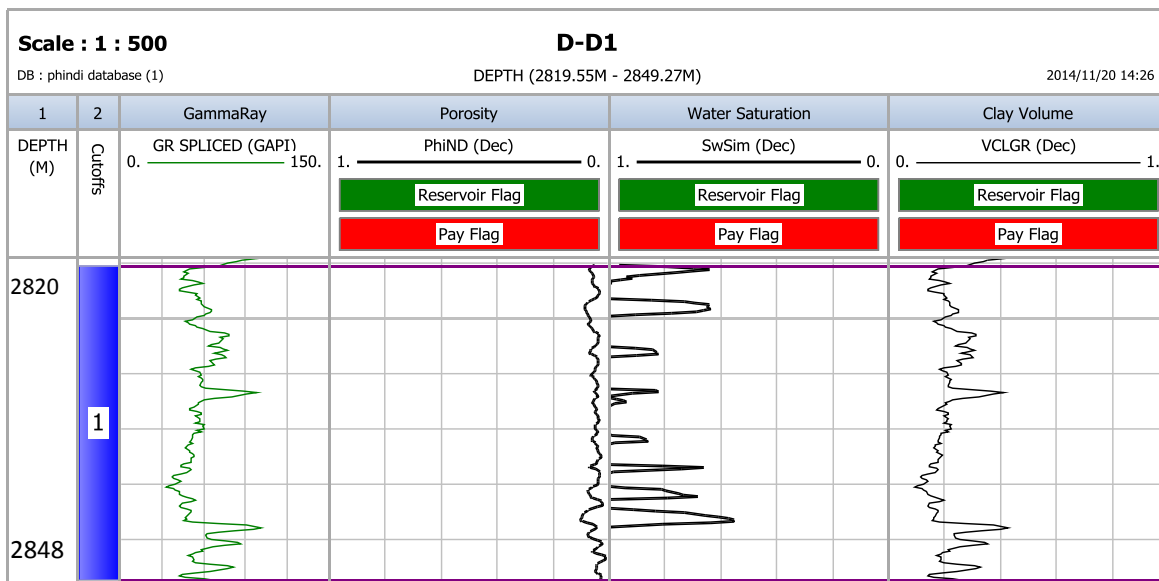
It is normal to apply cut-offs to each calculated result to eliminate poor quality or unproductive zones. Cut-offs are usually applied to shale volume, porosity, water saturation, and permeability. Flag curves were generated using cut-off limits in the database of gross reservoir interval and net reservoir. The net to gross ratio determined can be used to calculate the volume of gas originally in place (GOIP) but this study does not cover this aspect. Illustrated below in Tables 5.8.1 and 5.8.2 are calculated net pay summary for wells with corresponding graphics.

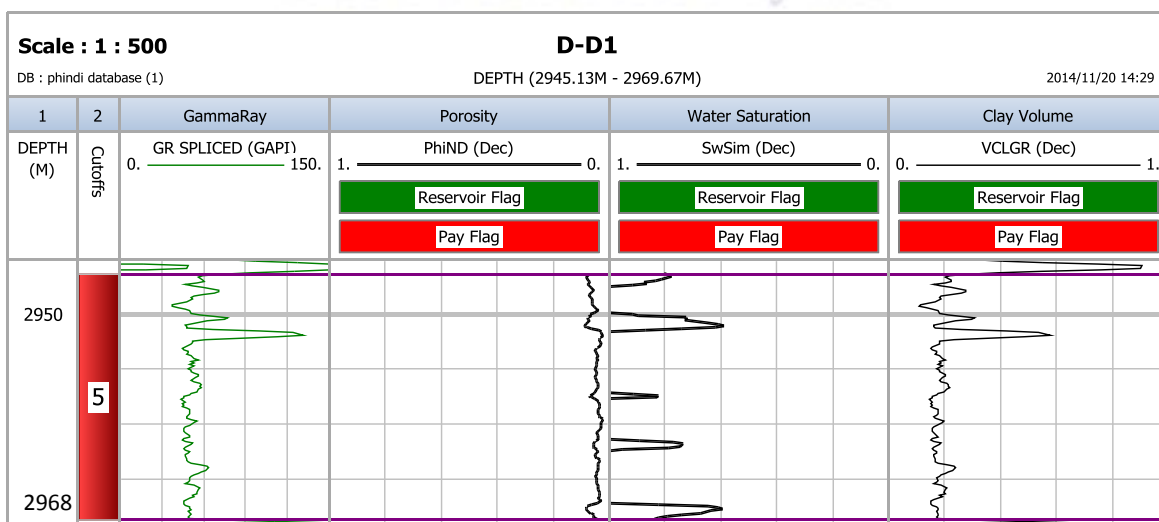
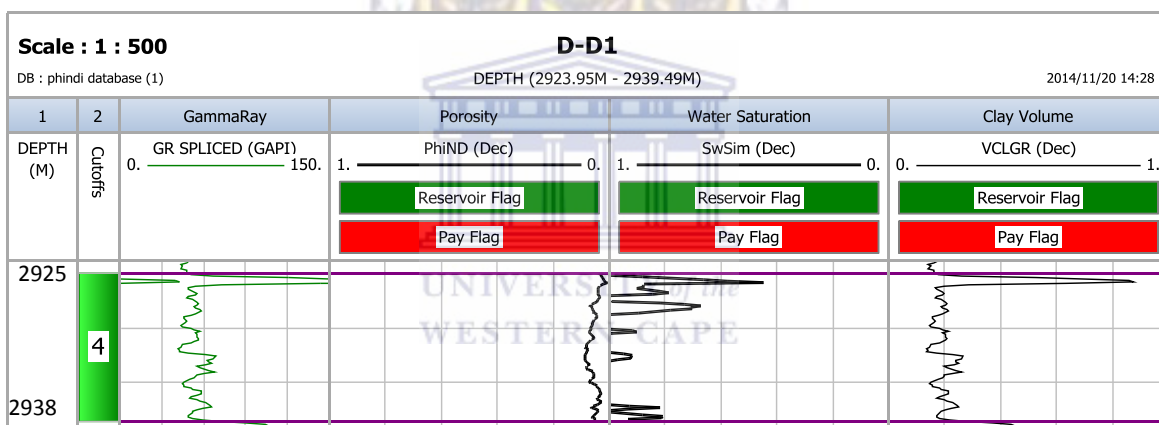
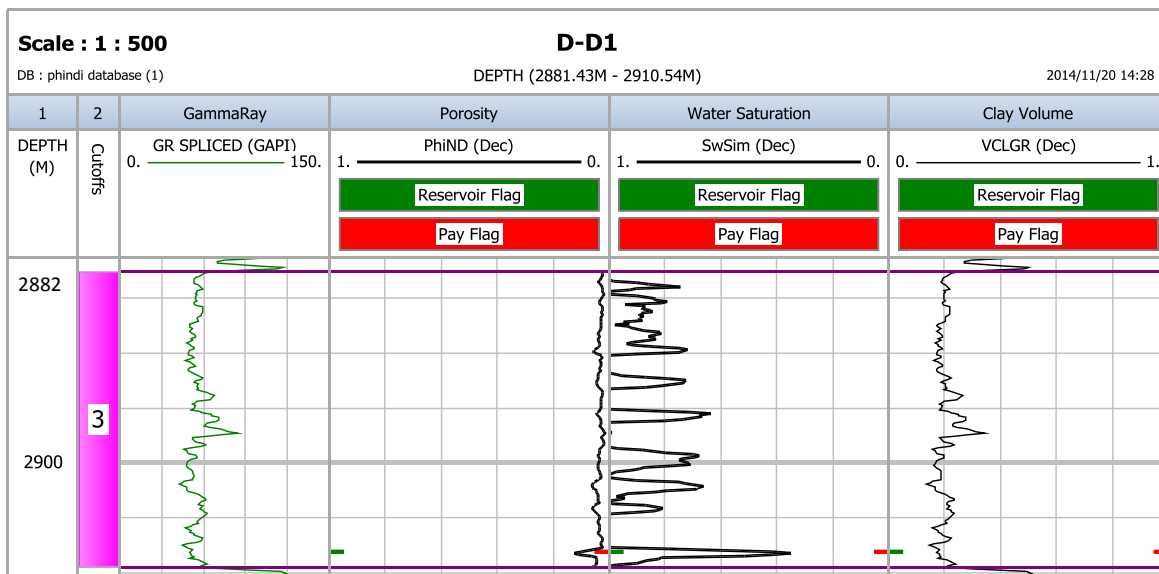
Table 5.8.1: Summary of calculated pay parameters for well D-D1

Zone Name	Top (m)	Bottom (m)	Gross (m)	Net (m)	N/G	Av Phi (v/v)	Av Sw (v/v)	Av Vcl (v/v)
Reservoir 1	2820.20	2848.8	28.60	0.00	0.000	---	---	---
Reservoir 2	2853.1	2879.3	26.20	0.00	0.000	---	---	---
Reservoir 3	2882.6	2909.5	26.90	0.30	0.011	0.113	0.215	0.265
Reservoir 4	2925	2938.6	13.60	0.00	0.000	---	---	---
Reservoir 5	2946.3	2968.8	22.50	0.00	0.000	---	---	---
Reservoir 6	2973.9	3018.4	44.50	0.00	0.000	---	---	---
Reservoir 7	3030.2	3079.5	49.30	0.61	0.012	0.160	0.061	0.340
All zones	2820.20	3079.50	211.60	0.91	0.004	0.144	0.101	0.315

Two reservoirs with pay parameters were encountered in well D-D1, reservoir 3 and 7. Reservoir 3 had a net-pay of 0.30m with an average porosity of 11.3%; water saturation of 21.5% and volume clay of 26.5%. Reservoir 7 had a net-pay of 0.61m with an average porosity of 16%; water saturation of 0.61% and volume clay of 34%. These calculations are also presented in figure 5.8.1.

UNIVERSITY of the
WESTERN CAPE
RESPICE PROSPICE





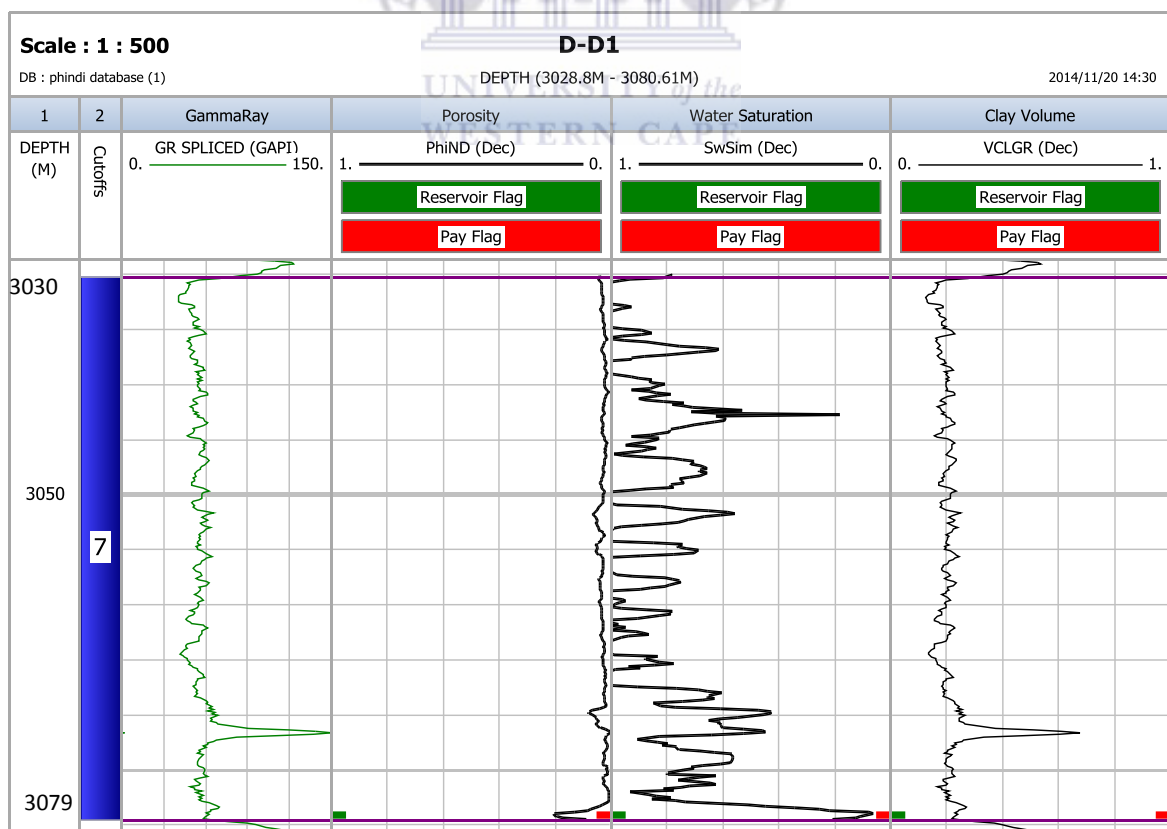
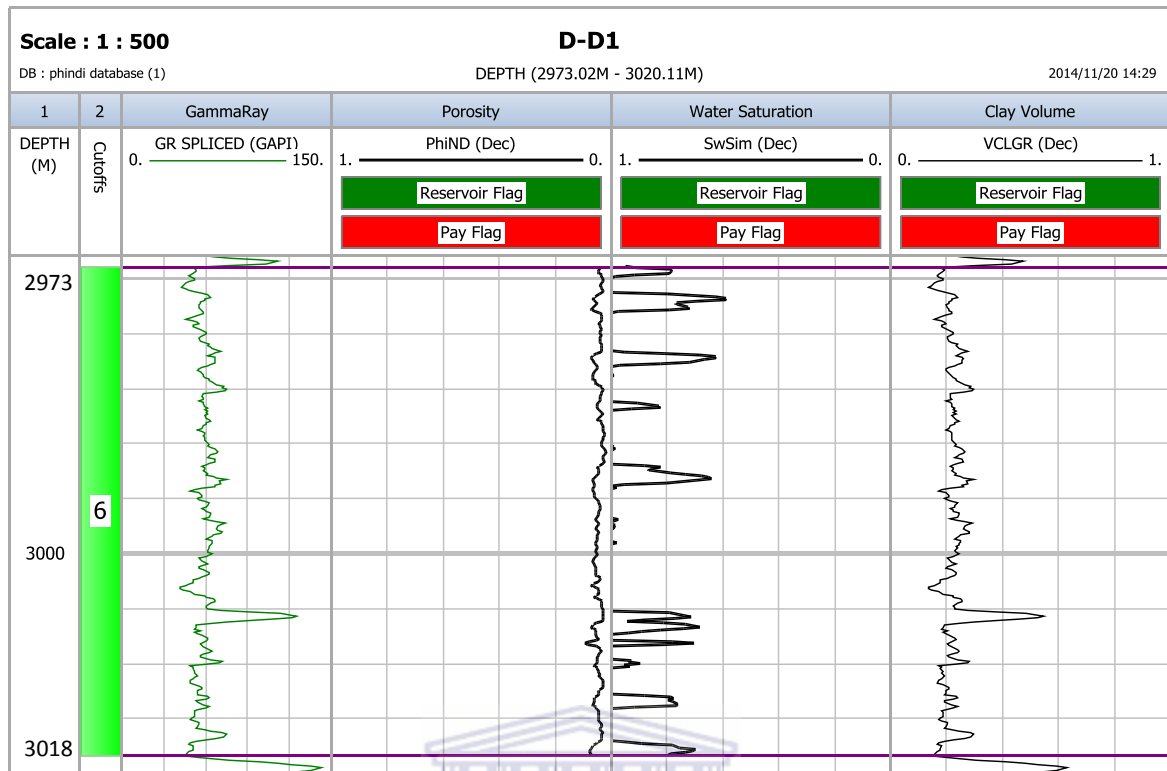


Figure 5.8.1: Well D-D1 displaying calculated reservoir parameters and pay flag

5.8.2 Well E-AP1 Net pay

Table 5.8.2 (a): Summary of calculated reservoir parameters for well E-AP1

Zone Name	Top (m)	Bottom (m)	Gross (m)	Net (m)	N/G	Av Phi (v/v)	Av Sw (v/v)	Av Vcl (v/v)
Reservoir 1	1908.2	1973.9	65.70	53.04	0.807	0.193	0.996	0.116
Reservoir 2	2028.7	2124.2	95.50	65.99	0.691	0.168	1.000	0.169
Reservoir 3	2149.9	2227.3	77.40	45.72	0.591	0.154	0.998	0.128
Reservoir 4	2232.1	2312.7	80.60	51.36	0.637	0.161	0.997	0.142
Reservoir 5	2676	2696.3	20.30	8.23	0.405	0.139	0.982	0.134
All zones	1908.2	2696.30	339.50	224.33	0.661	0.169	0.997	0.155

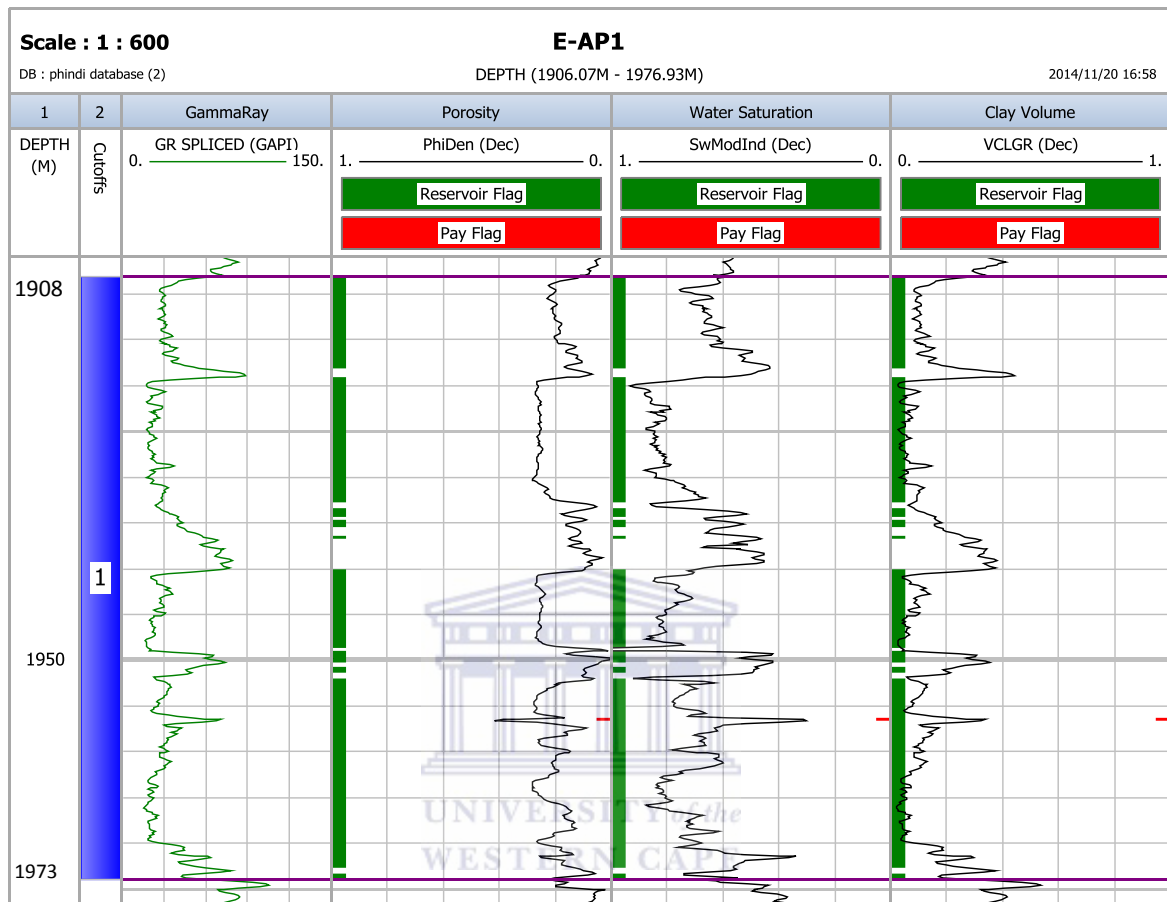
Five reservoirs were encountered in well E-AP1. Reservoir 1 had a net of 53.04m with an average porosity of 19.3%; water saturation of 99.6% and volume of clay of 11.6%. Reservoir 2 had a net of 65.99 m with an average porosity of 16.8%; water saturation of 100% and volume of clay of 16.9%. Reservoir 3 had a net of 45.72m with an average porosity of 15.4%; water saturation of 99.8% and volume of clay of 12.8%. Reservoir 4 had a net of 51.36 m with an average porosity of 16.1%; water saturation of 99.7% and volume of clay of 14.2%. Reservoir 5 had a net of 8.23m with an average porosity of 13.9%; water saturation of 98.2% and volume of clay of 13.4%.

Although five reservoirs were encountered, well E-AP1 had no pay parameters as seen in Table 5.8.2 (b) this is an indication that the well does not produce. These calculations are presented in figure 5.8.2

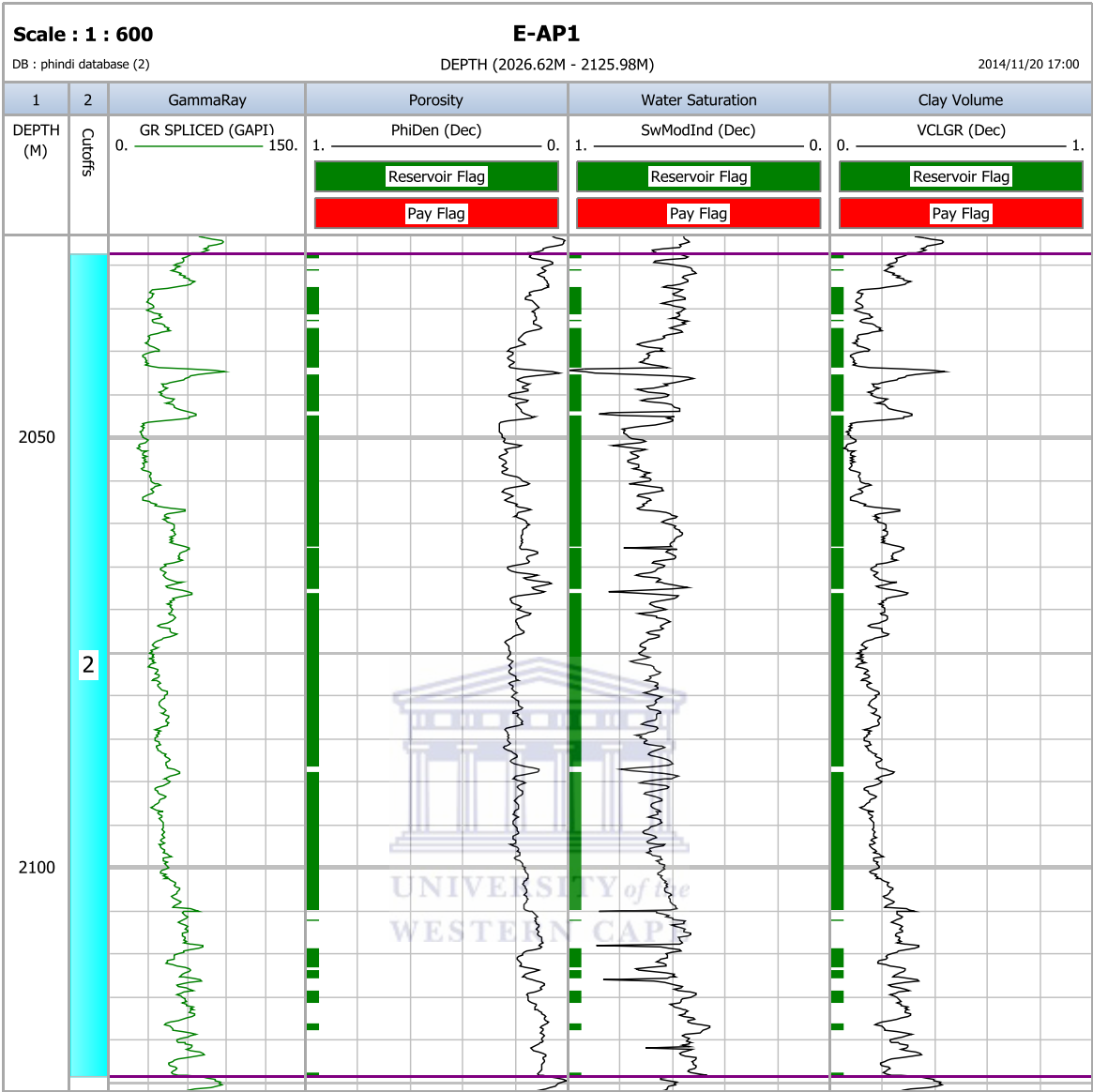
Table 5.8.2 (b): Summary of calculated pay parameters for well E-AP1

Zone Name	Top (m)	Bottom (m)	Gross (m)	Net (m)	N/G	Av Phi (v/v)	Av Sw (v/v)	Av Vcl (v/v)
Reservoir 1	1908.2	1973.9	65.70	0.00	0.000	---	---	---
Reservoir 2	2028.7	2124.2	95.50	0.00	0.000	---	---	---
Reservoir 3	2149.9	2227.3	77.40	0.00	0.000	---	---	---
Reservoir 4	2232.1	2312.7	80.60	0.00	0.000	---	---	---
Reservoir 5	2676	2696.3	20.30	0.00	0.000	---	---	---

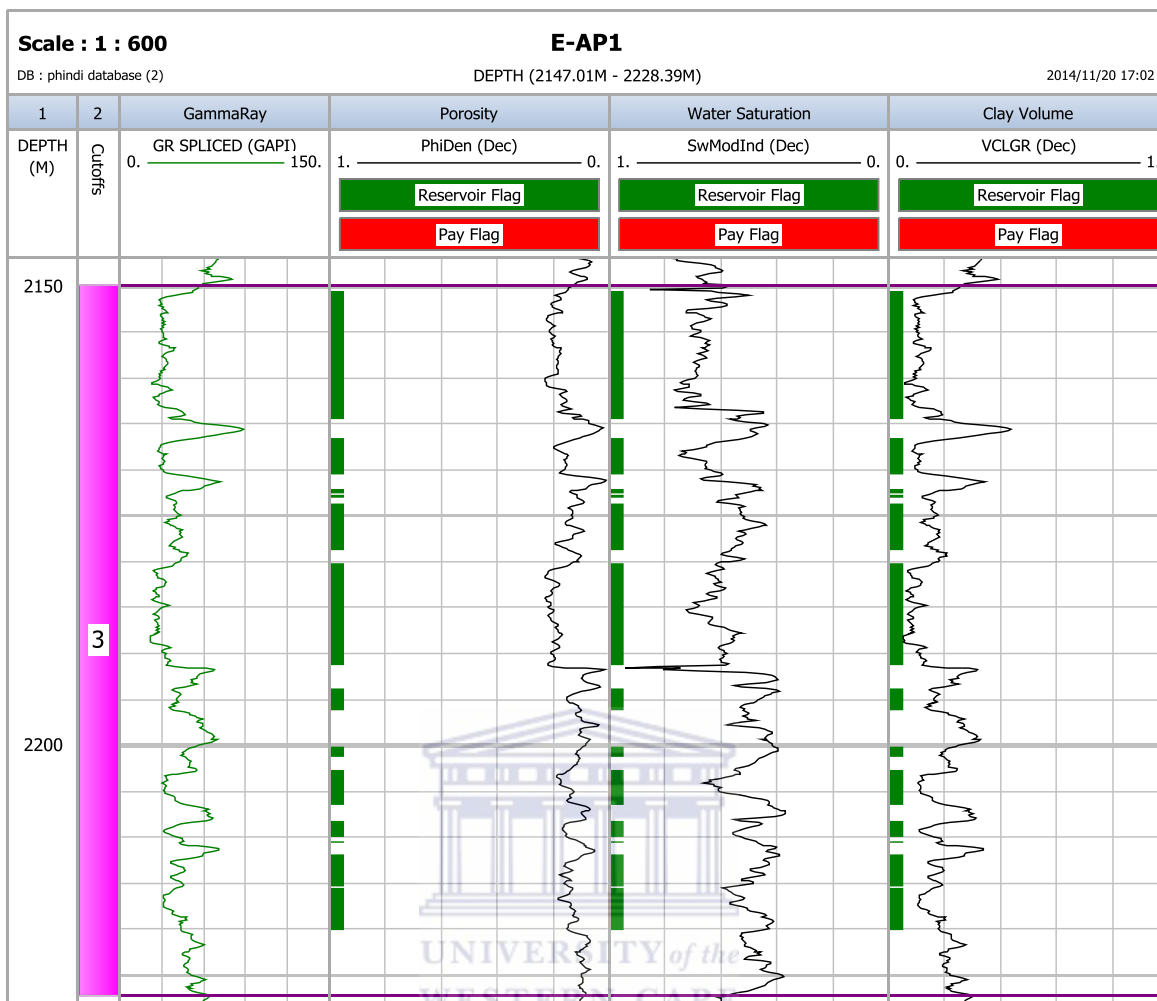
All zones	1908.2	2696.30	339.50	0.00	0.000	---	---	---
-----------	--------	---------	--------	------	-------	-----	-----	-----



UNIVERSITY of the
WESTERN CAPE



WESTERN CAPE



UNIVERSITY of the
WESTERN CAPE

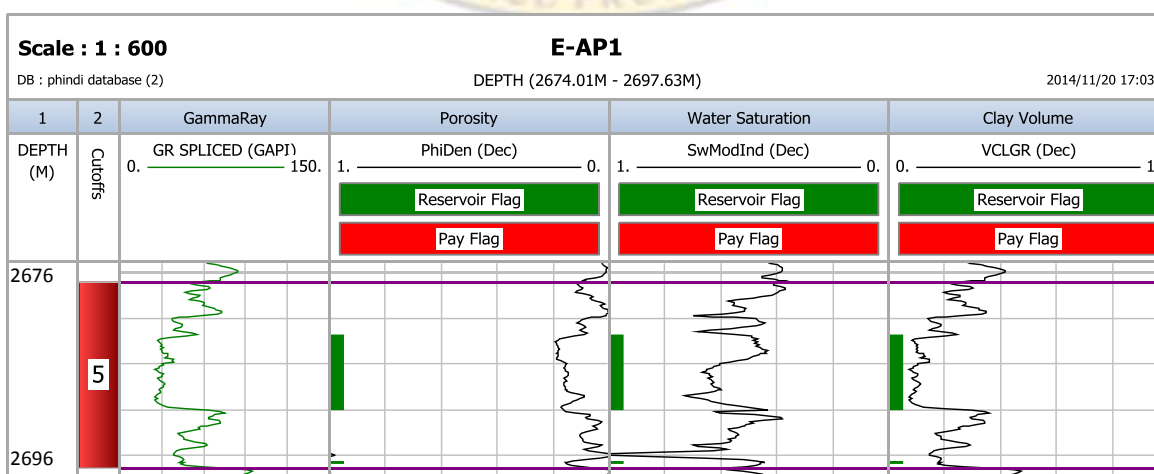
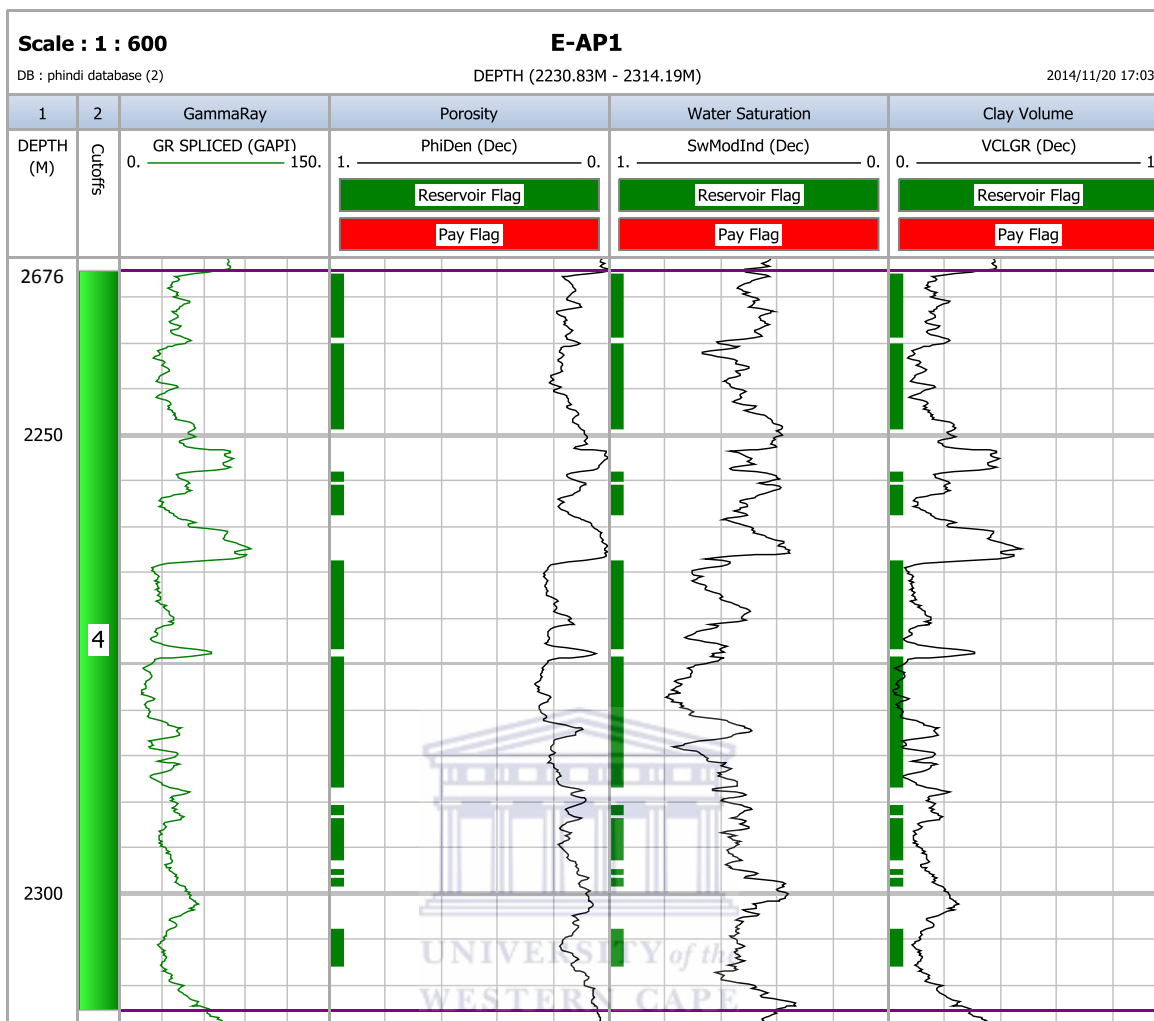


Figure 5.8.2: Well E-AP1 displaying calculated reservoir parameters

CHAPTER 6

Conclusions

The lithofacies were described on the basis of lithology, sedimentary structures, facies

distribution, grain size variation, sorting of grains, fossils and bioturbation. Lithofacies defined by core examination for both well D-D1 and E-AP1 were; facies A1 (Poorly sorted carbonaceous sandstone facies), facies A2 (Massive clean sandstone facies), facies A3 (Dark grey claystone facies), facies A4 (Conglomerate with subrounded grains) and facies A5 (Well sorted siltstone). Facies A1, A2 and A4 tend to have higher porosity and permeability compared to facies A3 and facies A5.

The grain density of core samples was calculated from the measured dry weight divided by the grain volume. The grain density value for all wells with core analysis results showed a range of 2.64 to 2.76 g/cc with a mean value of 2.68 g/cc and a standard deviation of 0.027 g/cc. The core porosity values for well E-AP1 ranged from 1.8 % to 16.2 % at cored intervals while well D-D1 values ranged from 1.2 % to 10.1 % at cored intervals.

The air permeability values for well D-D1 ranged from 0.021 mD to 0.169 mD while the liquid permeability values varied from 0.01 mD to 0.10 mD. The air permeability values for well E-AP1 ranged from 0.01 mD to 20.00 mD while the liquid permeability values varied from 0.01 mD to 16.00 mD. Liquid permeability values were used in this study.

The fluid saturations recorded in well D-D1 were water saturation with an average value of 84.5 %, oil saturation of an average value of 1.31 % and gas saturation value of 15.1%. Fluid saturations were only recorded at sandstone intervals (facies type A1 and A2). The fluid saturations recorded in well E-AP1 were water saturation with an average value of 61 %, oil saturation of an average value of 6.3 % and gas saturation value of 33 %. Fluid saturations were only recorded at intervals associated with sandstone (facies type A1 and A2). Only two reservoirs in well D-D1 indicated to have pay parameters with an average porosity ranging from 11.3% to 16%, average saturation from 0.6% to 21.5% and an volume of clay from 26.5% to 31.5%. Well E-AP1 showed good quality reservoir sandstones occurring in the 1908.2m to 2696.3m intervals though predominantly water-saturated. Pay parameters for all five reservoirs in this well showed zero or no average porosity, saturation and volume of clay

In this study, cut-off values of porosity, volume of shale and water saturation were used to classify pay intervals, viz. intervals with porosity equal to and greater than 8 percent and volume of shale less or equal to 35 percent and water saturation less than or equal to 65 percent were considered as net pay intervals.

Recommendations

The main use of logs is for the identification of the depth of stratigraphic formation boundaries and their correlation between wells. In addition, logs also provide valuable information on the study area because they can be used for rock type recognition; sandstone can usually be distinguished easily from shales in most logs observed in the study. This information can be used to give both depth and thickness of sandstones at the well location, as well as for tracing them between wells.

- In future, the petrophysical evaluation of the study area ought to be used to prepare the petrophysical and engineering data needed for building the 2D/3D model of the selected study area in the Bredasdorp Basin. Property analogue model and cut-off values determination will thus be more accurate.
- More wells can be used in future, including more data on well D-A1 for better analysis of the study area.
- Conventional and special core analysis data ought to be provided in future in order to obtain capillary pressure and electrical properties so that they can be contracted to assist calibrate water saturation.
- XRD provides a fast and reliable tool for routine mineral identification and thus XRD values should also be provided to help calibrate mineral volume calculations derived from well log data.
- It could be essential to carry out an analogous outcrop base modelling in order to understand the permeability distribution and simulate flow patterns in these reservoirs.
- This work could be reviewed with more data input from PASA (well, seismic and production data) for further studies, particularly with respect to reservoir modelling and flow simulation.
- Well D-D1 produces a small amount of gas while E-AP1 has good quality reservoirs that are water saturated thus not producing anything. It is not advisory to explore any of the two well.

References

- Bray, E. E. and Evans, E. D., 1961. Distribution of n-paraffin as a clue to recognition of source rocks. *Geochim. Cosmochim. Acta*. 22, 2.
- Broad, D.S. (2000). Petroleum exploration offshore South Africa: *Journal of African Sciences*, 31 (1), pp 50-51.
- Broad, D.S., Jungslager, E.H.A., McLachlan, I.R., & Roux, J., (2006). Offshore Mesozoic Basins. In: Johnson, M.R., Anhaeusser, C.R., Thomas, R.J. (Eds.). *The Geology of South Africa*. Geological Society of South Africa, Johannesburg/Council for Geosciences, Pretoria, p. 553–571.
- Brown, L.F., J.M., Brink, G.J., Doherty, S., Jollands, A., Jungslager, E.H.A., Keenan, J.H.G., Muntigh, A. and Van Wyk, N.J.S. (1995). Sequence stratigraphy in offshore South African divergent basins. In: *Am. Ass. Petrol. Geol., Studies in Geology*, 41, An Atlas on Exploration for Cretaceous Lowstand traps, by Soeker (Pty) Ltd, pp 83-131.
- Brown, L.F., Brown, L.F, Jr., Benson, J.M., Brink, G.J., Doherty, S., Jollands, A., Jungslager, E.H.A., Keenan, J.H.G., Muntingh, A. and Van Wyk, N.J.S. (1996). Sequence stratigraphy in offshore South Africa divergent basins. An atlas on exploration for cretaceous lowstand traps by SKEKOR (Pty) Ltd. *Am. Ass. Petro. Geol. Stud. In Geology*. 41, 184pp.
- Crain, E.R. (2003). *The New Role of Petrophysics in Geophysical Interpretation* P.Eng., Spectrum 2000 Mindware Ltd., Calgary. 477 pp.
- De Wit, M.J. and Ransome, I.G.D. (1992). *Inversion Tectonics of the Cape Fold Belt, Karoo and Cretaceous Basins of the Southern Africa*, A.A. Balkem, Netherlands, pp 49.

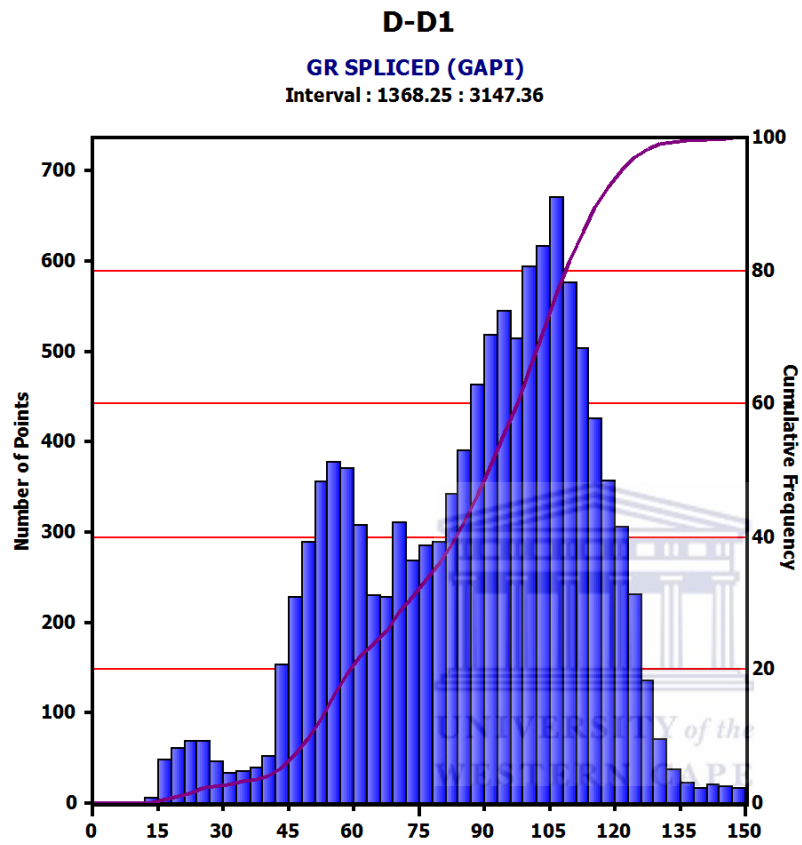
- Dow, W.G. and Williams, H. (1974). Application of Oil-Correlation and Source-Rock, Data to Exploration in Williston Basin: AAPG Bulletin, v. 58, no7, p. 1253-1262.
- Dingle, R.V., Siesser, W.G. and Newton, A.R. (1983). Mesozoic and Tertiary Geology of Southern Africa. A.A. Balkema/Rotterdam, pp 99-106.
- Eglinton, G., and Calvin, J.R., 1984. The Bengal submarine fan, northeastern Indian Ocean. *Geo-Mar, Lett.*, 3:119-124.
- George, C.J. and Stile, L.H. (1978). Improvements techniques for evaluating carbonate water floods in West Texas, *Journal of Petroleum Technology*, vol 30, no6; pp 1547-1554.
- Gilbert, C.E. (1990). Sandstone distribution in the 14At1 level in the E-G area, south-central Bredasdorp Basin: implication for a predictive depositional model. In: Abstracts Geocongress 90. *Geol. Soc. S. Afr.*, Cape Town, pp 177-180.
- Gilbert, D. (1977). Organic facies variation in the Mesozoic South Atlantic. In: Initial Reports Deep Sea Drilling Project Leg 75. (eds.) Hay, W.W., Sibuet, J-C, et al., Washington (US Govt. Printers Office), pp 1035-1049.
- IHS Energy, 2010. Outeniqua Basin, South Africa. Basin Monitor.
- Khanna, S.N. and Pillay, G. (1986). Seychelles: petroleum potential of this Indian Ocean paradise. *Oil and Gas Jour.*, 84/12, pp 136-139.
- Ketzer, J.M. (2002). Diagenesis and sequence stratigraphy: An integrated Approach to constrain Evolution of Reservoir Quality in Sandstone. Dissertation for the Degree of Doctor of Philosophy in Mineral Chemistry, Petrology and Tectonics at the Department of Earth Science, Uppsala University. Sweden.

- Lawver, L.A., Gahagan, L.M. and Coffin, M.F. (1992). The development of palaeoseaways around Antarctica, In “The Antarctic palaeoenvironments: a perspective on global change”. (eds.) Kennett, J.P. and Warnke, D.D., Antarctic Res. Ser. 56, pp 7-36.
- Lombard, D. and Akinlua, A. (2009) Reservoir characterization of wells KD1, KE1, KF1, KH1, in block 3, Orange Basin, offshore South Africa. 11th SAGA Biennial Technical Meeting and Exhibition Swaziland, pp 574.
- Mc Millan, I.K., Brink, G.J., Broad, D.S. and Maier, J.J. (1997), late Mesozoic Sedimentary Basins off the South Coast of South Africa, In: African Basins. Sedimentary Basins of the World 3, Edited by R.C. Selley, Series Editor K.J. Hsu, Elsevier Science B.V., Amsterdam, pp 319-376.
- Petroleum Agency SA (2003). South African Exploration Opportunities, South African Agency for Promotion of Petroleum Exploration and Exploitation, Cape Town, pp 27.
- Petroleum Agency SA (2004/5). South African Exploration Opportunities, South African Agency for Promotion of Petroleum Exploration and Exploitation, Cape Town, pp 27.
- Rider, M. (1996). The Geological Interpretation of Well Logs. 2nd Edition. Whittles Publishing Strack, K. M. (2002) KMS Technologies, KJT Enterprises Inc. Reservoir Characterization with Borehole Geophysics.
- Rider, M. (2000). The geological interpretation of well log . Scotland : Whittles publishing.
- Schlumberger (2005). Schlumberger Oil Field Glossary: Where the oil Field Meets the Dictionary. [URL:http://www.glossary.Oilfields.slb.com](http://www.glossary.Oilfields.slb.com)
- Suzanne, G.C. and Robert, M.C. (2004). Petrophysics of the Lance sandstone reservoirs in the Jonah Field, Sublette County, Wyoming. AAPG Studies in Geology 52 and Rocky Mountain Association of Geologists 2004 Guidebook; pp 226-227.

- Tissot, R.P. and Welte, D.H. (1984). Petroleum formation and occurrence. Springer-Verlag, New York, 699 pp.
- Turner, J.R., Grobber, N. and Sontundu, S. (2000). Geological modelling of the Aptian and Albian sequences within Block 9, Bredasdorp Basin, Offshore South Africa, Journal of African Earth Sciences, Geocongress 2000: A new millennium on ancient crust, 27th Earth Science Congress of the Geological Society of South Africa, edited by Kisters, A.F.M. and Thomas, R.J., pp 80.
- Western Atlas, 1992, Introduction to Wireline Log Analysis, WA92.
- Worthington, P.F. and Cosentino, M. (2005). The role of cut-offs in integrated reservoir studies. SPE Reservoir evaluation and engineering (4). SPE 84387.
- Serra, O. (1984). Fundamental of well logging interpretation. Elsevier Science Publisher, BV; pp 142.
- Wahl, J.S., Nelligan, W.B., Frentrop, A.H., Johnstone, C.W., and Schwartz, R.J. (1964). The thermal neutron decay time log: SPE Journal, 10, pp364-379.
- Jensen, J.L. and Menke, J.Y. (2006). Some statistical issues in selecting porosity cut-offs for estimating net-pay. Petrophysics 47(4), pp 315-320.
- Worthington, P.F. (2008). The application of cut-offs in integrated reservoir studies. SPE reservoir evaluation and engineering 11(6), pp 968-975.
- Van Ditzhuijzen, R., Oldenziel, T., and Van Kruijsdijk., C. (2001). Geological parametrization of a reservoir model for history matching incorporating time-lapse seismic based on a case study of Stratfjord field, SPE 71318, SPE Annual Technical Conference and Exhibition, New Orleans, USA.
- Djebbar, T. and Donaldson, E.C. (1999). Theory and practise of measuring reservoir rock and fluid transportation properties. Butterworth-Heimann, USA.

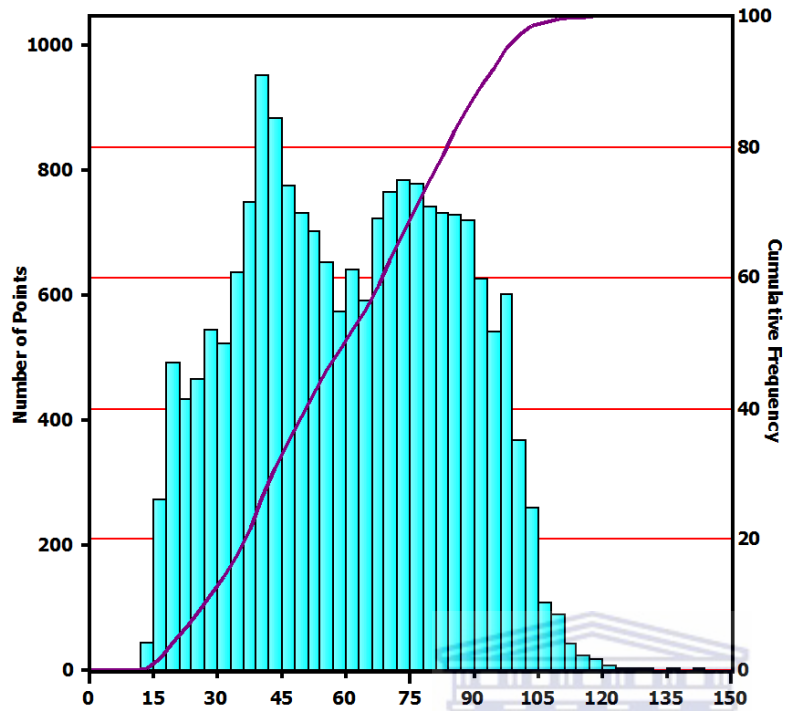
Appendices

Appendix A: Gamma Ray histogram for wells

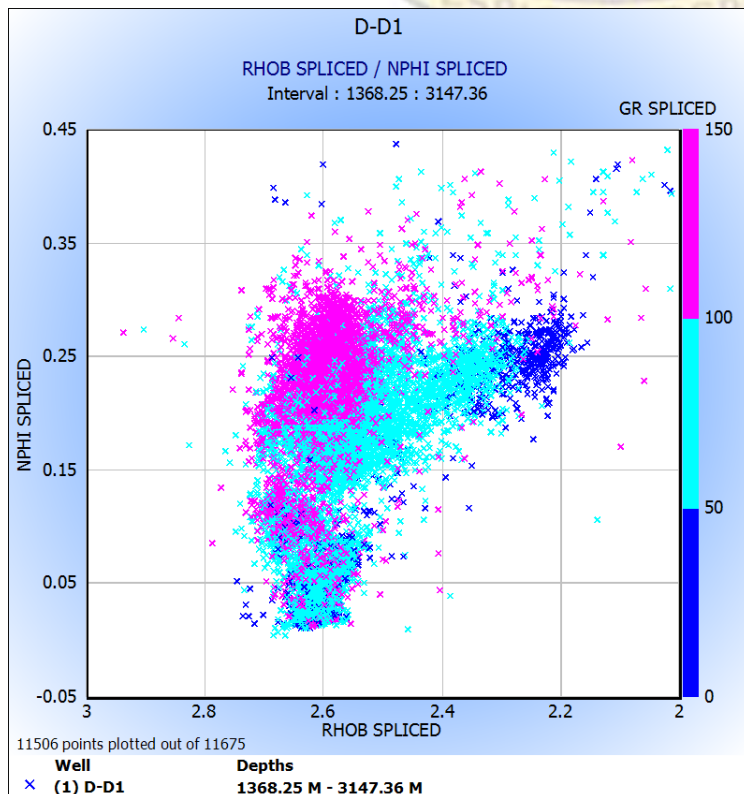


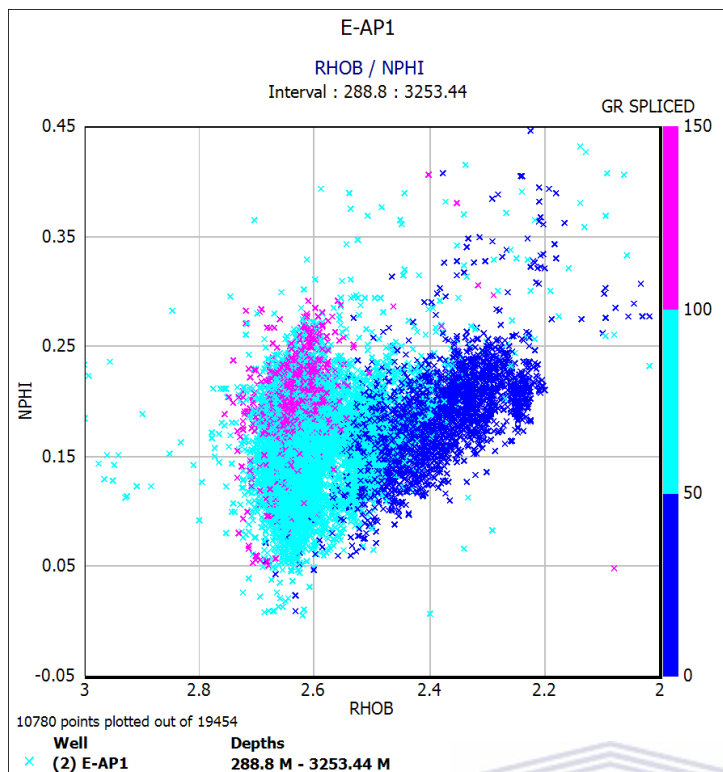
E-AP1

GR SPLICED (GAPI)
Interval : 288.8 : 3253.44

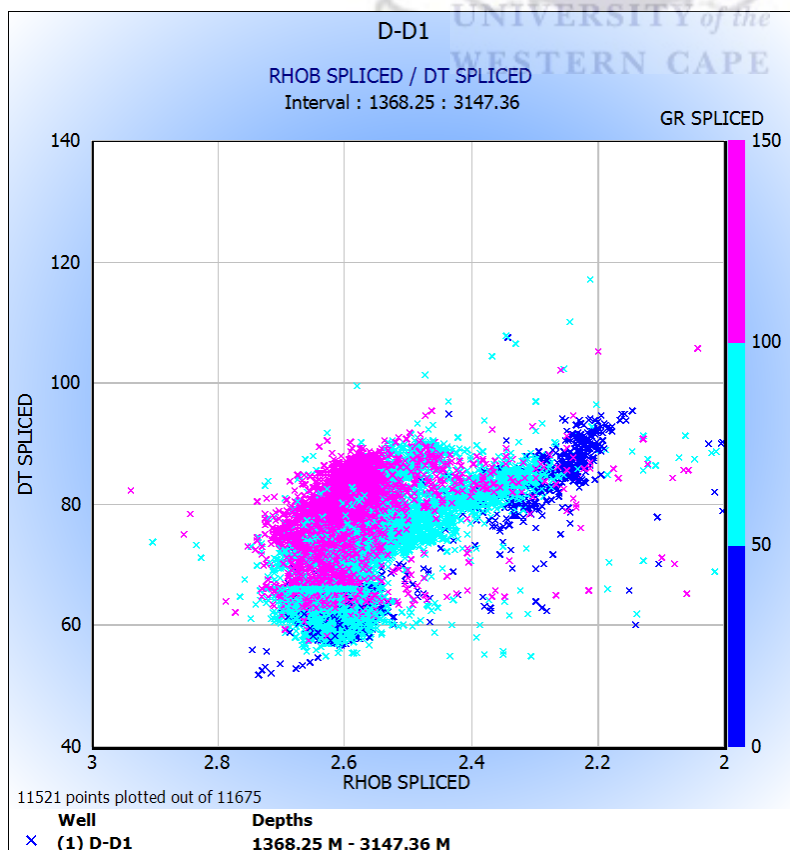


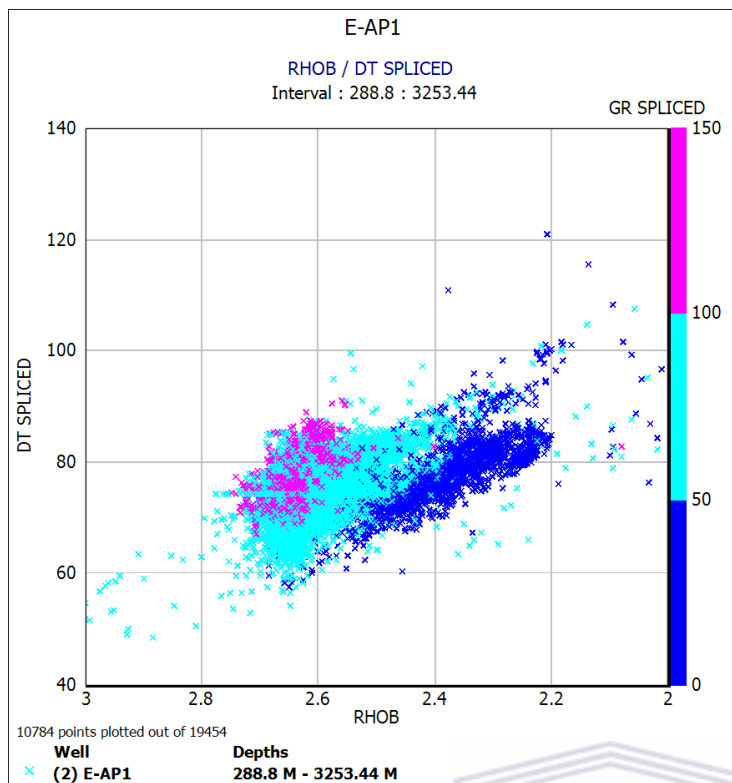
Appendix B: RHOB vs NPHI for wells



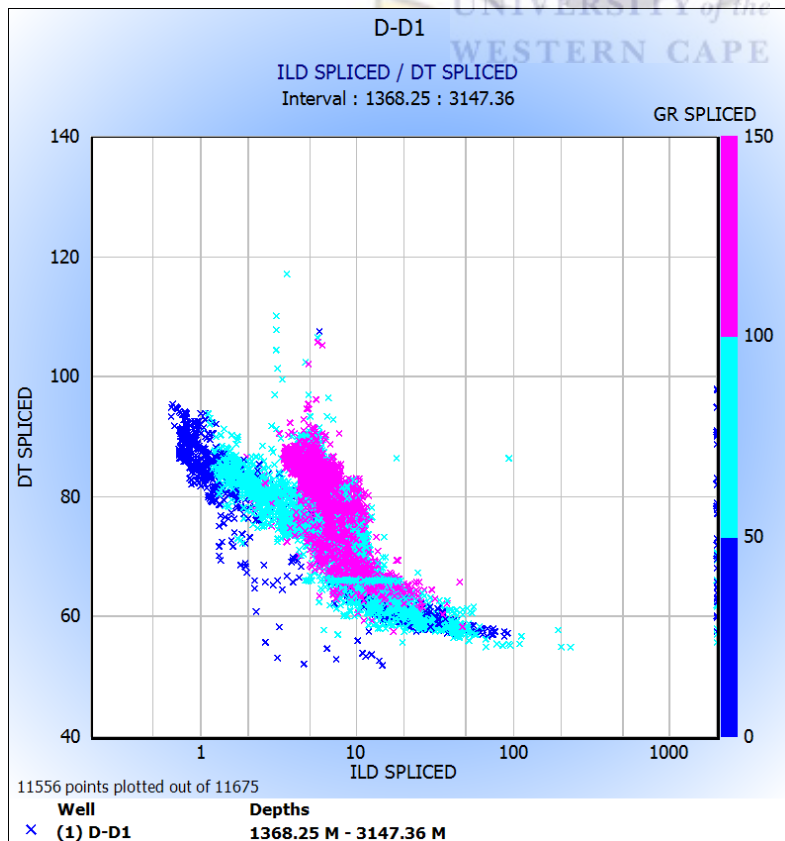


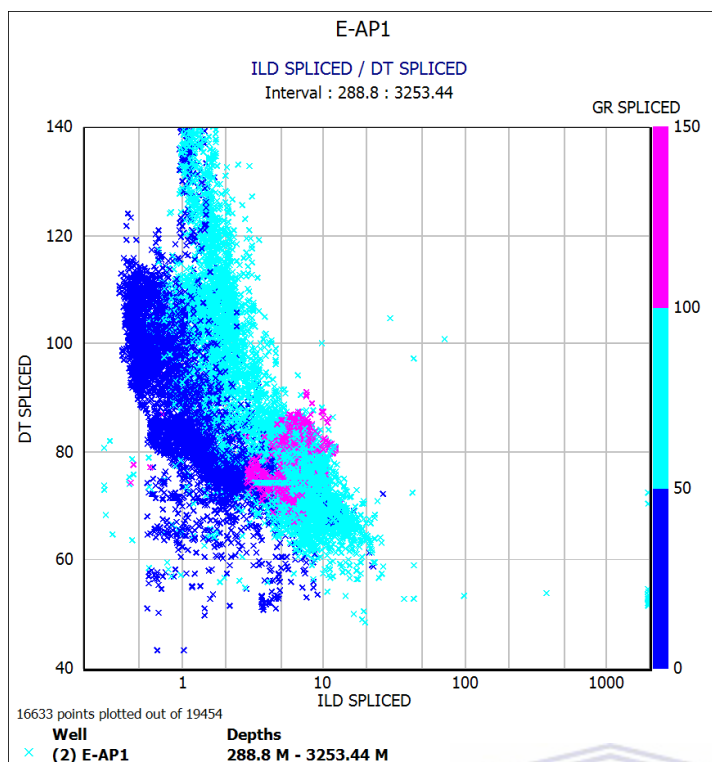
Appendix C: RHOB vs DT for wells



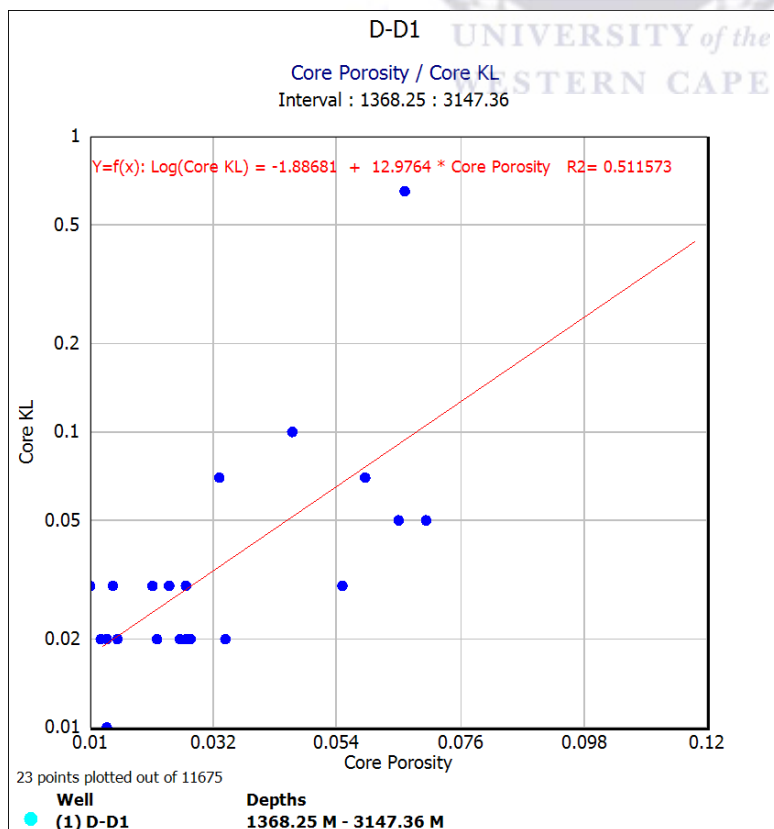


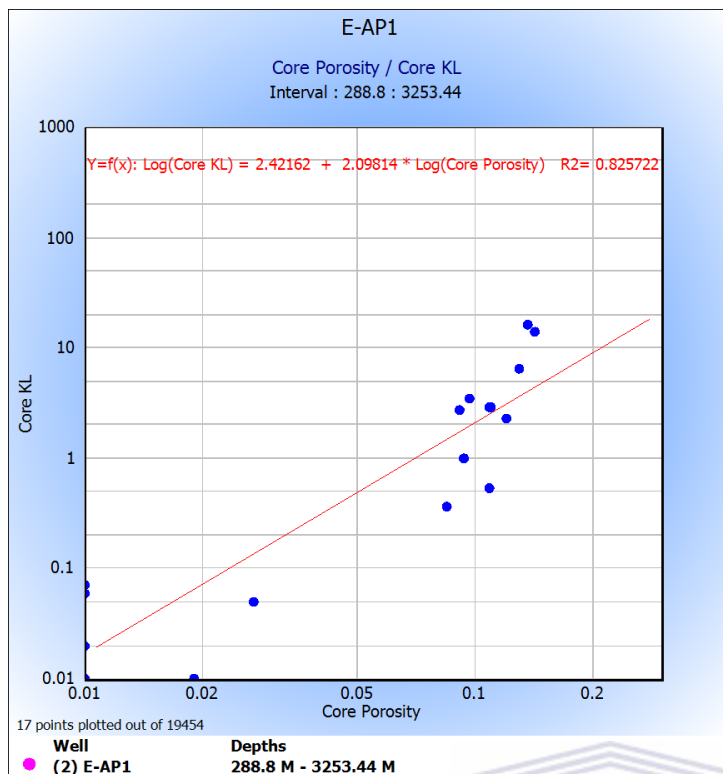
Appendix D: ILD vs DT for wells



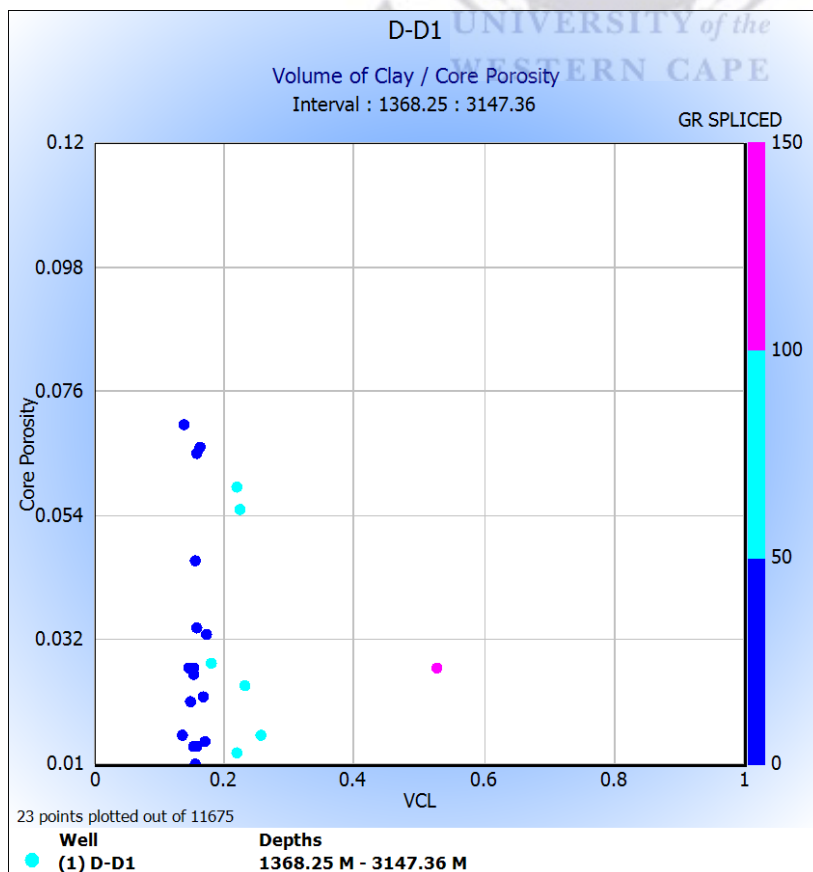


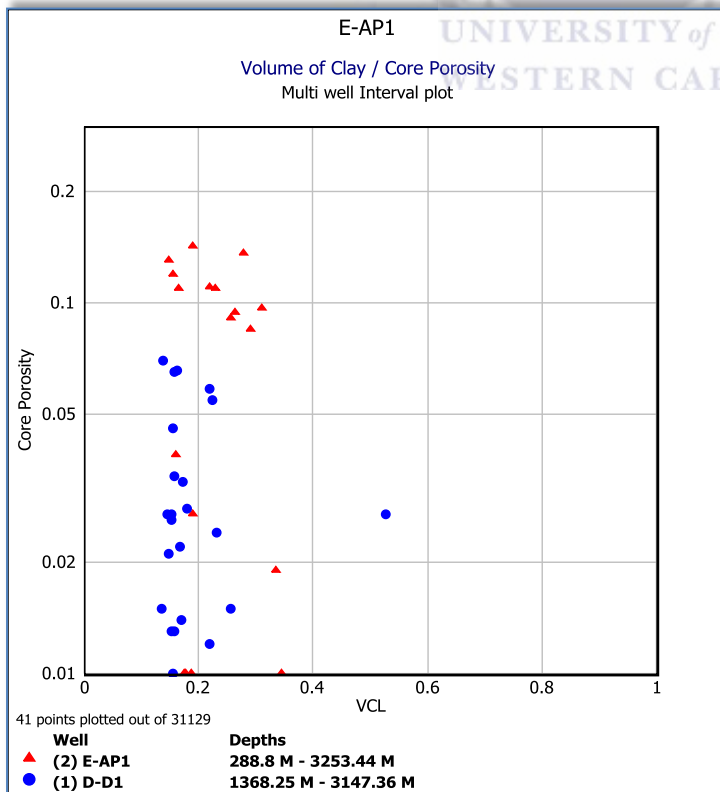
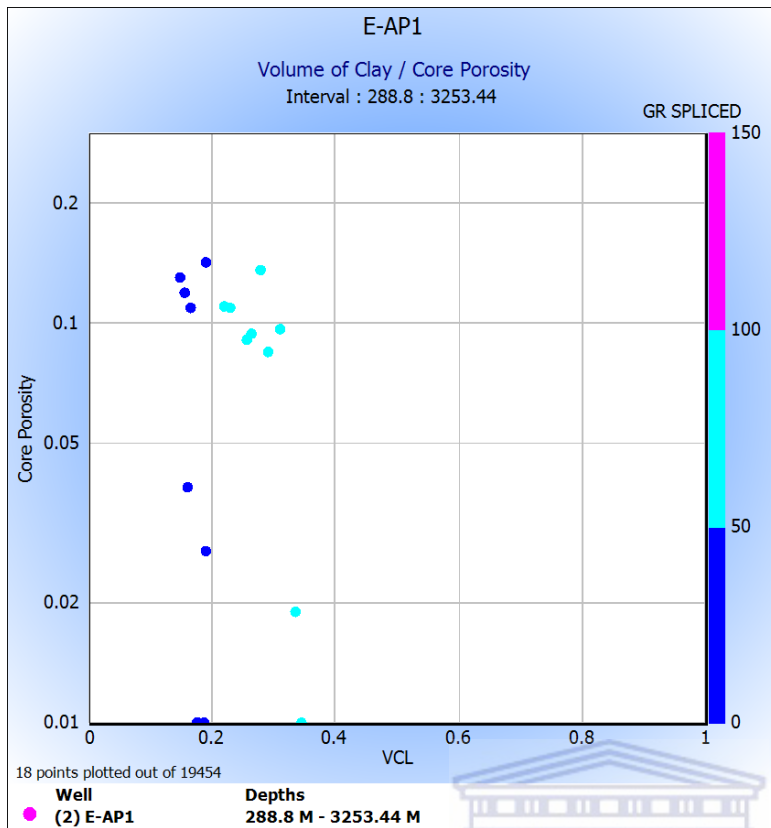
Appendix E: Core Porosity vs Core Permeability



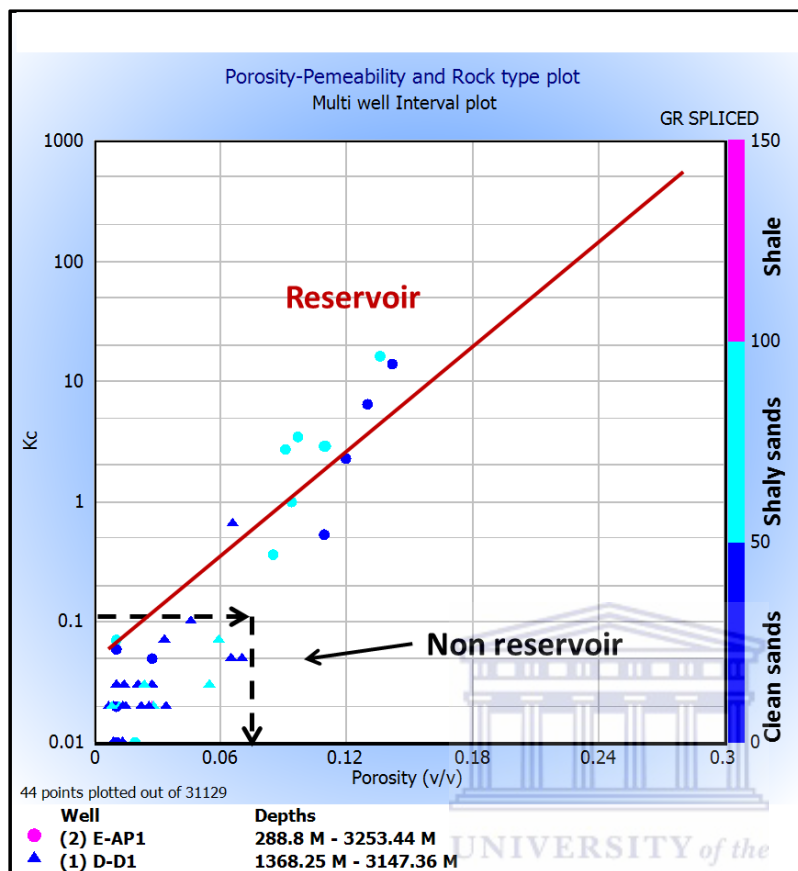


Appendix F: Volume of Clay vs Core Porosity for wells

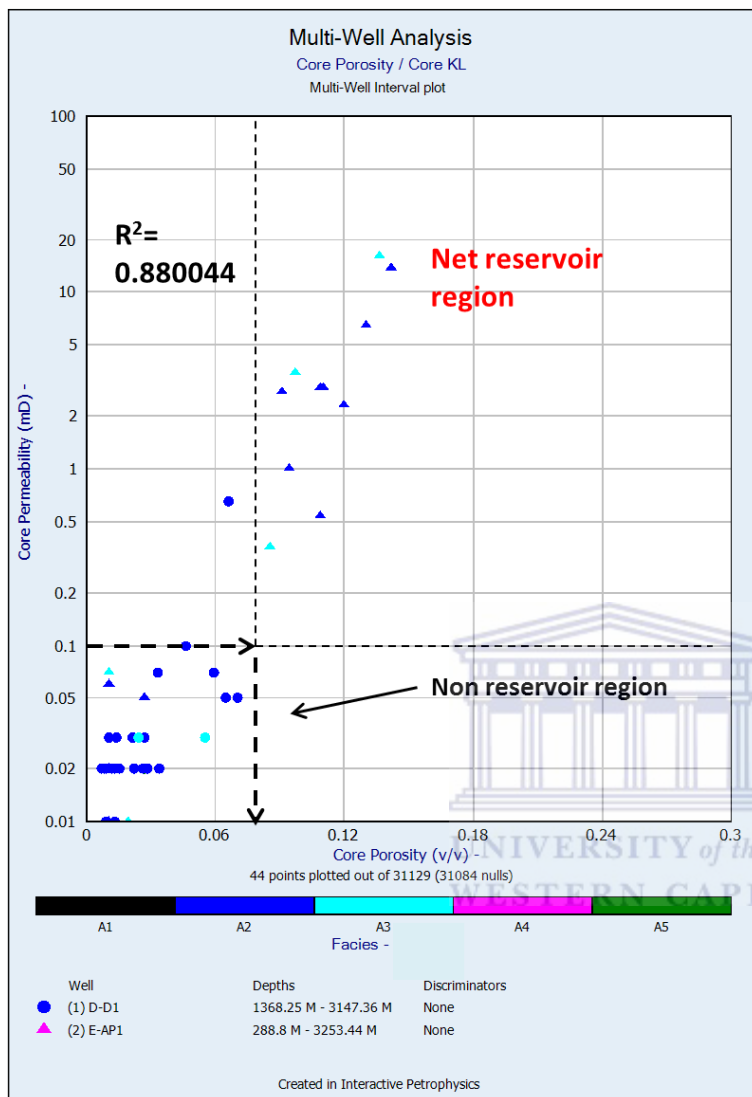




Appendix G: Porosity-Permeability and Rock type plot

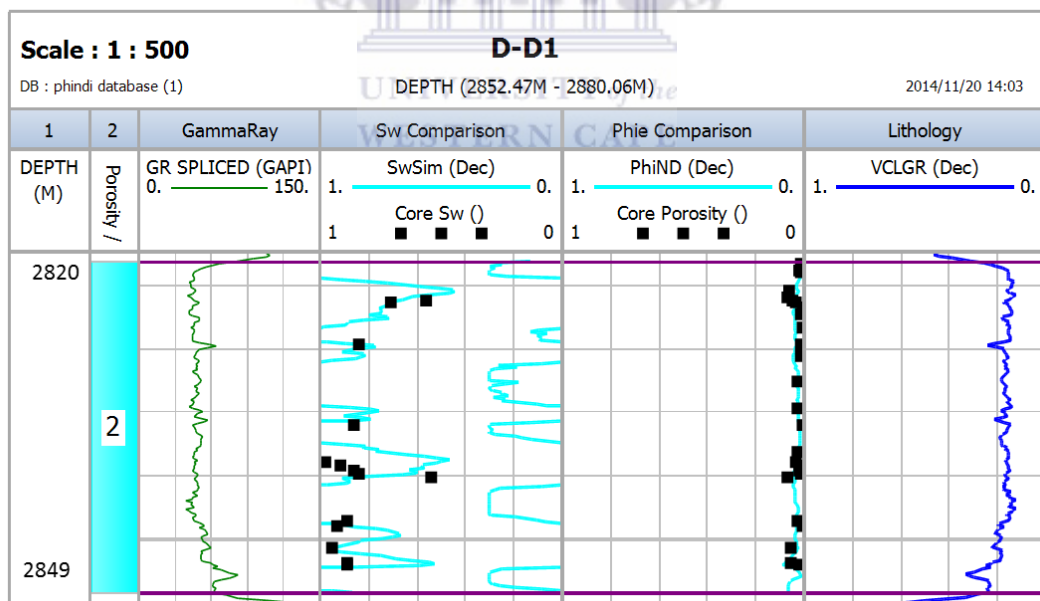
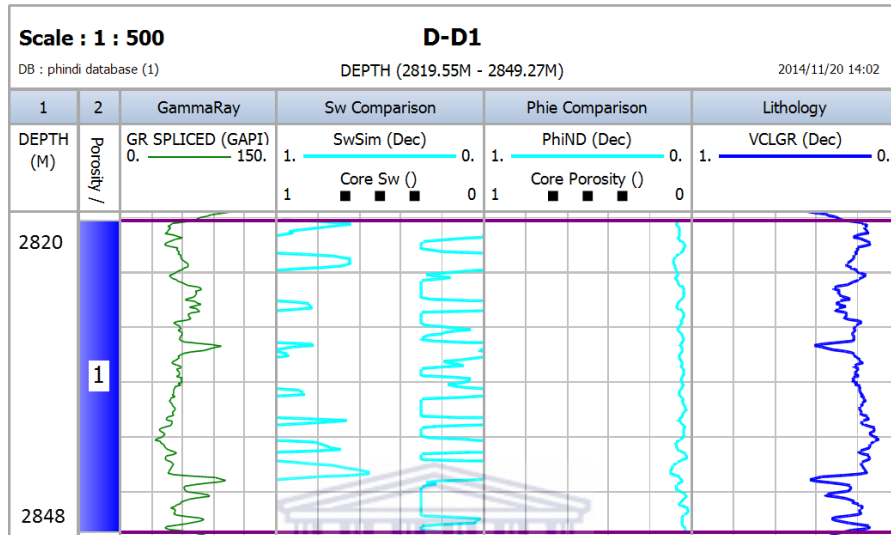


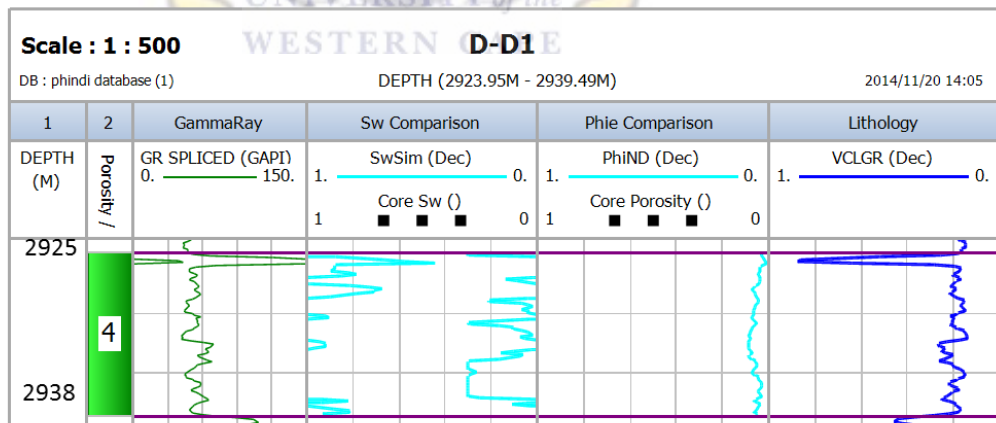
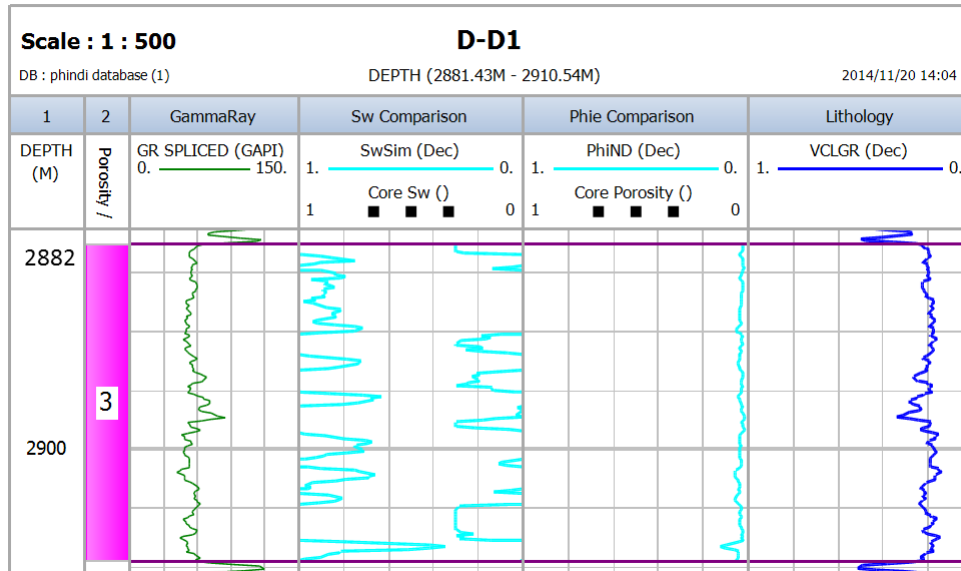
Appendix H: Core Porosity vs Core Permeability

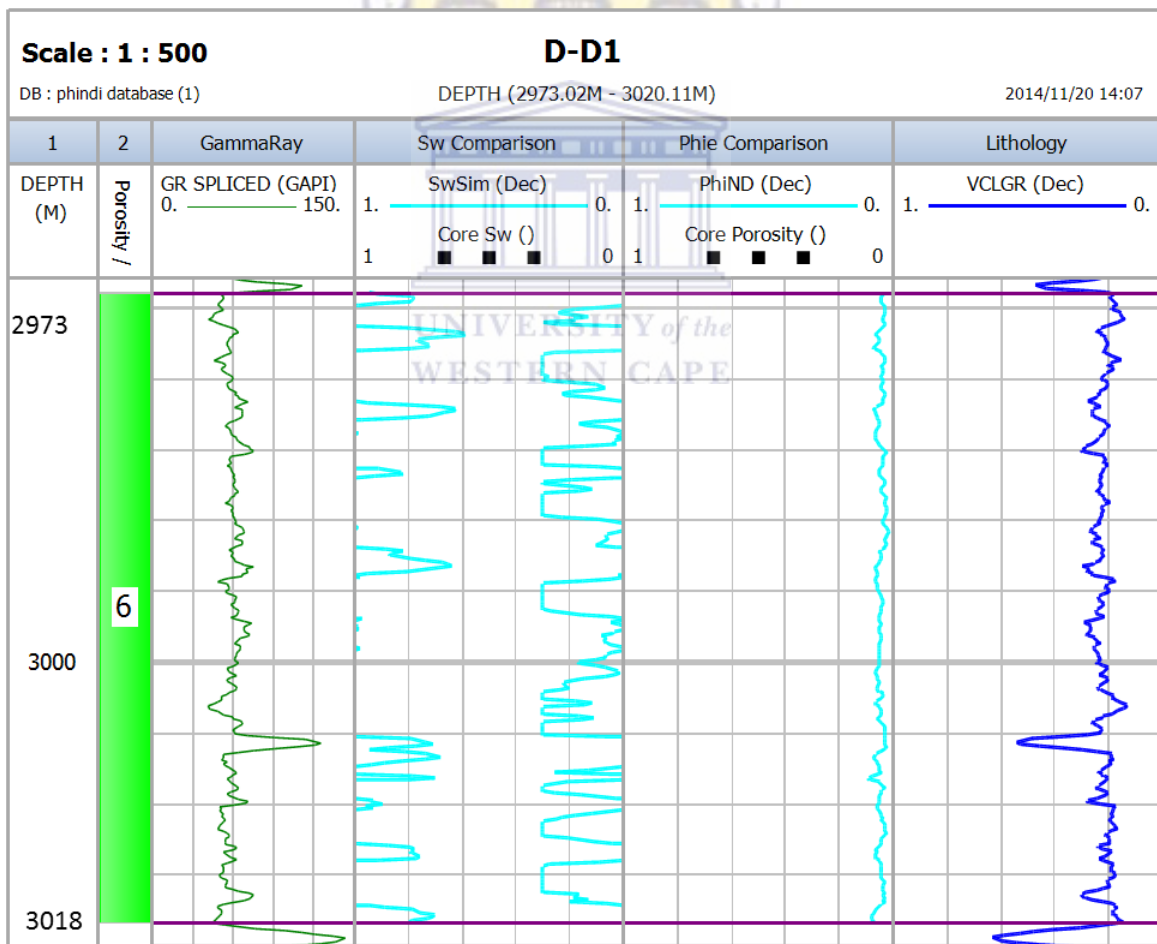
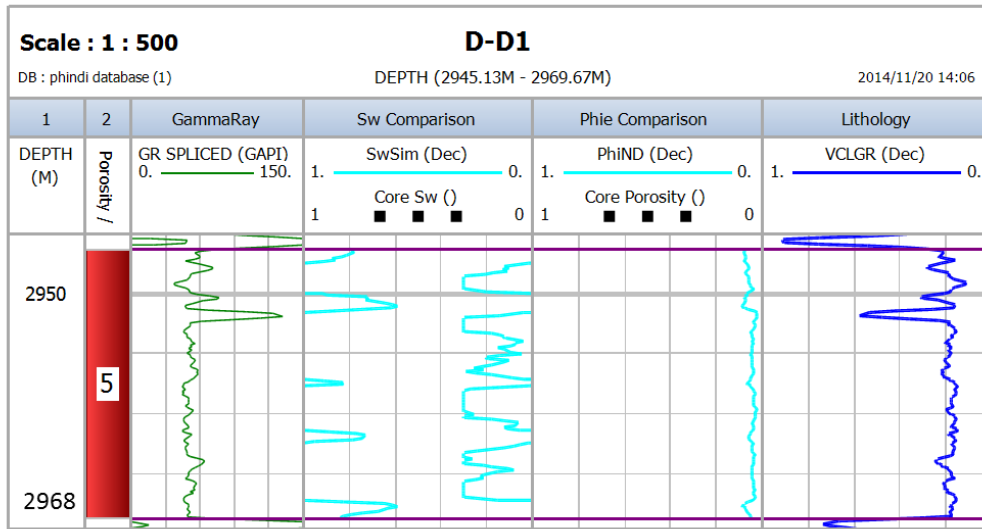


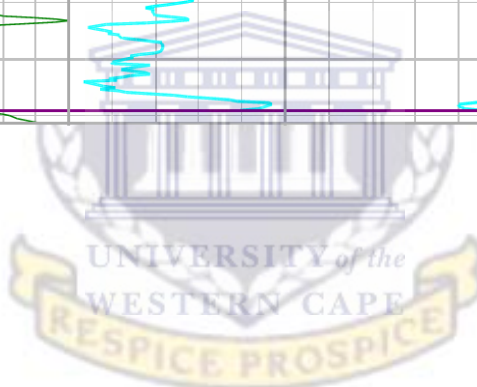
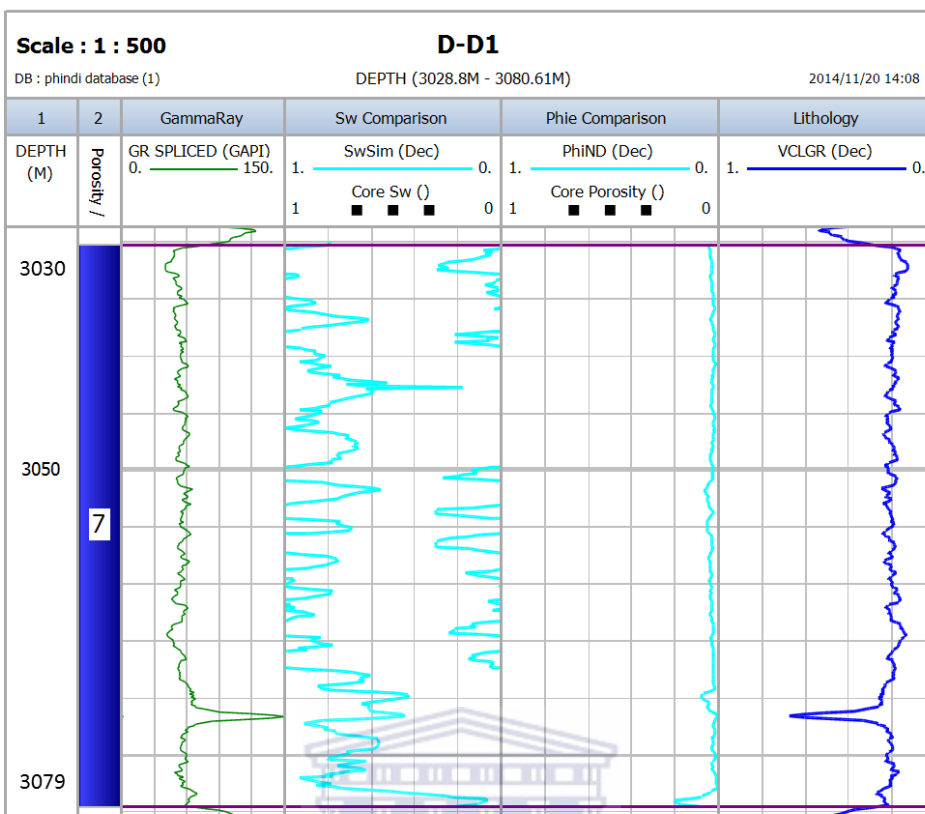
Appendix I: Comparison of log and core saturation and Porosity for reservoirs

Well D-D1



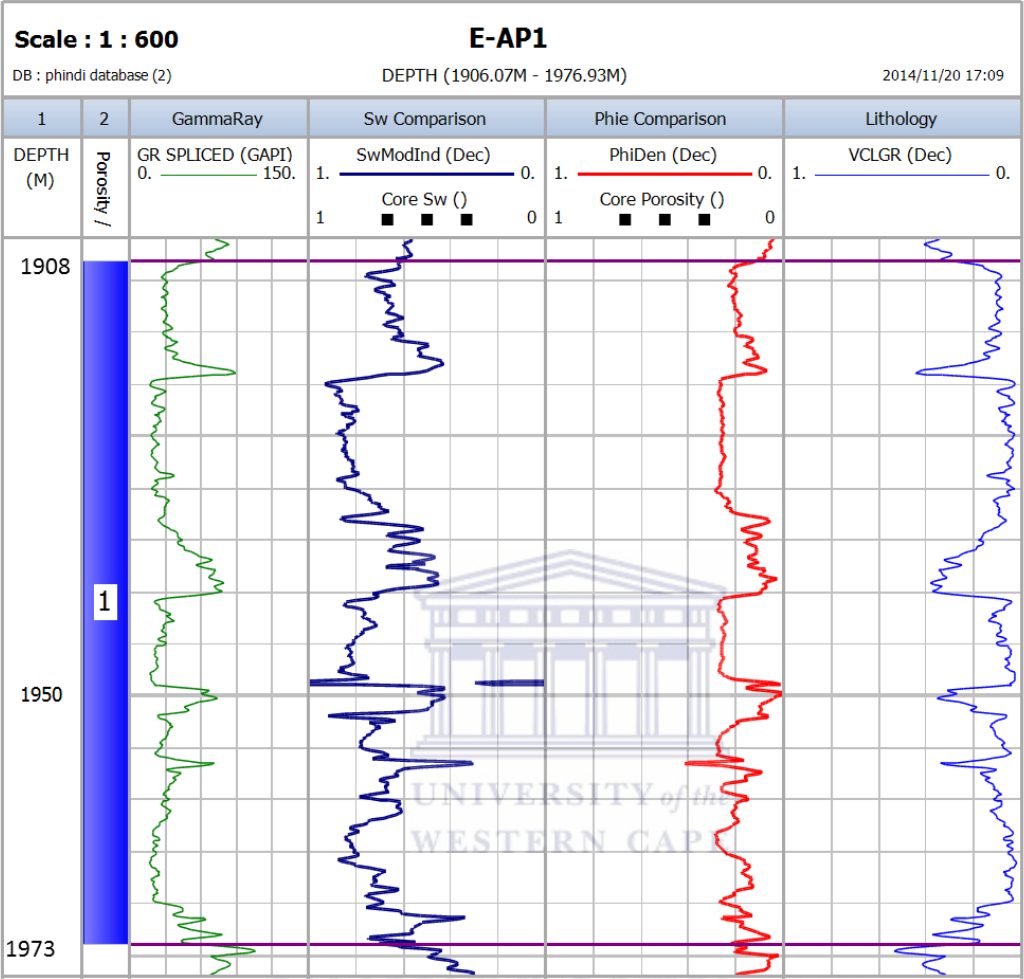


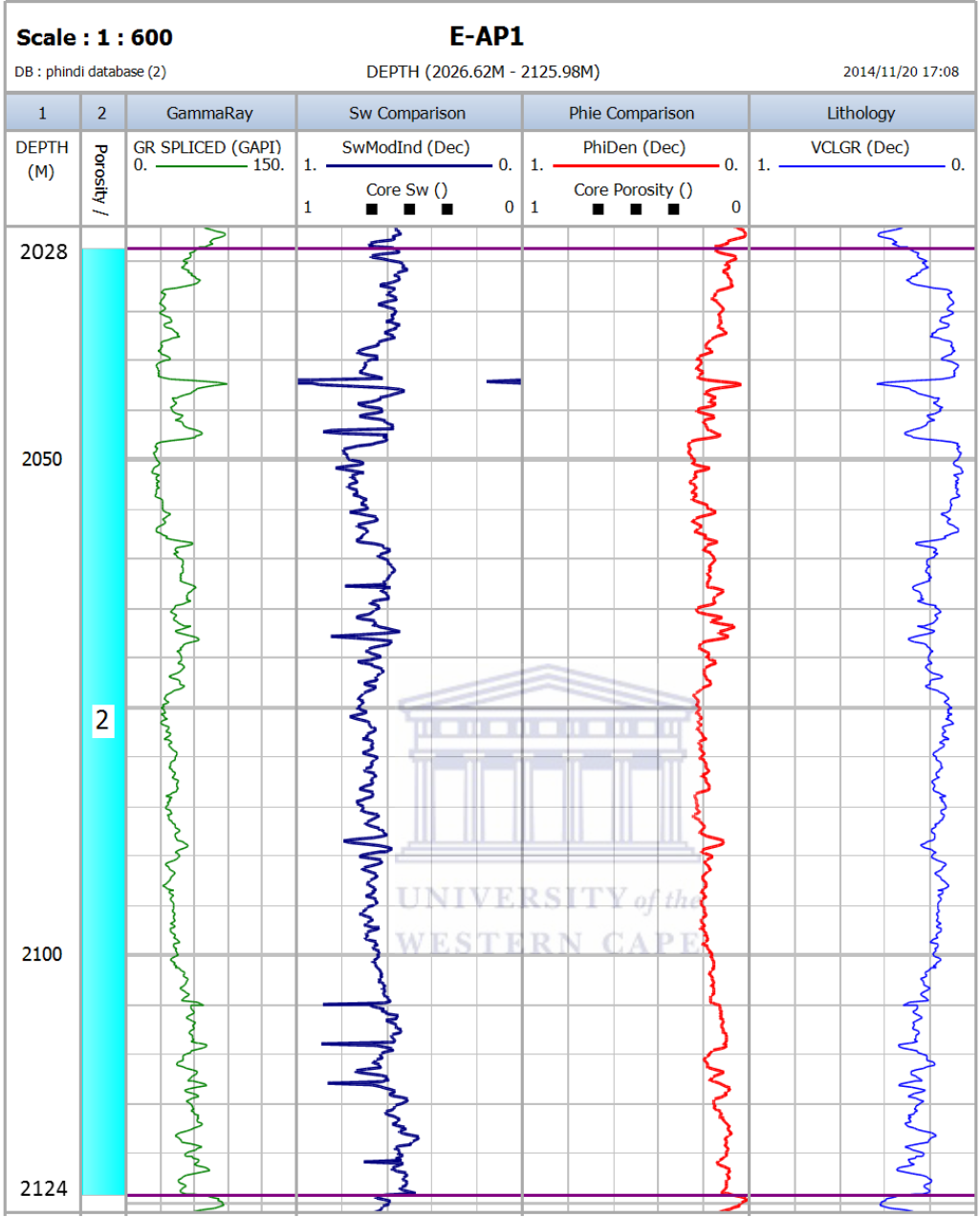


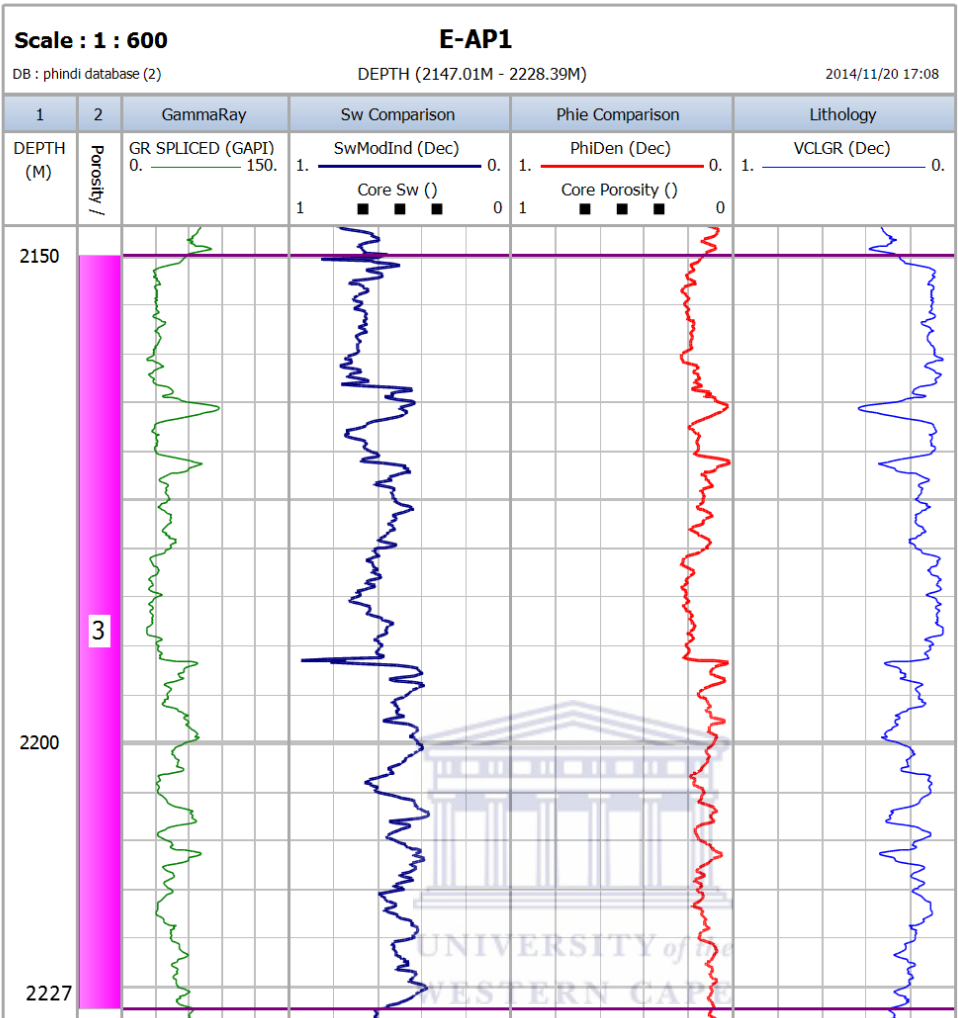


UNIVERSITY of the
WESTERN CAPE

Well E-AP1







UNIVERSITY of the
WESTERN CAPE

